Digital Microfluidics: A Versatile Platform For Applications in Chemistry, Biology and Medicine

By

Mais J. Jebrail

A thesis submitted in conformity with the requirements
for the degree of Doctor of Philosophy – Interdisciplinary

Department of Chemistry
University of Toronto

Digital Microfluidics: A Versatile Platform For Applications in Chemistry, Biology and Medicnine

Mais J. Jebrail

Doctor of Philosophy – Interdisciplinary

Department of Chemistry
University of Toronto

2011

Abstract

Digital microfluidics (DMF) has recently emerged as a popular technology for a wide range of applications. In DMF, nL-mL droplets containing samples and reagents are controlled (i.e., moved, merged, mixed, and dispensed from reservoirs) by applying a series of electrical potentials to an array of electrodes coated with a hydrophobic insulator. DMF is distinct from microchannel-based fluidics as it allows for precise control over multiple reagent phases (liquid and solid) in heterogeneous systems with no need for complex networks of microvalves. In this thesis, digital microfluidics has been applied to address key challenges in the fields of chemistry, biology and medicine.

For applications in chemistry, the first two-plate digital microfluidic platform for synchronized chemical synthesis is reported. The new method, which was applied to synthesizing peptide macrocycles, is fast and amenable to automation, and is convenient for parallel scale fluid handling in a straightforward manner. For applications in biology, I present the first DMF-based method for extraction of proteins (via precipitation) in serum and cell lysate. The performance of the new method was comparable to that of conventional techniques, with the advantages of automation and reduced analysis time. The results suggest great potential for digital microfluidics for proteomic biomarker discovery. Furthermore, I integrated DMF with

microchannels for in-line biological sample processing and separations. Finally, for applications in medicine, I developed the first microfluidic method for sample clean-up and extraction of estrogen from one-microliter droplets of breast tissue homogenates, blood, and serum. The new method is fast and automated, and features >1000x reduction in sample use relative to conventional techniques. This method has significant potential for applications in endocrinology and breast cancer risk reduction. In addition, I describe a new microfluidic system incorporating a digital microfluidic platform for on-chip blood spotting and processing, and a microchannel emitter for direct analysis by mass spectrometry. The new method is fast, robust, precise, and is capable of quantifying analytes associated with common congenital disorders such as homocystinuria, phenylketonuria, and tyrosinemia.

This thesis is dedicated to my parents John and Mary, for their love, support and understanding.

"This I do know beyond any reasonable doubt. Regardless of what you are doing, if you pump long enough, hard enough and enthusiastically enough, sooner or later the effort will bring forth the reward."
~ Zig Ziglar

Acknowledgments

This dissertation was made possible under the guidance and support of Professor Aaron Wheeler who is an exceptional mentor and first-class researcher. As a student of Professor Wheeler, I gained tremendous wealth of knowledge and research experience, and more importantly I developed a great enthusiasm and appreciation for scientific research. I am grateful for his positive-attitude, kind and humble approach in research which motivated me to be creative and hard working. I am confident that I can apply what I have learned from him and be successful in my scientific career. I will always look up to him and hope in the future I can make him proud. It's been truly a blessing working with Professor Wheeler.

I would like to extend my deepest gratitude to my committee members Professors Ulrich Krull and Rebecca Jockusch for their encouragement and valuable advice over the course of my graduate studies. Furthermore, I would like to thank them for finding the time in their busy schedules to take part in all of my committee meetings and for reviewing this thesis. I am also grateful to Professor Andrei Yudin for being on my comprehensive oral examination committee and final defense. My sincere thanks also go to my external appraiser for this thesis, Professor Stephen Jacobson for his efforts and expertise.

I am indebted to my colleagues and friends in the Wheeler Lab from whom I learned to enjoy research and graduate life: Dr. Mohamed Abdelgawad, Sam Au, Dr. Irena Barbulovic-Nad, Dario Bogojevic, Alex Chebotarev, Irwin Eydelnant, Lindsey Fiddes, Dr. Sergio Freire, Ryan Fobel, Dr. Yan Gao, Andrea Kirby, Nelson Lafreniere, Vivienne Luk, Dr. Beth Miller, Alphonsus Ng, Nikoo Shahrestani, Steve Shih, Suthan Srigunapalan, Uvaraj Uddayasankar, Dr. Mike Watson, Hao Yang, and Dr. Edmond Young.

It is a pleasure to pay tribute to the collaborators. To Professor Robert Casper and Noha Mousa from Mount Sinai Hospital (Toronto, ON) I would like to thank you for your guidance with the analysis of hormones in clinical samples. Special thanks also go to Professor Andrei Yudin and group members, Vishal Rai and Ryan Hili for their expertise with synthesizing peptide macrocycles. Finally, to the Ontario Newborn Screening Program (Ottawa, ON) crew, Dr. Pranesh Chakraborty, Christine McRoberts, Dr. Osama Al-Dirbashi and Lawrence Fisher thank you for guidance with the newborn screening project. The opportunity to work with these

experts has made me realize how vital collaborative research is when confronting difficult scientific problems.

I am also thankful to Dr. Henry Lee and Dr. Yimin Zhou from the ECTI cleanroom for their help with using the instruments and discussions. I would like to also thank Dr. Timothy Burrow and Dmitry Pichugin for their help with the NMR analysis.

I thank my best friend and fiancée Nadine for her support, encouragement, patience and unwavering love. Last, but certainly not least, I thank my loving parents John and Mary for sacrificing so much in life so I can reach this point. They are the bedrock upon which my accomplishments in life are built on. Finally, special thanks to my younger brother Fadie for his support and company during the long drives to school.

Overview of Chapters

This thesis describes a series of projects that I completed during my Ph.D. studies in Aaron Wheeler's research group at the University of Toronto. The theme of this thesis is the invention and development of new digital microfluidic (DMF) device architectures for applications in the fields of chemistry, biology and medicine. The unique capabilities of DMF are highlighted in the various chapters, ranging from straightforward integration of syncrhonized synthesis (chapter two), to preparation of biological and clinical samples for proteomic, hormonal and inborn metabolic disorder analysis (chapters three-six). Here, I provide a brief description of each chapter.

Chapter one is a literature review of DMF with special emphasis on topics encountered during the course of the projects described in my thesis. This chapter describes the state-of-the-art in digital microfluidics as applied to a wide range of applications in chemistry, biology and medicine.

Chapter two presents the first two-plate digital microfluidic platform for chemical synthesis, suitable for control of multiplexed, multi-component, multi-step reactions in parallel. For proof-of-principle, the method was used to carry out synchronized synthesis of peptide macrocycles. The results suggest that there is significant potential for digital microfluidics for fast and automated synthesis of libraries of compounds for applications such as drug discovery and high-throughput screening.

Chapter three describes the first DMF-based method for extracting proteins from heterogeneous fluids, including the key steps of precipitation, rinsing, and resolubilization. The method is compatible with proteins representing a range of different physicochemical properties, as well as with complex mixtures such as fetal bovine serum and cell lysate. The work represents an important first step in efforts to develop fully automated microfluidic methods for proteomic analyses.

Chapter four introduces a new multilayer "hybrid microfluidics" device configuration, in which a DMF device is formed on a top substrate which is mated to a network of microchannels below. In this hybrid device, droplets are dispensed from reservoirs, merged, mixed, and split on the top layer, and are subsequently transferred to microchannels through a vertical interface into channels for chemical separations. To validate the capabilities of the new

method, on-chip serial dilution experiments and multi-step enzymatic digestion regimens were implemented. The new multilayer hybrid microfluidic device has the potential to become a powerful new tool for biological assays.

Chapter five describes the application of DMF to the extraction of estrogen in 1-microliter samples of breast tissue homogenate, whole blood, and serum. This technique was developed in response to the conventional methods that require invasive biopsies of hundreds to thousands of milligrams of tissue which can result in scarring and require many hours of laboratory time for analysis. The new integrated sample cleanup method may prove useful for a wide range of clinically relevant applications, specifically conditions requiring frequent analysis of hormones in clinical samples (e.g., infertility and cancer).

Chapter six presents a new integrated microfluidic system developed to quantify amino acids in samples of newborn blood. The method is capable of processing two kinds of samples: blood spotted directly onto the chip and dried, and discs of filter paper bearing dried blood. For some applications, the device was integrated with a microchannel emitter for direct analysis by mass spectrometry. The presented method is fast and precise, and is capable of screening blood samples for inborn metabolic disorders.

The Appendices describe two side-projects that are outside of the scope of the main text. Appendix 1 describes a fully integrated digital microfluidic system with automated droplet control for protein extraction by precipitation followed by solution-phase processing. Appendix 2 describes an inexpensive and fast method for generating an insulating and hydrophobic layer using laboratory wrap (Parafilm®) for DMF devices.

Overview of Author Contribution

This work described in my thesis was made possible with the help of colleagues from the Wheeler Microfluidics Lab and from outside of the lab. Here, I outline the contributions that each author made towards the work.

For the literature review in ***Chapter one***, I conceived of the ideas and wrote the text and assembled the figures. As I wrote the text, I had valuable conversations with Dr. Mohamed Abdelgawad (a former graduate student in the Wheeler lab). A version of this paper has been submitted for publication as a review article. The initial version of the paper was written by me and revised by Prof. Wheeler. I am the first author.

The project described in ***Chapter two*** was carried in collaboration with Prof. Andrei Yudin's group in chemistry department at the University of Toronto. I designed and fabricated DMF devices, carried out DMF-based synthesis and characterized the products with the help of Alphonsus Ng (then an undergraduate student in the Wheeler Lab). Dr. Vishal Rai (a post-doc in the Yudin Group) and Dr. Ryan Hili (then a graduate student in the Yudin Group) designed the synthetic protocol, and carried out synthesis and characterization on the macroscale. A version of this chapter was published in the journal *Angewandte Chemie International Edition* (*Angew. Chem. Int. Ed.*, 2010, 49, 8625). The initial version of the paper was written by me and revised by Profs. Wheeler and Yudin. I am the first author.

For the project described in ***Chapter three***, I designed and fabricated DMF devices, developed the methods and carried out the extraction and purification of proteins by DMF, and completed all of the characterisation of proteins extracted by the DMF and conventional macroscale method. This work was published in the journal *Analytical Chemistry* (*Anal. Chem.*, 2009, 81, 330). The initial version of the paper was written by me and revised by Prof. Wheeler. I am the first author.

The project described in ***Chapter four*** was carried out in close collaboration with Dr. Michael (Mike) Watson, who was then a graduate student in Wheeler Lab. I designed the hybrid microfluidic device, established a fabrication protocol and together with Mike fabricated the devices. The calibration curve experiments were carried out by me, and the separations and post-analysis by Mike. The protein digestion experiments and analysis were completed by Mike. A version of this chapter was published in the journal *Analytical Chemistry* (*Anal. Chem.*, 2010, 82,

6680). The initial version of the paper was written by Mike and me, and revised by Prof. Wheeler. Mike and I are co-first authors.

The project described in ***Chapter five*** was completed in collaboration with Dr. Robert Casper's research group at Mount Sinai Hospital. In addition, we were supported by staff from the Ontario Cancer Biomarker Network (OCBN). Dr. Noha Mousa (then a graduate student in the Casper group) and I designed the experiments and fabricated the devices. Mass spectrometry analyses were designed and carried out by Hao Yang (a graduate student in the Wheeler lab), Pavel Metalnikov and Jian Chen (technicians at OCBN). Dr. Mohamed Abdelgawad (then a graduate student in the Wheeler lab) participated in the initial development of digital microfluidic device design and operation. A version of this chapter was published in the journal *Science Translational Medicine* (*Sci. Trans. Med.*, 2009, 1, 1ra2). The initial version of the paper was written by Noha and me, and revised by Prof. Aaron Wheeler. Noha and I are co-first authors.

The project described in ***Chapter six*** was carried out in collaboration with the Ontario Newborn Screening Program (ONSP). I designed the device and carried out the experiments in which samples were processed by DMF and analyzed off-line, I had help from Jared Mudrik (then an undergraduate student in the Wheeler lab) and Nelson Lafrenière (a graduate student in the Wheeler Lab) in fabricating these devices. Hao Yang (a graduate student in the Wheeler lab) designed and fabricated the DMF devices that were integrated with a microchannel emitter for in-line mass spectrometry analysis. Hao Yang and I worked together to carry out the analysis of mass spectrometry results from all devices. Christine McRoberts (a technician at ONSP), Dr. Osama Al-Dirbashi (a scientist at ONSP). Lawrence Fisher (a technician at ONSP), and Dr. Pranesh Chakraborty (the director of ONSP) contributed valuable suggestions and provided newborn patient samples, and McRoberts, Al-Dirbashi, and Fisher carried out analyses using conventional methods. A version of this chapter has been submitted and is currently under review. The initial version of the paper was written by me and Hao, and revised by Prof. Wheeler. Hao and I are co-first authors.

The project described in ***Appendix 1*** was carried out with Vivienne Luk and Steve Shih, (graduate students in the Wheeler lab). Vivienne and I designed the experiments and fabricated the devices, and carried out the protein processing experiments. Steve designed the control box and wrote the algorithms used to automate the processes. Other Wheeler lab

members (Ryan Fobel, Alphonsus Ng, Hao Yang and Dr. Sergio Freire) were involved in assisting with fabrication and analysis. A version of appendix 1 was published in the *Journal of Visualized Experiments* (*J. Vis. Exp.*, 2009, 33, DOI: 10.3791/1603). The initial version of the report was written by me, Vivienne and Steve, and revised by Prof. Wheeler. Vivienne, Steve and I are co-first authors.

The project described in ***Appendix 2*** was carried out with assistance from two graduate students from the Wheeler Lab, Nelson Lafrenière and Hao Yang. A version of appendix 2 was published online as an article in Chips and Tips – an online supplement to *Lab on a Chip* (http://www.rsc.org/Publishing/Journals/lc/Chips_and_Tips/digitalmicrofluidics.asp, Jul. 6, 2010).

Table of Contents

List of Abbreviations

1. Acetonitrile (**ACN**)
2. Alexa fluor 488 (**AF**)
3. Amino acid (**AA**)
4. Bovine serum albumin (**BSA**)
5. Charge coupled device (**CCD**)
6. Cell Lysate (**CL**)
7. Collision induced dissociation (**CID**)
8. Deoxyribonucleic acid (**DNA**)
9. Dibutyroyl-*sn*-glycero-3-phosphocholine (**PC**)
10. Dichloromethane (**DCM**)
11. Digital microfluidics (**DMF**)
12. Dried blood sample (**DBS**)
13. Electrospray Ionizatio (**ESI**)
14. Fetal bovine serum (**FBS**)
15. Fibrinogen (**Fb**)
16. Hexamethyldisilazane (**HMDS**)
17. High pressure liquid chromatography (**HPLC**)
18. Indium Tin Oxide (**ITO**)
19. Internal diameter (**i.d.**)
20. Iodoacetamide (**IAM**)
21. Isoelectric point (**pI**)
22. Isoleucine (**Ile**)
23. Liquid chromatography (**LC**)
24. Mass Spectrometry (**MS**)
25. Methanol (**MeOH**)
26. Methionine (**Met**)
27. Micro total analysis systems (**μTAS**)
28. Myoglobin (**Mb**)
29. Newborn screening Ontario (**NSO**)
30. Nuclear Magnetic Resonance (**NMR**)
31. Peptide-based macrocycle (**PM**)
32. Phenylalanine (**Phe**)
33. Phenylmethylsulfonyl fluoride (**PMSF**)
34. Phosphate buffered saline (**PBS**)
35. Poly(dimethylsiloxane) (**PDMS**)
36. Proline (**Pro**)
37. Proline-Leucine (**ProLeu**)
38. Proton NMR (**^{1}HNMR**)
39. Ring-opened products (**ROP**)
40. Selected reaction monitoring (**SRM**)
41. Sodium dodecyl sulfate (**SDS**)
42. Tandem mass spectrometry (**MS/MS**)
43. Tert-butyl isocyanide (**^{t}BuNC**)

44. Thiobenzoic acid (**PhCOSH**)
45. Threonine (**Thr**)
46. Trichloroacetic acid (**TCA**)
47. Trifluoroethanol (**TFE**)
48. Tris(2-carboxyethyl)phosphine (**TCEP**)
49. Tyrosine (**Tyr**)
50. Valine (**Val**)

List of Equations

List of Schemes

List of Tables

List of Figures

Chapter 1

Chapter 2

Chapter 3

Chapter 4

Chapter 5

Chapter 6

Appendix 1

Appendix 2

Chapter 1 Review of Digital Microfluidics

1.1 Digital Microfluidics

The most common format for microfluidics is based on enclosed microchannels in planar platforms. While such systems have been used for applications in chemistry,[1-5] biology[6-9] and medicine,[10-12] in this minireview, we focus on a related but distinct technology called digital microfluidics. Like microchannel-based fluidics, digital microfluidics is being used to miniaturize a wide range of applications, with the advantages of reduced reagent and solvent consumption, faster reaction rates, and capacity for integration (i.e., the lab-on-a-chip concept). In digital microfluidics, discrete droplets of samples and reagents are manipulated (i.e., dispensed from reservoirs, split, merged and mixed) on an open surface by applying a series of electrical potentials to an array of electrodes.[13,14] Although microchannels can also be used to manipulate droplets,[15,16] digital microfluidics is a distinct paradigm that offers several unique advantages.

One unique advantage of digital microfluidics is the capacity to address each reagent individually with no need for complex networks of tubing or microvalves (Figure 1.1a). A second advantage is the capacity to control liquids relative to solids with no risk of clogging -- thus, as shown in Figure 1.1b, digital microfluidics is a good match for the analysis of solid samples.[17,18] A third advantage for digital microfluidics is compatibility with a large range of volumes (see Figure 1.1c), making it useful for preparative-scale sample handling. This is contrasted with microchannels, in which volumes are typically much smaller and are suitable for analytical applications (but not preparative applications). There are of course many advantages for microchannels relative to digital microfluidics (e.g., suitability for separations and reactions in continuous flow). The key capabilities and challenges for digital microfluidics are summarized in Table 1.1

In the following sections, I describe my contributions to the field of digital microfluidics, the physics and formats of digital microfluidics, followed by a discussion of the state-of-the-art for applications in chemistry, biology, medicine, and beyond.

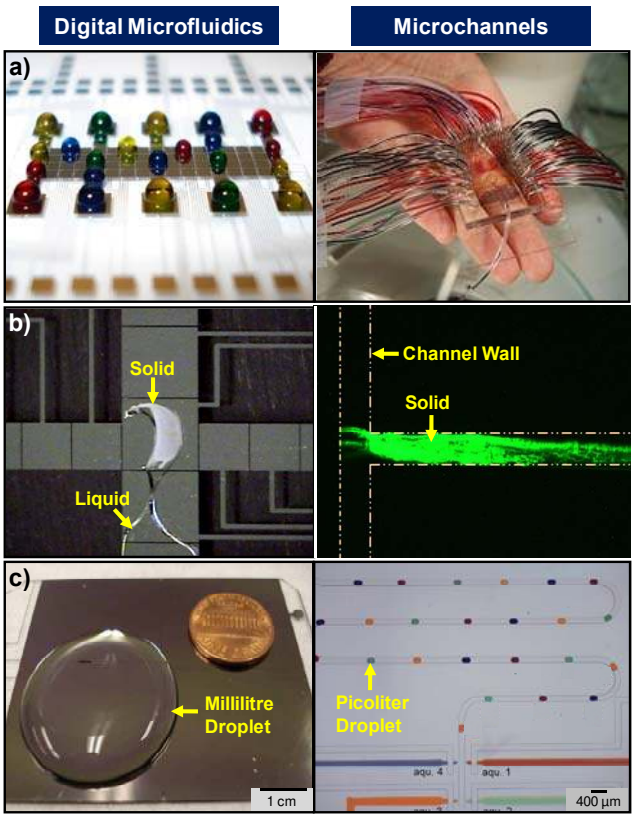

Figure 1.1 Digital microfluidics vs. microchannels. a) Digital microfluidic platform (left) controlling more than twenty reaction droplets with no need for external hardware (i.e., pumps, connectors and tubing) or microvalves vs. a microchannel platform (right) with requiring a complex network of hardware and microvalves. Reproduced with permission from [19] Copyright © 2010 John Wiley & Sons, Inc. and [4] Copyright © 2009 The Royal Society of Chemistry. b) Digital microfluidic platform (left) in which a droplet of supernatant liquid is driven away from a solid precipitate with no clogging vs. a microchannel platform (right) depicting a channel clogged with bacteria lysate. Reproduced with permission from [17] Copyright © 2009 The American Chemical Society and [20] Copyright © 2009 Elsevier. c) Digital microfluidic platform (left) Picture of a used to manipulate a ~3 mL sample droplet vs. a microchannel platform (right) used to manipulate 740 pL sample droplets. Reproduced with permission from [21] Copyright © 2008 The Royal Society of Chemistry and [22] Copyright © 2009 The Royal Society of Chemistry.

Table 1.1 Capabilities of and challenges for digital microfluidics

Capabilities	Challenges
- Easy to manipulate reagent droplets with no need for pumps, tubing and microvalves - Can handle wide range of volumes (nL-mL), suitable for preparative applications - Compatible with aqueous and organic solvents - Straightforward control over different phases	- Not suitable for chemical separations or continuous-flow synthesis - Incompatible with high temperatures (above 35 °C) and pressures (above 1 mbar) if device open to atmoshphere. - Fouling of device surfaces can result in droplet sticking - Incompatible with centrifugation

1.2 My Contributions

This thesis is a compilation of the innovations that I have contributed to the technique of digital microfluidics, which includes the development of new digital microfluidic device architectures and demonstrating their capabilities for applications in chemistry, biology and medicine.

For applications in chemistry, I developed the first two-plate DMF platform for carrying out synchronized synthesis of peptide macrocycles. The new method is fast, compatible with a wide range of solvents, liberated from external hardware (e.g., tubing, microvalves, etc.), and is particularly well-suited for parallel processing. For applications in biology, I designed and built the first-of-its-kind DMF device capable of separating a liquid phase from solid which facilitated the extraction and purification of proteins from complex biological mixtures (e.g., serum and cell lysate) for proteomic application. Furthermore, I designed and fabricated the first multilayer hybrid microfluidic configuration, in which a digital microfluidic device is formed on a top substrate for biological sample preparation mated to a network of microchannels below for separation.

For applications in medicine, I developed a novel DMF device capable of carrying key processes (i.e., solid-liquid and liquid-liquid extractions) for extracting and purifying hormones from clinical samples (e.g., whole blood and tissue homogenates). As a second application in medicine, I developed a new integrated microfluidic system incorporating a DMF platform for on-chip blood spotting and processing, and a microchannel emitter for direct analysis by mass spectrometry. The method is fast, robust and capable of screening samples for metabolic disorders.

The following sections describe the physics and format of digital microfluidics, followed by a review of applications of digital microfluidics in the areas of chemistry, biology, and medicine, as well as miscellaneous applications that defy categorization.

1.3 Physics and Formats of Digital Microfluidics

Digital microfluidics was popularized in the early 2000s by the Fair[23] and Kim[24] groups at Duke and UCLA, respectively. In this pioneering work, droplets were made to move across an insulating surface upon application of electrical potentials to electrodes positioned under the

insulator. The technique was explained as being a phenomenon driven by surface tension, and was called “electrowetting” or “electrowetting-on-dielectric” (EWOD). This naming convention arose from the observation that the contact angle between an aqueous droplet and the device surface is dramatically reduced (i.e., wetted) during droplet movement. In the "electrowetting" paradigm, the two phenomena (wetting and movement) were viewed as being cause-and-effect: droplet movement was understood as being a consequence of capillary pressure arising from non-symmetrical contact angles. However, this understanding does not explain droplet motion for liquids with low surface tension that have no apparent changes in contact angle;[25] nor can it explain related phenomena, such as contact angle saturation (i.e., the observed limit on contact angle change above a threshold in applied potential).

A better understanding of the physics of droplet actuation is derived from electromechanical analysis,[26-29] which explains both the wetting and the droplet movement phenomena in terms of electrical forces generated on free charges in the droplet meniscus (in case of conductive liquids) or on dipoles inside of the droplet (in case of dielectric liquids). For the purposes of modeling, these forces can be estimated by integrating the Maxwell–Stress tensor, T_{ij} (Eq. 1) (which can be derived from the Lorenz equation[30]), over any arbitrary surface surrounding the droplet[27,31]:

$$T_{ij} = \varepsilon\left(E_i E_j - \frac{1}{2}\delta_{ij} E^2 \right)$$

where $\mathcal{E}$ is the permittivity of the medium surrounding the droplet, i and j refer to pairs of x, y, and z axes, δ_{ij} is the Kronecker delta, and E is the electric field surrounding the droplet. Unlike electrowetting, this formulation explains the motion of dielectric liquids and liquids that do not experience a change in contact angle. In addition, it provides a rationale for the phenomenon of contact-angle saturation as an equilibrium between electrical and surface-tension forces.[27,28]

Digital microfluidics is typically implemented in one of two different configurations (Figure 1.2a) – the closed format (also known as the two-plate format) in which droplets are sandwiched between two substrates patterned with electrodes (the substrates house driving and ground electrodes, respectively) and the open format (also known as the single-plate format) in which droplets are placed on top of a single substrate housing both actuation and ground electrodes. In both configurations, an insulating layer is deposited on top of the actuation

electrodes, and the insulating layer is typically covered by an additional hydrophobic coating to reduce droplet sticking to the surface.

The closed and open digital microfluidic configurations have complementary advantages. Closed digital microfluidic devices are well suited for a wide range of fluidic operations – droplet dispensing, moving, splitting, and merging are all feasible.[32] In contrast, open digital microfluidic devices are typically not capable of splitting and dispensing; however, the open format facilitates fast sample and reagent mixing,[33] the capacity to move large droplets,[21] and better access to samples for external detectors.[34] Additionally, evaporation rates are higher in open format devices, which may be advantageous or inconvenient, depending on the application. Digital microfluidic devices are typically fabricated in a clean-room facility using conventional techniques such as photolithography and etching; electrodes are formed from substrates common to such facilities (e.g., chromium, gold, indium-tin oxide (ITO), doped polysilicon, etc.). The insulating layer can be formed using a variety of techniques, including vapor deposition (parylene, amorphous fluoropolymers, silicon nitride, etc.), thermal growth (silicon oxide), or spin coating (PDMS or SU-8). The hydrophobic coating is usually formed by spin-coating a thin layer of a fluorinated polymer such as Teflon-AF or Cytop.

After devices have been fabricated and assembled, a second key distinction in format is the nature of the matrix surrounding droplets on the device. For many applications, this matrix is simply ambient air. This format is the most striaghtforward, but is susceptible to evaporation and may require humidified chambers to overcome this issue.[35] Another common format uses a matrix of oil,[36] which limits evaporation and reduces the surface energy, and thus allows for lower electrical potentials for droplet actuation. Oil-immersed systems have drawbacks, however, including the requirement of gaskets or other structures to contain the oil bath, the potential for liquid-liquid extraction of analytes into the surrounding oil,[21] the incompatibility with oil-miscible liquids (e.g., organic solvents), and the incompatibility with assays requiring drying droplets onto the device surface.[37]

While digital microfluidics is typically implemented in planar formats (Figure 1.1a), the use of flexible platforms is growing in popularity. For example, Abdelgawad et al.[21] described the format of “All Terrain Droplet Actuation” (ATDA) using devices fabricated on flexible substrates, and demonstrated droplet actuation on non-planar (i.e., inclined, declined, upside-down, etc.) surfaces. This format allows for straightforward integration of multiple

physicochemical environments on the same device for applications such as temperature cycling (Figure 1.2b). Similarly, Fan et al.[38] developed a wearable "droplet-on-a-wristband" device formed from flexible polyethylene terephthalate substrates that can fit around patients' wrists for potential point-of-care applications (Figure 1.2c).

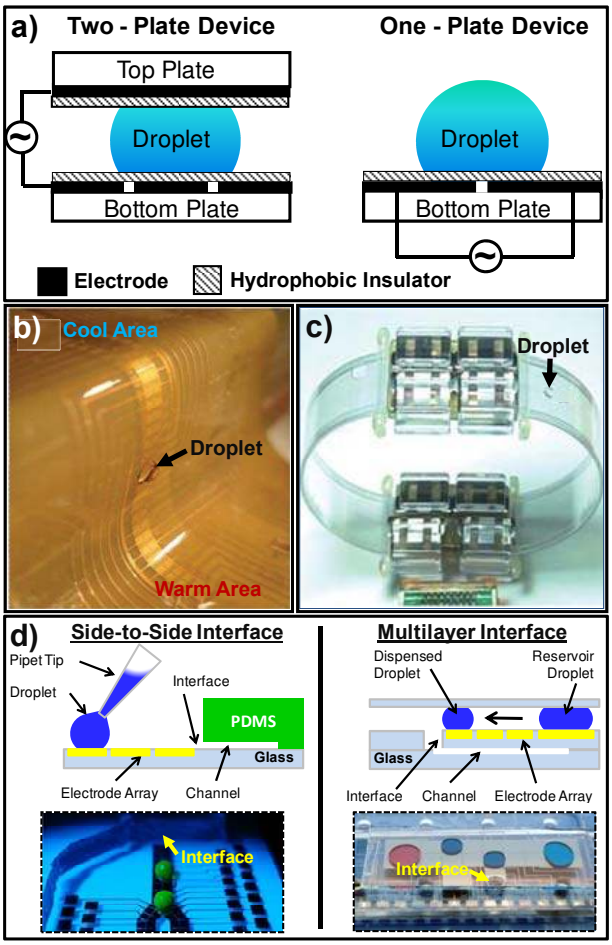

Figure 1.2. Digital microfluidic formats. a) Side-view schematics of two- (left) and one-plate (right) digital microfluidic formats. b) Picture of a flexible "All-Terrain Droplet Actuation" device moving a droplet from a warm to a cool area. Reproduced with permission from [21] Copyright © 2008 The Royal Society of Chemistry. c) Picture of a wearable "droplet-on-a-wristband" device. Reproduced with permission from [38] Copyright © 2011 The Royal Society of Chemistry. d) Side-view schematics (top) and aerial pictures (bottom) of two formats of "hybrid microfluidics," which combines digital microfluidics for sample processing with microchannels for separations. The side-to-side configuration (left) comprises a one-plate digital microfluidic device mated to a PDMS microchannel on a common substrate and the multilayer design (right) comprises a digital microfluidic array patterned on a top substrate mated to a network of microchannels in a glass substrate below. Side-view schematics and aerial picture of multilayer interface were reproduced with permission from [39] Copyright © 2010 The American Chemical Society, and aerial picture of side-to-side configuration was reproduced with permission from [40] Copyright © 2008 The Royal Society of Chemistry.

Another recent trend for digital microfluidic device design is integration with microchannels. For example, "hybrid microfluidics"[39,40] combines digital microfluidics for sample processing with microchannels for separations. The Wheeler group developed a side-on configuration of hybrid microfluidics,[40] which comprises a one-plate digital microfluidic device mated to a PDMS microchannel (Figure 1.2d, left). Devices formed in this manner were demonstrated to be useful for applications such as in-line sample labelling with fluorogenic reagents followed by separations. A multilayer configuration was then developed[39] (see Chapter 4) which comprises a two-plate digital microfluidic substrate on a top layer mated to a network of channels on a bottom layer (Figure 1.2d, right). This more elegant format facilitates the implementation of complex processing regimens (e.g., multi-enzyme digestion of a proteomic sample) followed by electrophoretic separations. A similar strategy was reported by Gorbatsova et al.[41], who mated samples controlled by digital microfluidics to the inlet of an external capillary for separations. In on-going work, methods are being developed to couple digital microfluidics with integrated nanoelectrospray ionization emitters for direct analysis by mass spectrometry.[42] Given the myriad applications requiring sample pre-processing and chemical separations, hybrid microfluidics and related techniques have the potential to become a useful new strategy for micro total analysis systems.

1.4 Digital Microfluidic Applications in Chemistry

The format of digital microfluidics, in which droplets can be used as individually addressable microreactors, seems well suited for chemical synthesis. This assertion was greatly strengthened when Chatterjee et al.[25] demonstrated the capacity to actuate organic solvents including acetone, acetonitrile, ethanol, dichloromethane and others. In an early demonstration of chemical applications in digital microfluidic format, Millman et al.[43] synthesized a wide variety of different kinds of micro-particles, including capsules, semiconducting microbeads, and anisotropic striped and "eyeball" particles (Figure 1.3a). Droplets containing suspensions of micro/nano particles, polymer solutions, and polymer precursors were merged, mixed, and dried to yield the different types of particles. In the most unique design ("eyeball" beads), darker microparticles (forming the "iris") were driven to the droplet surface by internal convection currents induced by evaporation. In another example of synthesis applications on digital microfluidc devices, Dubois et al.[44] implemented Grieco's reaction using ionic liquid droplets as

microreactors to synthesize tetrahydroquinolines. In this reaction (scheme 1), a task-specific onium salt (1) is reacted with benzaldehydic derivatives (2a-c) and excess indene (3) in ionic liquid matrix ([tmba][NTf2]) to obtain tetrahydroquinolines (4a-c), see Figure 1.3b . Ionic liquids are advantageous for this application because of their low vapor pressure – reactions can be implemented in small droplets (<1 μL) on single-plate devices with no evaporation. In addition, ionic liquids have other advantages for use with digital microfluidics, such as intrinsic conductivity and thermal stability.

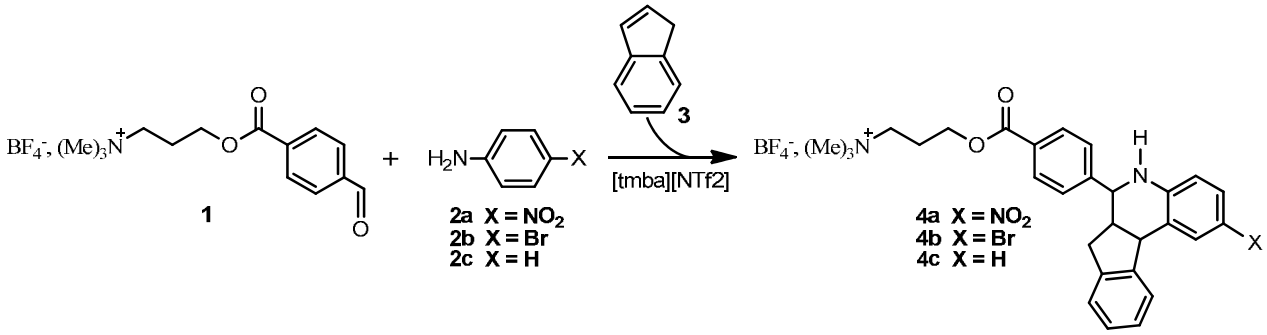

Scheme 1.1 Synthesis of tetrahydroquinolines in ionic liquids by Grieco reaction.[44]

The studies described above established the compatibility of digital microfluidics with chemical synthesis; however, they used fairly simple devices that were capable of carrying out only a single, serial reaction (with no dispensing, splitting, active mixing, or flexibility in droplet volumes). I recently introduced the first two-plate digital microfluidic platform for chemical synthesis that is suitable for control of many different multi-component, multi-step reactions in parallel[19] (see Chapter 2). The platform was used to carry out synchronized synthesis of five peptide macrocycles from three different components followed by late-stage modification with thiobenzoic acid 5 to generate aziridine ring-opened products. The digital microfluidic device featured ten reagent reservoirs and eighty-eight actuation electrodes dedicated to dispensing, merging, and mixing droplets of reagents and products.

In comparison with other miniaturized fluidic technologies (e.g., enclosed microchannels), digital microfluidics is particularly well-suited for applications in synthesis, as digital microfluidics allows for precise control over multiple reagent phases. Moreover, there are no limits (nL - mL) on the volume of solvent used to re-dissolve a particular solid. This stands in contrast to microchannels, in which volumes are defined by channel dimensions and cannot be changed.

The most useful features of digital microfluidics for synthesis include individual addressing of all reagents with no need for complex networks of microvalves,[45,46] chemically inert Teflon-AF-based device surfaces that facilitate the use of organic solvents and corrosive chemicals, and easy access to reasonably large amounts of products for off-chip analysis. On the other hand, digital microfluidics is not appropriate for all synthetic applications; for example, reactions performed at high temperature and pressure that require in-line purification are better suited for closed microchannel systems[47] and there are several unique advantages associated with modular continuous flow reactors formed in microchannels (also known as mesofluidics[1,48]). Nevertheless, as a synthetic platform, digital microfluidics is under-used relative to its advantages and has tremendous room for innovation.

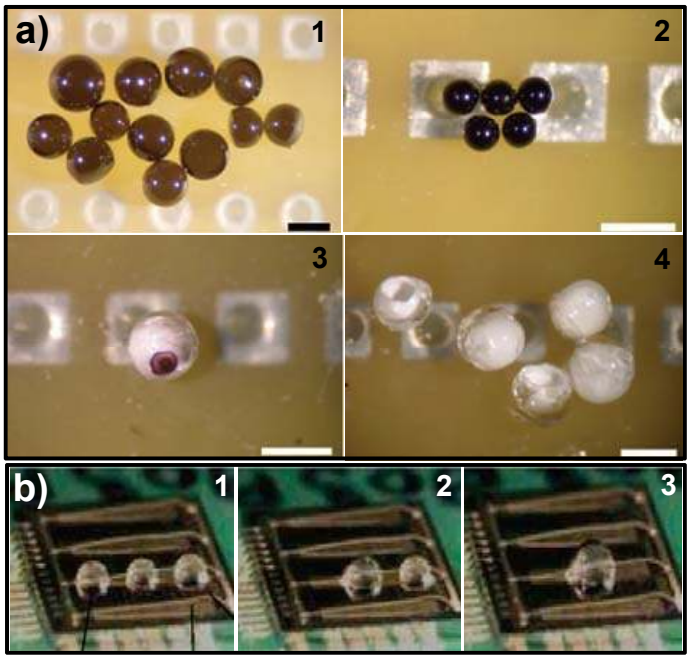

Figure 1.3 Digital microfluidic applications in chemistry. a) Pictures depicting microparticles synthesized using digital microfluidics. The products include conductive gold/SU-8 particles (1), semiconducting polypyrrole particles (2), "eyeball" microbeads (3), and cup-shaped particles formed by drying water droplets that were originally encapsulated in latex (4). Scale bars are 1 mm; reprinted with permission from [43] Copyright © 2005 Nature Publishing Group. b) Pictures depicting synthesis of tetrahydroquinolines in ionic liquids by digital microfluidics. The process includes merging three ionic liquid droplets containing task-specific onium salt, benzaldehydic derivative and excess indene (1-3). Reproduced with permission from [44] Copyright © 2009 The American Chemical Society.

1.5 Digital Microfluidic Application in Biology

Digital microfluidics is an attractive platform for biological applications, which often require the use of expensive or precious reagents. However, a non-trivial challenge is non-specific adsorption of biological molecules to device surfaces (or fouling), which can lead to sample loss, cross-contamination, or droplet sticking (which renders devices useless). Several strategies have been developed to overcome this problem. Srinivasan et al.[49] demonstrated that fouling could be minimized by suspending droplets in an immiscible oil, which facilitates manipulation of a variety of fluids containing high concentrations of potential surface fouling molecules (i.e., blood, serum and plasma). Oil is not compatible with all applications, and an alternative strategy is to mix samples and reagents with low concentrations of amphiphilic polymer additives, which facilitates the actuation of serum and other concentrated biochemical reagents with reduced fouling.[50] Finally, a third technique is to use a removeable hydrophobic insulator, such that each successive experiment is implemented on a fresh device surface.[51] These advances and others have made digital microfluidics compatible with a wide range of applications in biology, including proteomics, enzyme assays and immunoassays, applications involving DNA, cell-based assays, and clinical applications. These topics are reviewed below.

1.5.1 Proteomics

Proteomic experiments typically require tedious, multi-step sample processing prior to analysis by mass spectrometry, and the capacity of digital microfluidics for individual addressing of many reagents simultaneously makes it a good fit for such processes. In an early demonstration of proteomics in a DMF format, the Garrell and Kim groups developed DMF-based methods to purify peptides and proteins from heterogeneous mixtures.[52,53] The methods comprised a series of steps, including drying the sample droplet, rinsing the dried spot with DI water droplet to remove impurities, and finally delivering a droplet of matrix assisted laser desportion/ionization (MALDI) matrix to the purified proteins for analysis on-chip by mass spectrometry. The same team then improved upon this process by implementing simultaneous purification of 6 samples (Figure 1.4a).[37] Recently, I developed a DMF-based protocol for extracting and purifying proteins from complex biological mixtures by precipitation, rinsing, and resolubilization (see Chapter 3) [17]. The method had comparable protein recovery efficiencies (≥80 %) relative to conventional techniques, combined with the advantages of no centrifugation,

and 2x faster extraction and purification. In a separate study, Luk et al.[54] applied DMF to key proteomic processing steps that commonly follow protein extraction, including protein reduction, alkylation, and digestion. Peptide mixtures processed in this manner were analyzed off-chip by MALDI-MS, and identified by Mascot database search engine yielding correct sample identifications with confidence levels >95%. In related work, Garrell's group demonstrated on-chip protein biochemical processing combined with *in situ* analysis by MALDI-MS,[55] and were able to speed the rates of biochemical processes by introducing localized Joule heating.[56] For a complete proteomic sample workup, I developed an automated DMF-based platform integrating all common processes, including protein precipitation, rinsing, resolubilization, reduction, alkylation, and digestion[57] (see Appendix 2).

1.5.2 Immunoassays and Enzyme Assays

Immunoassays and enzyme assays are routinely used to detect analytes in biological samples with high selectivity, and the former (immunoassays) has recently emerged as a good match for DMF. Sista et al.[58] reported a droplet-based magnetic bead immunoassay using digital microfluidics to detect insulin and interleukin-6. In this work, a droplet of analyte and a second droplet containing magnetic beads (modified with primary capture antibodies), blocking proteins, and reporter antibodies were merged to form capture antibody–antigen–reporter antibody complexes. A magnetic field was then used to immobilize the beads such that the supernatant could be driven away by DMF. Close to 100% bead recovery was realized after 8000-fold dilution-based washing of the supernatant. The beads were then resuspended in a new buffer droplet and the analytes were detected by chemiluminescence. The assay had low detection limits: less than 10 pmol L^{-1} and 5 pg mL^{-1} for insulin and interleukin-6. In a separate study, the same group implemented a similar method to perform immunoassays for cardiac troponin I in whole blood in less than 8 minutes.[59] Recently, Miller et al.[60] developed a digital microfluidic platform for similar immunoassay applications[60] without the requirement for beads or magnets. As shown in Figure 1.4b, the method relied on device surfaces modified with spots of capture antibody (Fc-specific anti-human IgG), which binds antigens in the droplet sample, which is in turn recognized by detection antibodies.

Enzyme assays have long been a popular target for digital microfluidics. In one of the first reports, Taniguchi et al.[61] demonstrated a bioluminescence assay for ATP using the enzyme,

luciferase. In another early report, the Fair group developed an automated glucose assay compatible with a range of physiological fluids (serum, saliva, plasma, and urine) on a DMF device.[36] Droplets of glucose oxidase were merged with sample droplets spiked with glucose, then mixed, and the glucose concentration was measured using an integrated LED/photodiode detector. Nichols and Gardeniers[62] carried time-sensitive measurement-using DMF to mix reagents and MALDI time-of-flight mass spectrometry to investigate pre-steady-state kinetics of the enzyme, tyrosine phosphatase. Miller et al.[63] applied DMF to the study of enzyme kinetics by mixing and merging droplets of alkaline phosphatase with fluorescein diphosphate on a multiplexed DMF device (Figure 1.4c). Enzyme reaction coefficients, K_m and k_{cat}, generated by DMF agreed with literature values, and the assays used much smaller volumes and had higher sensitivity than conventional methods. Finally, Martin et al.[64] described initial steps for constructing artificial Golgi organelle through the use of DMF, recombinant enzymes, and magnetic nanoparticles.

1.5.3 Applications Involving DNA

Handling, purifying, detecting, and characterizing samples of DNA have become critical steps for a wide range of basic and applied fields of science. Thus, it is not surprising that such processes have been an attractive match for DMF. For example, Miller et al. demonstrated the first of these processes, DNA handling and purification, using digital microfluidics to implement liquid-liquid extraction of a heterogenous mixture of DNA and proteins.[21] In this work, All-Terrain Droplet Actuation (ATDA) was used to drive aqueous droplets containing a mixture of DNA and proteins into and out of a pool of phenolic oil, which had the effect of removing proteins from the droplet and purifying the nucleic acid. A second application, repair of oxidized lesions in oligonucleotides, was implemented in DMF format by Jary et al.[65] In this work, droplets containing a DNA repair enzyme and damaged DNA were merged by DMF, incubated, and then the repaired DNA was detected by fluorescence microscopy. Liu et al.[66] demonstrated a similar application, in which a DMF device was developed to facilitate DNA ligation by merging droplets containing vector DNA and the enzyme, DNA ligase. In a different application, Malic et al.[67] carried out on-chip immobilization of thiolated DNA probes followed by hybridization with droplets containing complementary oligonucelotide target sequences. Surface plasmon resonance

imaging measurements revealed a two-fold increase in the efficiency of DNA immobilization under an applied potential in comparison to passive immobilization.

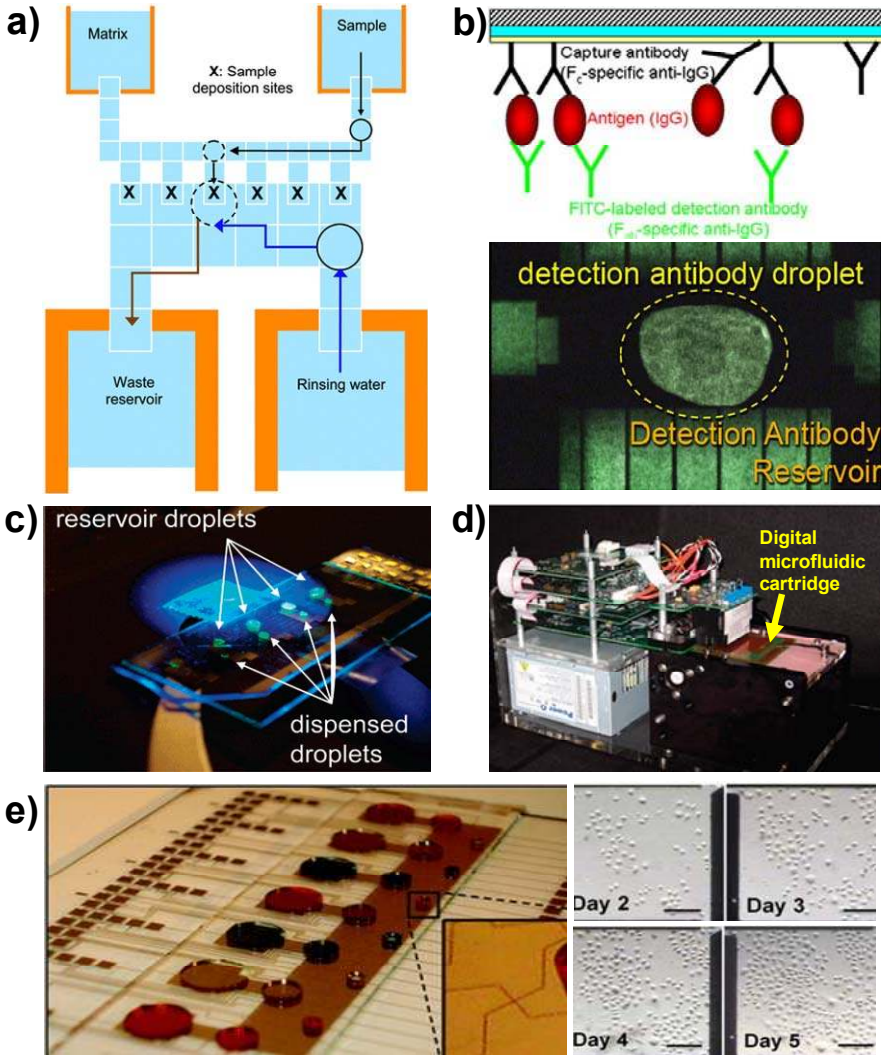

Figure 1.4 Digital microfluidic applications in biology. a) Schematic of a digital microfluidic device used to perform multiplexed proteomic sample de-salting. Reproduced with permission from [37] Copyright © 2006 The Royal Society of Chemistry. b) Schematic (top) depicting an IgG sandwich immunoassay, and picture (bottom) a droplet containing detection antibody (FITC-labeled anti-IgG). Reproduced with permission from [60] Copyright © 2011 Springer. c) Picture of a multiplexed digital microfluidic device used to study enzyme kinetics. Reproduced with permission from [63] Copyright © 2008 The American Chemical Society. d) Picture of self-contained digital microfluidic system for multiplexed real-time PCR. Reproduced with permission from [68] Copyright © 2010 The American Chemical Society. e) Pictures of a digital microfluidic platform developed for complete cell culture (left) and sequence of frames (right) from a movie illustrating HeLa cells on a device from day 2 to day 5 of culture. Reproduced with permission from [35] Copyright © 2010 The Royal Society of Chemistry.

The most complete DNA application using DMF was initially reported by Chang et al.,[69] who implemented the polymerase chain reaction (PCR). In this work, a digital microfluidic device with an embedded micro-heater was developed to facilitate thermal cycling. The fluorescent signals from DNA amplified on-chip were comparable to those generated using a bench-scale PCR machine with 50% and 70% reductions in total time and sample consumption, respectively. Sista et al.[59] improved on this technique, performing a 40-cycle real-time PCR in 12 minutes by shuttling droplet through two different temperature zones on a DMF cartridge capable of accommodating other assays (immunoassays and sample preparation). More recently, Pollack and coworkers expanded on this technique to develop an automated and self-contained multichannel DMF platform for multiplexed real-time PCR assays [68]. The entire system is the size of a shoebox and comprises all of the required control and detection capabilities, and a disposable microfluidic cartridge in which sample processing and PCR takes place (Figure 1.4d). The system has an amplification efficiency of 94.7% and is capable of detecting the equivalent of a single genome of test samples (methicillin-resistant *S.aureus*). As a proof-of-concept for high-throughput multiplexed PCR applications, the authors demonstrated that multiple DNA samples could be amplified and detected simultaneously.

1.5.4 Cell-Based Assays

Cell-based assays have been a popular target for miniaturization, as the reagents and other materials are often prohibitively expensive. Despite this obvious match, cell-based assays have only recently been embraced by the DMF community: in the past two years, five papers have been published describing DMF applications involving cells.[35,70-73] In the first,[70] Barbulovic-Nad et al. implemented a toxicity assay in which droplets carrying Jurkat-T cells were merged with droplets containing different concentrations of the surfactant Tween 20 (lethal to cells) and were then merged again with droplets carrying viability dyes. The DMF assay was more sensitive than an identical one performed in a 384-well plate, such that the DMF-generated results gave a better approximation of the empirical value of the 100% lethal concentration, and also had a 30x reduction in reagent consumption. Additionally, actuation by DMF was found to have no significant effects on cell vitality. This agrees with the second DMF/cell study, in which Zhou et al.[71] reported no increase in number of dead osteoblasts after droplet actuation. In the third study, Fan et al. used dielectrophoresis to separate neuroblastoma cells to different regions of droplets

that were manipulated by digital microfluidics.[72] The original droplets were then split into daughter droplets containing different cell densities. In the fourth study, Shah et al. developed an integrated DMF-lateral field optoelectronic tweezer microfluidic device for cell handling.[73] Finally, Barbulovic-Nad et al.[35] recently developed the first microfluidic platform capable of implementing all of the steps required for mammalian cell culture—cell seeding, growth, detachment, and re-seeding on a fresh surface.[35] The new DMF technique demonstrated cell growth characteristics comparable to those found in conventional tissue culture and were used for on-chip transfection of cells (Figure 1.4e).

1.6 Digital Microfluidic Applications in Medicine

The precise control over different reagents, phases, and volumes afforded by digital microfluidics makes it a good match for applications in medicine. In an important first step towards this aim, the Fair group developed a series of glucose assays in physiological fluids (serum, saliva, plasma, and urine) with actuation by digital microfluidics[36] (see Figure 1.5a). More recently, Sista et al.[59] developed a digital microfluidic technique to extract DNA from whole blood samples using magnetic beads with integrated analysis with immunoassays and PCR, see Figure 1.5b. Recently, I reported a digital microfluidic-driven method for sample clean-up and extraction of estradiol (the most biologically active form of estrogen) in 1 μL samples of human breast tissue homogenate, as well as from whole blood and serum[18] (see Chapter 5). In a typical assay, a sample was chemically lysed, the estradiol extracted into a polar solvent, unwanted constituents extracted into a nonpolar solvent, and the extract was delivered to a collection reservoir for off-chip analysis (Figure 1.5c). The digital microfluidic method used a sample size that is 1000-4000x smaller than the conventional methods for extraction and quantification of steroids, and was 20-30x faster. Similar advantages are leveraged in a new digital microfluidic technique for analyzing newborn blood samples for screening for metabolic disorders.[42] This new method is integrated with hybrid microfluidics and an integrated nanoelecrospray ionization emitter for direct detection by mass spectrometry, which results in analysis techniques that are faster and more efficient than the state-of-the-art (see Chapter 6).

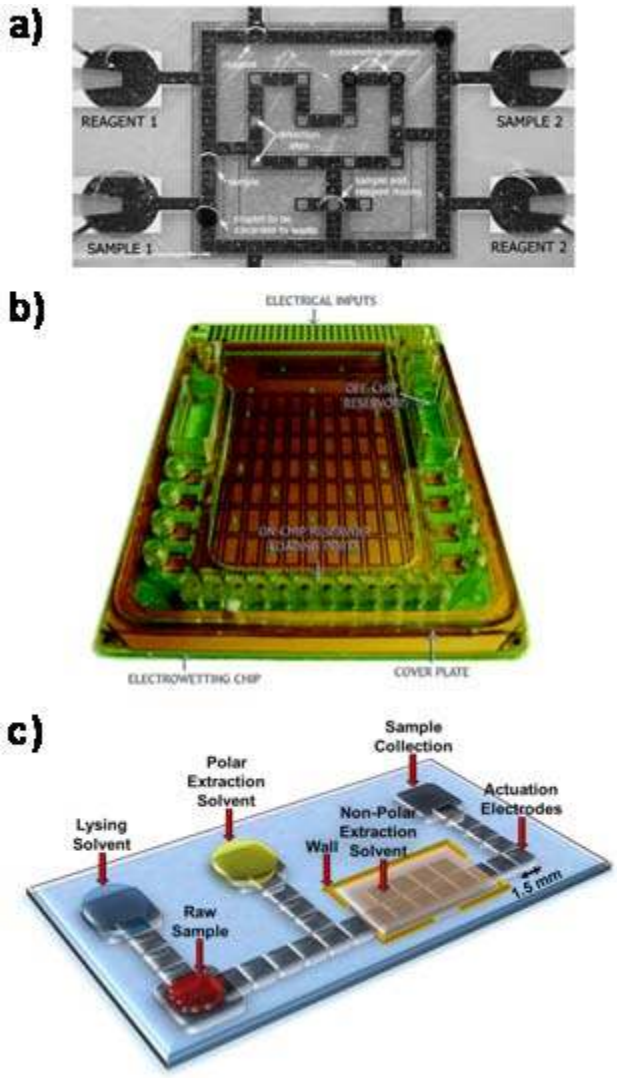

Figure 1.5 Digital microfluidic applications in medicine. a) Picture of digital microfluidic device used to perform glucose assays. Reproduced with permission from [36] Copyright © 2004 The Royal Society of Chemistry. b) DMF cartridge capable of performing magnetic bead-based immunoassays, PCR, and sample preparation. Reproduced with permission from [59] Copyright © 2008 The Royal Society of Chemistry. c) Schematic of DMF device for extracting and purifying estrogen from 1 µL human breast tissue homogenate, whole blood and serum. The device includes sample and solvent reservoirs, and a liquid-liquid extraction zone (bounded by a photoresist wall). Reproduced with permission from [18] Copyright © 2009 The American Association for the Advancement of Science.

1.7 Miscellaneous Applications

The unique characteristics of digital microfluidics have made the technology attractive for a diverse set of applications that do not fit into any of the categories described above. For example, Zhao et al.[74] manipulated air bubbles, instead of droplets, on digital microfluidic devices, and used these bubbles to effect a chemical reaction between gaseous reagents. Moon et al.[75] used digital microfluidics to form a conveyer system by placing a piece of thin silicon wafer

on top of four water droplets that were moved on a track of electrodes (Figure 1.6a). In another creative marriage of technology and application, droplets controlled by digital microfluidics were used to collect particles from surfaces of perforated microfilter membranes, which may be useful for sampling bioaerosols for environmental applications as shown in Figure 1.6b.[76] Finally, Polous et al.[77] developed an integrated digital microfluidic device bearing thin-film Ag/AgCl electrodes for the formation and analysis of lipid bilayer membranes (Figure 1.6c). In this work, aqueous droplets surrounded by a lipid-containing organic oil were moved close to each other and lipid bilayer formation at the interface was measured using electrochemical techniques.

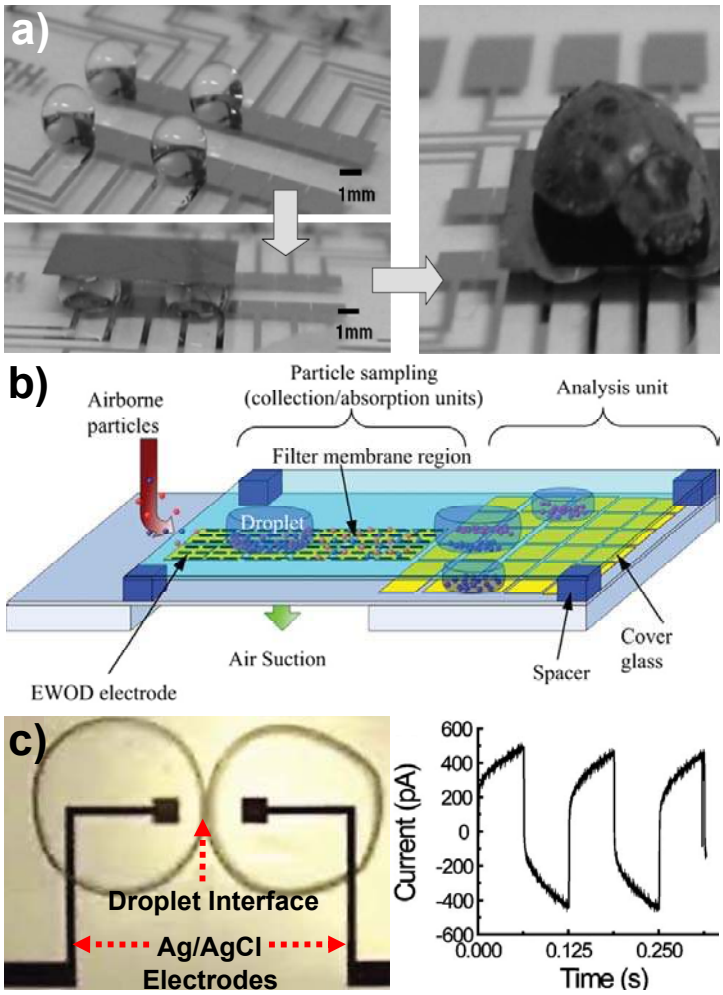

Figure 1.6 Miscellaneous applications of digital microfluidics. a) Pictures of a micro-belt conveyer system based on digital microfluidics; the picture on the right shows a lady bug carried on a silicon wafer supported by 4 droplets. Reproduced with permission from [75] Copyright © 2006 Elsevier B.V. b) A schematic of a digital microfluidic-powered monitoring system for airborne particle sampling and analyses. Reproduced with permission from [76] Copyright © 2009 IOP Publishing. c) Picture (left) of a digital microfluidic device integrated with Ag/AgCl electrodes positioning two aqueous droplets (surrounded by lipid-containing organic phase) in contact, and electrical measurnment (right) of bilayer formation at the droplets interface by electrodes. Reproduced with permission from [77] Copyright © 2009 American Institute of Physics.

1.8 Conclusion

As a lab-on-a-chip technology, digital microfluidics is making unique contributions in the fields of chemistry, biology and medicine. This success is a result of the advantages it offers, including the ability to manage reagents in an assay individually with no cross-talk, capacity to control liquids relative to solids and compatibility with a wide range of volumes. However, this technology is still in its infancy and this thesis presents work utilizing digital microfluidics solely and in combinations with the traditional microfluidic format (i.e., microchannels) to address key issues in the fields of chemistry (e.g., miniaturized chemical synthesis), biology (e.g., proteomics) and medicine (e.g., hormone assays and newborn screening).

Chapter 2 Synchronized Synthesis of Peptide-Based Macrocycles by Digital Microfluidics

In this chapter, a new microfluidic technique is reported for synchronized chemical synthesis of peptide-based macrocycles and their analogues. The method relies on digital microfluidics, a technique in which discrete nL-mL droplets of samples and reagents are controlled in parallel by applying a series of electrical potentials to an array of electrodes coated with a hydrophobic insulator. There is significant potential for digital microfluidics for fast and automated synthesis of libraries of compounds for applications such as drug discovery.

2.1 Introduction

There has been considerable interest in peptide-based macrocycles,[78-82] as their topology allows them to resist digestion by exopeptidases while retaining high affinities for their biochemical targets.[81,83,84] Recently, Hili et al. described a novel macrocyclization strategy that is enabled by amphoteric aziridine aldehydes (Scheme 2.1).[85] Peptide macrocycles can now be made with high chemoselectivity from amino acids or linear peptides, isocyanides, and amphoteric aziridine aldehydes in a one-step process. Importantly, the resulting products possess useful structural features that allow specific modification at defined positions. In initial work, serial batches of peptides were formed using conventional macroscale synthetic techniques. The utility of this method is limited, however, without a high-throughput approach for generating focused libraries of peptide macrocycles. Such a method would be automated and would enable multistep reactions to be handled in parallel. Herein, a new miniaturized technique for synchronized on-chip synthesis of peptide macrocycles and related products is presented.

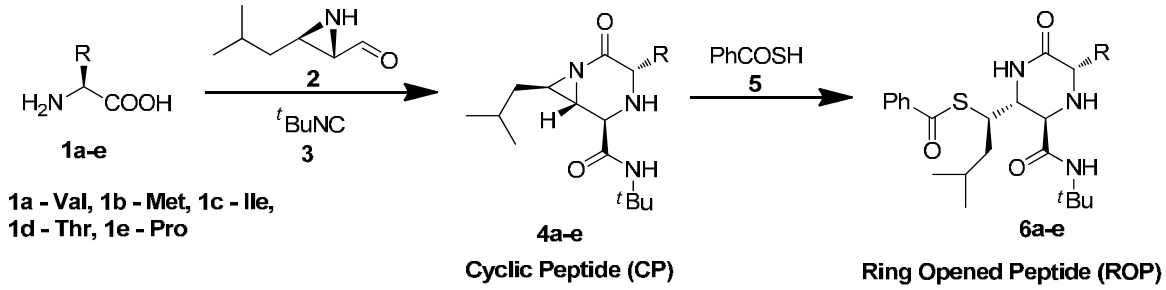

Scheme 2.1 Synthesis of peptide-based macrocycles and their ring-opened peptide derivatives.

The most common format for miniaturized synthesis is enclosed microchannels in planar platforms. Such systems have been used for conventional organic synthesis,[4,46,86-88] polymerization reactions,[89,90] formation of biomolecules, such as peptides and DNA,[91-93] and generation of nanoparticles and colloids.[3,94,95] However, there are some challenges that limit the scope of their use for parallel chemical synthesis. For example, many microchannel platforms are formed from poly(dimethylsiloxane), a material that is susceptible to degradation in common organic solvents.[96,97] Furthermore, control of many reagents simultaneously (a feature required to implement parallel synthetic reactions) in microchannels requires pumps, tubing, valves, and/or three dimensional channel networks that can be difficult to fabricate and operate.[45,46] This has

prompted researchers to develop specialized techniques[98,99] to overcome this limitation. Another disadvantage associated with the microchannel format is the challenge inherent in the removal of solvents and re-dissolution of solids that are common steps in synthesis. Solid reagents and products can clog microchannels, making targeted reagent delivery difficult to control. Finally, the small volumes of samples in microchannels makes it difficult to recover them in sufficient quantities for off-line analysis techniques, such as NMR spectroscopy.

In need of a platform capable of generating a) peptide macrocycles for downstream transfer onto functionalized surfaces, and b) spatially resolved macrocyclic peptide products in the solid state, we implemented an alternative format for automation of synthesis, called digital microfluidics.[14] In digital microfluidics, discrete nL to mL sized droplets of samples and reagents are controlled in parallel by applying a series of electrical potentials to an array of electrodes coated with a hydrophobic insulator (Figure 2.1). Digital microfluidics has become popular for biological and chemical applications, including cell culture and assays,[35,70,100] enzyme assays,[36,49,63] immunoassays,[58,59] protein processing (see chapter 3),[17,37,53-55,57] clinical sample processing and analysis (see chapter 5),[18] and synthesis of anisotropic particles and tetrahydroquinolines.[43,44] The initial synthesis studies[43,44] used simple one-plate devices that are capable of carrying out only a single, serial reaction, with no reagent supply reservoirs, dispensing, splitting, or active mixing. The goal is to implement a fully integrated platform with reagent supply reservoirs, precise control over reagents (i.e., dispensing, splitting, and active mixing), and the capability to precipitate peptide macrocycles for hierarchical modification and analysis.

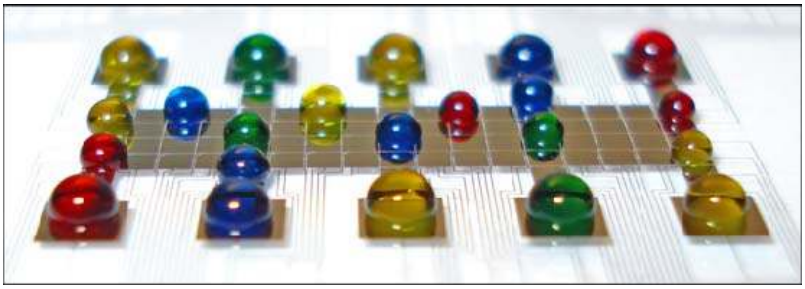

Figure 2.1 A digital microfluidic platform. Each droplet acts as a microvessel in which parallel reactions can take place with no cross-contamination.

In this chapter, the first two-plate digital microfluidic platform for chemical synthesis is used because it is suitable for control of many different multi-component, multi-step reactions in parallel. This system was used to carry out synchronized synthesis of peptide macrocycles from three different components. The resulting products contain aziridines as sites that are primed for specific, late-stage modification by nucleophilic ring-opening. Using the same chemistry, the synthesis of a nine-membered macrocycle was also demonstrated, a ring size that is associated with considerable synthetic difficulties in conventional cyclic peptide synthesis.[101] The new method is fast, amenable to automation, compatible with a wide range of solvents, liberated from external hardware (e.g., pumps, tubing, etc.), and is particularly well-suited for parallel processing.

2.2 Experimental

2.2.1 Reagents and Materials

L-Isoleucine (Ile), L-methionine (Met), L-Proline (Pro), L-Threonine (Thr), L-Valine (Val), proline-leucine (ProLeu), tert-butyl isocyanide (^{t}BuNC), thiobenzoic acid (PhCOSH), trifluoroethanol (TFE), methanol, water, boric acid, 50% formic acid, and fluorinert FC-40, were purchased from Sigma Chemical (Oakville, ON). Deuterated Met (d_3-Met) was obtained from Cambridge Isotope Laboratories (Andover, MA). Aziridine aldehyde was synthesized using method reported previously.[85,102] In all experiments, organic solvents were HPLC grade and deionized (DI) water had a resistivity of 18 Ω at 25°C. Parylene C dimer was from Specialty Coating Systems (Indianapolis, IN), and Teflon-AF was from DuPont (Wilmington, DE).

2.2.2 Device Fabrication and Operation

Digital microfluidic devices were fabricated in the University of Toronto Emerging Communications Technology Institute (ECTI) cleanroom facility, using a transparent photomask printed at Norwood Graphics (Toronto, ON). Glass devices bearing patterned chromium electrodes were formed by photolithography and etching as described elsewhere,[17,57] and were coated with 2.5 μm of Parylene-C and 50 nm of Teflon-AF. Parylene-C was applied using a vapor deposition instrument (Specialty Coating Systems), and Teflon-AF was spin-coated (1% wt/wt in Fluorinert FC-40, 2000 rpm, 60 s) followed by post-baking on a hot-plate (160 ºC, 10 min). The polymer coatings were removed from contact pads by gentle scraping with a scalpel to facilitate electrical contact for droplet actuation. In addition to patterned devices, unpatterned indium tin oxide (ITO) coated glass substrates (Delta Technologies Ltd, Stillwater, MN) were coated with Teflon-AF (50 nm, as above).

The device design featured an array of eighty-eight actuation electrodes (2.2 × 2.2 mm ea.) connected to ten reservoir electrodes (5 × 5 mm ea.), with inter-electrode gaps of 40 μm. Devices were assembled with an unpatterned ITO–glass top plate and a patterned bottom plate separated by a spacer formed from two pieces of double-sided tape (total spacer thickness 180 μm). Reagents were delivered to their respective reservoirs by simultaneously applying potential to reservoir and pipetting the reagent adjacent to the 180 μm gap between the bottom and top plates. Unit droplet and reservoir droplet volumes on these devices were ~900 nL and ~4.5 μL,

respectively. To actuate droplets, driving potentials (70–100 VRMS) were generated by amplifying the output of a function generator (Agilent Technologies, Santa Clara, CA) operating at 18 kHz. As described elsewhere,[17] droplets were sandwiched between the two plates and actuated by applying driving potentials between the top electrode (ground) and sequential electrodes on the bottom plate via the exposed contact pads. To ensure droplet actuation at all times, droplet must be larger than the footprint of home-electrode so that it overlaps its neighbouring electrode. Droplet actuation was monitored and recorded by a CCD camera mounted with a lens.

2.2.3 DMF Synthesis of Peptide-Based Macrocycles and Ring Opened Peptides

To synthesize cyclic peptide-based macrocycles, three 900 nL droplets containing a) amino acid (0.1M in dionized water, 90 nmol), b) aziridine aldehyde (0.05M in trifluoroethanol (TFE), 45 nmol), and c) tert-butyl isocyanide (0.1M in TFE, 90 nmol) were dispensed from their respective reservoirs and merged. The pooled droplet was mixed (20 s, RT) by periodically actuating in a circular motion on four electrodes and then incubated (1 h, RT) in a Petri dish sealed with parafilm to minimize evaporation. After the reaction, macrocycles were obtained by removing the top plate and allowing the solvent to evaporate (15 min, RT). After synthesizing and isolating macrocycles, some samples were re-dissolved in an appropriate solvent and collected by pipette for off-chip analyses, while others were subsequently processed on-chip to form aziridine ring-opened peptides. In the latter case, peptide-based macrocycle products were resolubilized by dispensing four droplets of TFE and driving them to the dried spot (combined volume 3.5 μL, 90 nmol). A droplet containing thiobenzoic acid (0.1M in TFE, 90 nmol) was then dispensed and merged with the resolubilized peptide, and the combined droplet was mixed (20 s, room temperature) and then incubated in a sealed Petri dish (1 h, RT).

The aziridine ring-opened peptides were obtained by removing the top plate and allowing the solvent to evaporate (15 min, RT). For analyses of peptide-based macrocycles and aziridine ring-opened peptides off-chip, isolated samples were resolubilized in 100 μL methanol containing 0.1% formic acid for mass spectrometry, or 250 μL CD_3OD for NMR spectroscopy. The synthesis of the nine-membered macrocycles was similar to that of the macrocycles. The

substrate in this reaction was proline–leucine (0.1m in TFE, 90 nmol), and the reaction required longer incubation (3 h, RT) and frequent mixing (20 s, every 30 min).

2.2.4 Macroscale Synthesis

Peptide-based macrocycle containing methionine (Met) and its aziridine ring-opened derivative were synthesized using methods we reported previously.[85] In brief, for synthesis of peptide-based macrocycle containing Met, in a screw-cap vial equipped with a magnetic stirring bar was added Met (0.2 mmol) and 1 mL of TFE:H_2O (20:1) and stirred until homogeneous solution has been obtained. Aziridine aldehyde dimer (0.1 mmol) and tert-butyl isocyanide (0.2 mmol) were then added sequentially and the resulting mixture was stirred for 1-3 h. For aziridine ring-opened derivative, in a screw-cap vial equipped with a magnetic stirring bar was added peptide-based macrocycle containing Met (0.06 mmol). Solvent (DCM, 0.2 ml) and thiobenzoic acid (0.12 mmol) were then added sequentially and the resulting mixture was stirred for 1 h.

2.2.5 Mass Spectrometry

For analysis by mass spectrometry, reaction products were diluted into methanol containing 0.1% formic acid (~870 μM final concentration of products) and injected into an LTQ linear ion trap mass spectrometer (Thermo Fischer Scientific, Waltham, MA) operating in positive ion mode. Samples were delivered via a fused silica capillary transfer line (100 μm i.d.) mated to a New Objective Inc. (Woburn, MA) nanoelectrospray emitter (100 μm i.d. tapering to 30 μm i.d.). The samples were delivered at a flow rate of 1.5 μL min^{-1}, with an applied voltage of 1.7–1.9 kV and capillary temperature of 170 ºC. Spectra were collected as an average of 50 acquisitions, and data shown here are representative of analysis of samples in triplicate.

2.2.6 Nuclear Magnetic Resonance

For analysis by nuclear magnetic resonance (NMR), concentrated solutions (~7 mM) of peptide-based macrocycle containing Met or its aziridine ring-opened derivative were prepared by re-suspending the reaction products synthesized in a single droplet by digital microfluidics in 12 μL MeOH-d_4. A Protasis CapNMR probe (Savoy, IL) was used for sample injection and ^{1}HNMR spectra were generated using a Varian UnityPlus 500 MHz NMR spectrometer referenced to MeOH-d_4 (3.31 ppm). ^{1}H-NMR spectra were recorded with a spectral window of 10998 Hz, using a 2.4 μs pulse with 45505 real plus complex points acquired with 256 scans. For

analysis of reaction products synthesized by macroscale, ^{1}H spectra were recorded on Varian Mercury 400 MHz spectrometers.

2.2.7 Reaction Rate Analysis

For reaction progress, the reaction rate of Met was analyzed. Two sets of five ~900 nL droplets containing Met (0.1 M) were dispensed on the same device. The first set of droplets were reacted with aziridine aldehyde and tert-butyl isocyanide (as above) for various periods of time (15, 30, 60 and 90 min), and the second set of control droplets were not reacted. After the reactions were completed, the top plate was removed and the two sets of droplets (reaction and controls) were allowed to dry. The solids were resolubilized in 100 μL methanol/water 50:50 ppm containing 250 μM deuterated Met (d_3-Met) as an internal standard, collected in a pipette, and evaluated by MS (as above). % conversion of Met reactant over time was determined by comparing the abundance ratio of the Met:d_3-Met peaks in the spectra of reacted samples to the abundance ratio of the Met:d_3-Met peaks in the spectra of the controls, and subtracting this ratio from 100%. Four replicate measurements were made for each sample and control. An analagous method (with volumes scaled appropriately) was used to evaluate reaction progress of macroscale synthesis.

2.3 Results and Discussion

2.3.1 Device and Peptide-based macrocycles Synthesis

Parallel synthesis of peptide-based macrocycles was implemented on a new digital microfluidic system (Figure 2.2a). The design features ten reagent reservoirs and eighty-eight actuation electrodes dedicated to dispensing, merging, and mixing droplets of reagents and products. The devices were designed to handle ten different reagents, including five amino acids, an aziridine aldehyde, tert-butyl isocyanide (^{t}BuNC), and thiobenzoic acid (PhCOSH) as stock solutions in trifluoroethanol (TFE) or water. As shown in Figure 2.2b, the digital microfluidic device facilitated the implementation of synchronized synthesis of five different macrocycles in three steps. First, five 900 nL droplets containing one of five amino acid substrates (Val, Met, Ile, Thr, and Pro) were dispensed from their respective reservoirs. Second, five 900 nL droplets containing aziridine aldehyde were dispensed and merged with the amino acid droplets and mixed. Third, five 900 nL droplets of tert-butyl isocyanide were dispensed and merged with the droplets containing the amino acids, and incubated. Finally, macrocyclic peptide products were isolated by allowing the solvent to evaporate.

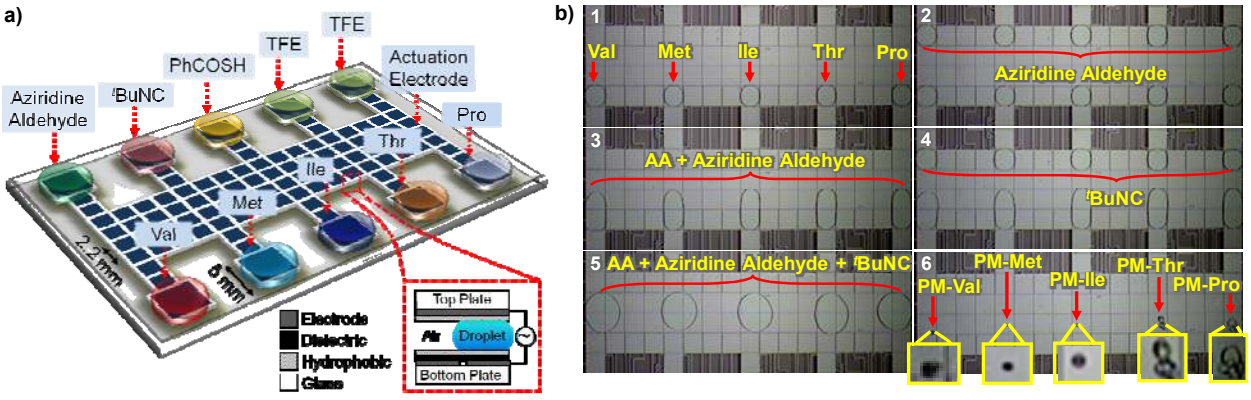

Figure 2.2 a) Top- and side-view schematics of the digital microfluidic device design used for peptide-based macrocycles (PM) synthesis. b) Sequence of frames from a movie illustrating digital microfluidic-based synthesis of PM. In frames 1-3, droplets (~900 nL) containing AA substrates and aziridine aldehyde were dispensed from their respective reservoirs, and merged and mixed. In frames 4-5, droplets of ^{t}BuNC were dispensed and merged with the droplets of AA substrates and aziridine aldehyde, and the reaction was allowed to proceed for 1 h at room temperature. Finally, in frame 6, PM products were isolated by allowing the solvent to evaporate. In these frames, the top plate is not visible, as it is formed from transparent ITO-glass.

Some macrocycles were further modified in three additional steps to form structurally modified products (Figure 2.3). First, each macrocyclic peptide product was re-dissolved in fresh trifluoroethanol. Second, five 900 nL droplets containing thiobenzoic acid were dispensed, and merged with macrocycle droplets, and the reactions were allowed to incubate. Third, the aziridine ring-opened products were isolated by allowing the trifluoroethanol to evaporate, delivering precipitated macrocycyclic peptide thioesters at defined positions. In all, this method constituted thirty processing steps—six steps each for five reactions in parallel.

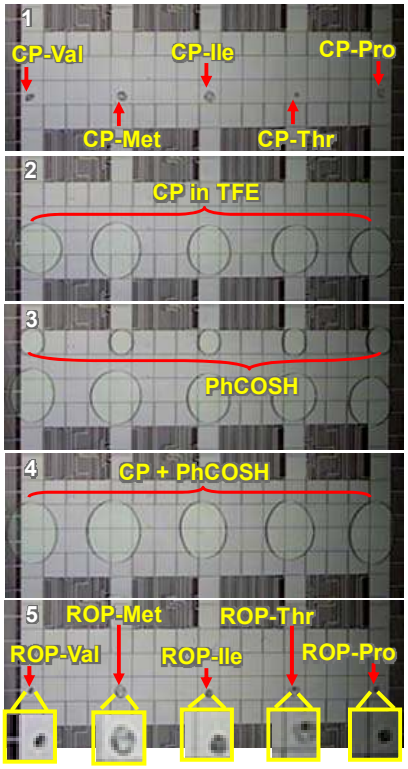

Figure 2.3 Sequence of frames from a movie illustrating the key steps in digital microfluidic-based synthesis of aziridine ring-opened products (ROP). Peptide-based macrocycles (PM) are solubilized in trifluoroethanol (frames 1,2), then merged (frames 3,4) with droplets containing thiobenzoic acid (PhCOSH), and then mixed and incubated for 1 h at room temperature, followed by isolation of RO products (frame 5) by allowing the trifluoroethanol solvent to evaporate.

2.3.2 Mass Spectrometry and Nuclear Magnetic Resonance Analysis

Mass spectrometry (MS) and NMR were used to evaluate the effectiveness of on-chip peptide macrocycle and aziridine ring-opened product synthesis. Figure 2.4 shows representative mass spectra generated from unreacted methionine (Met) and also peptide-based macrocycle-containing Met and its aziridine ring-opened derivative synthesized on a digital microfluidic

device, with peaks at m/z 150, 342, and 480, respectively (mass spectra of the other peptide-based macrocycles and their aziridine ring-opened products are given in Figures 2.5–2.8). The mass spectra of products from the microscale synthesis were nearly identical to those of the same products from macroscale synthesis (Figure 2.9a,b). Complementing the MS data, NMR spectra of the peptide-based macrocycle containing methionine (Figure 2.10) and its aziridine ring-opened derivative (Figure 2.11) synthesized on the digital microfluidic platform and on the macroscale had similar chemical shifts that correlated well with all the protons. The reaction progress was monitored as a function of Met conversion over time on the digital microfluidic platform (Figure 2.4d) and on the macroscale (Figure 2.9c). The reaction kinetics of the two methods were similar, with about 70% (digital microfluidic) and about 90% (macroscale) depletion of the initial reagent within one hour; we anticipate that future systems integrated with continuous, rapid mixing[103,104] will improve the kinetics of the microfluidic technique.

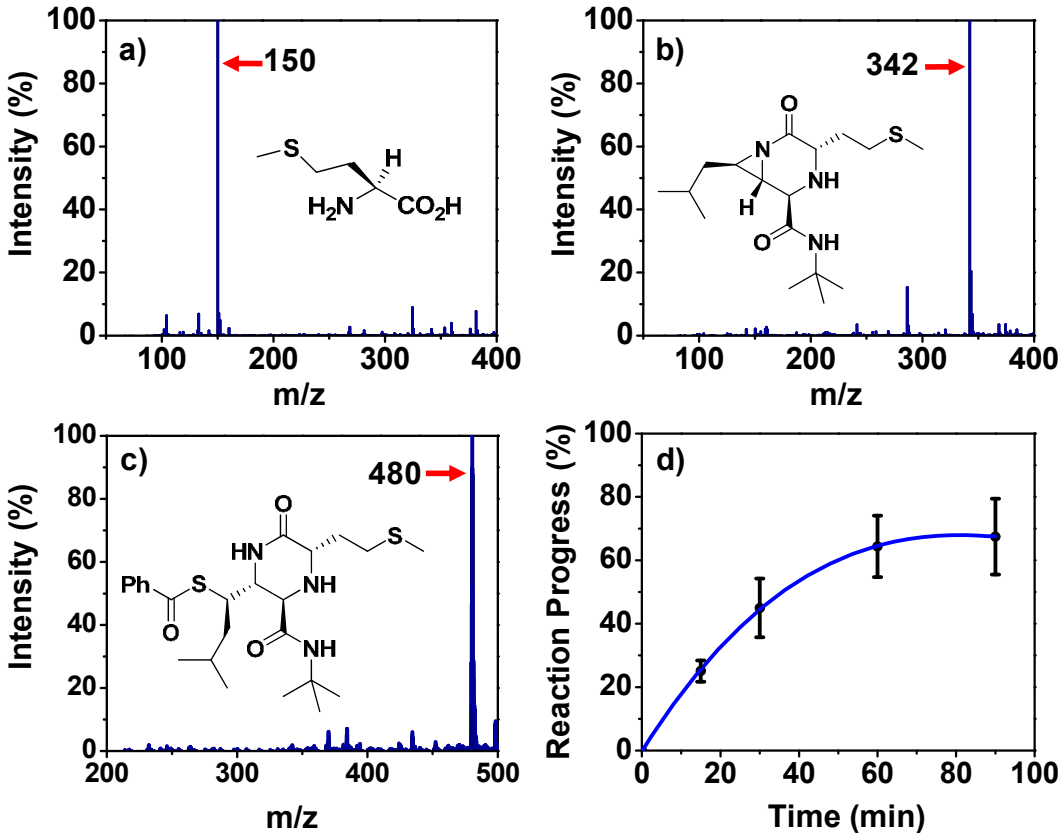

Figure 2.4 ESI-MS spectra of a) methionine (Met), and products synthesized by digital microfluidics, including a b) peptide-based macrocycle containing Met and c) the aziridine ring-opened derivative. d) Reaction progress by digital microfluidics as percentage conversion of Met over time. Each data point represents the mean ± standard deviation of 4 samples.

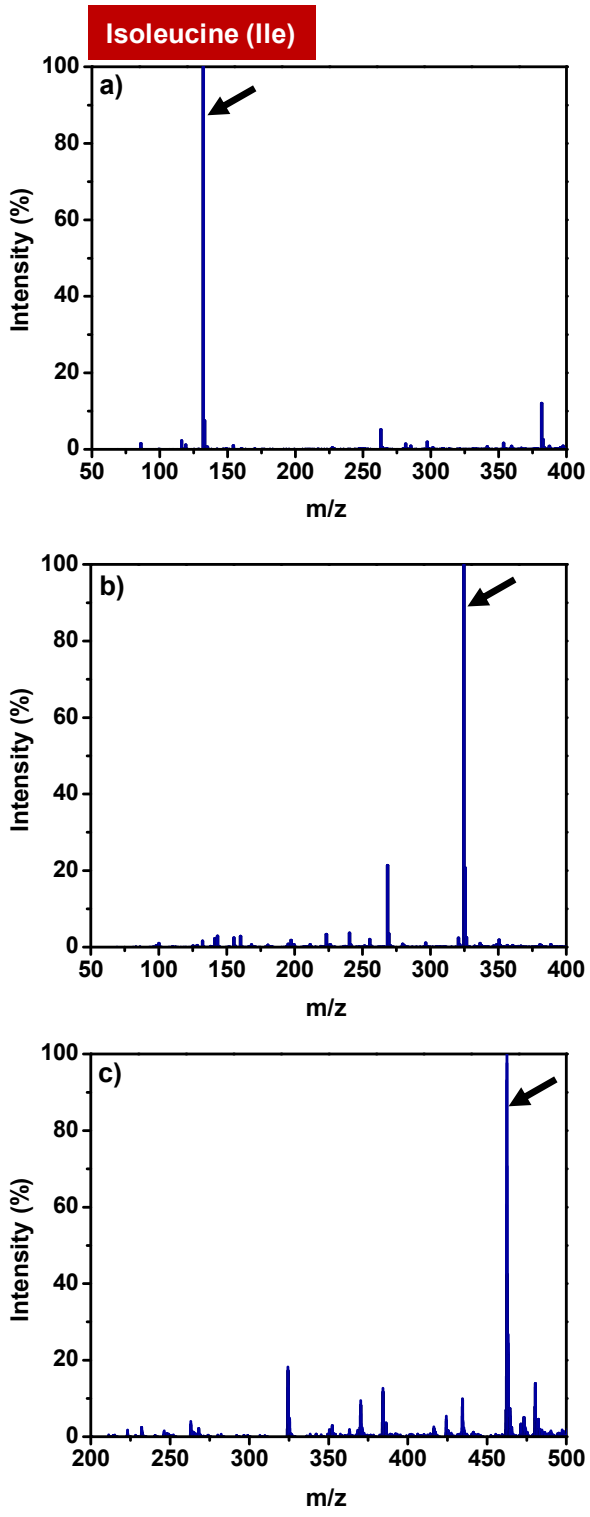

Figure 2.5 ESI-MS spectra generated from a) pure reactant solution of isoleucine (Ile) (m/z 132), b) on-chip synthesized peptide-based macrocycle containing Ile (m/z 324), and c) on-chip synthesized aziridine ring-opened derivative (m/z 462).

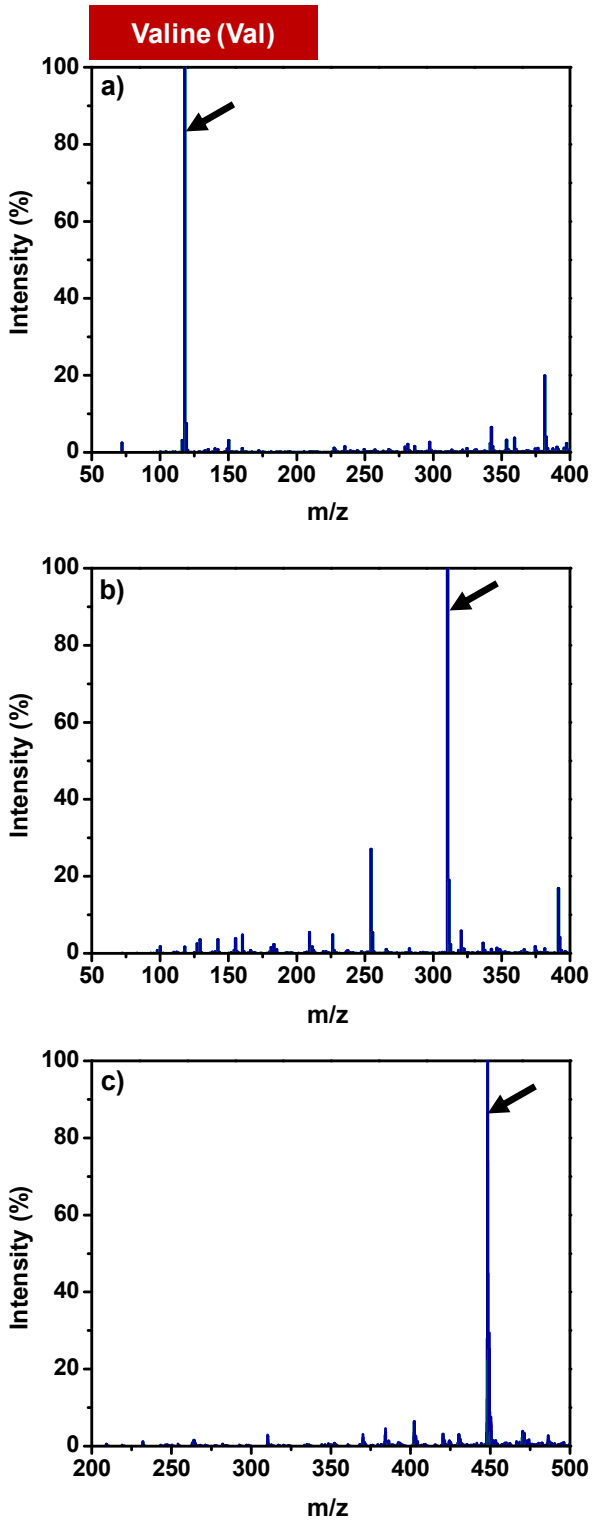

Figure 2.6 ESI-MS spectra generated from a) pure reactant solution of valine (Val) (m/z 118), b) on-chip synthesized peptide-based macrocycle containing Val (m/z 310), and c) on-chip synthesized aziridine ring-opened derivative (m/z 448).

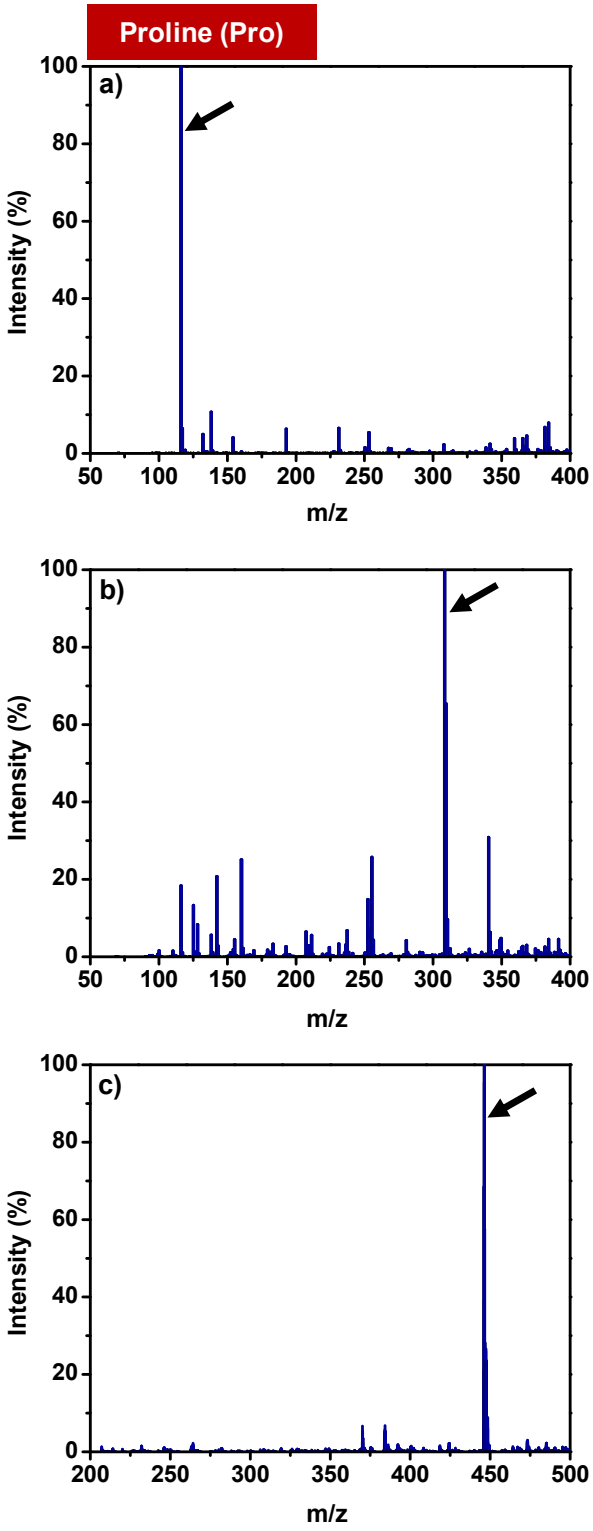

Figure 2.7 ESI-MS spectra generated from a) pure reactant solution of proline (Pro) (m/z 116), b) on-chip synthesized peptide-based macrocycle containing Pro (m/z 306), and c) aziridine ring-opened derivative (m/z 446).

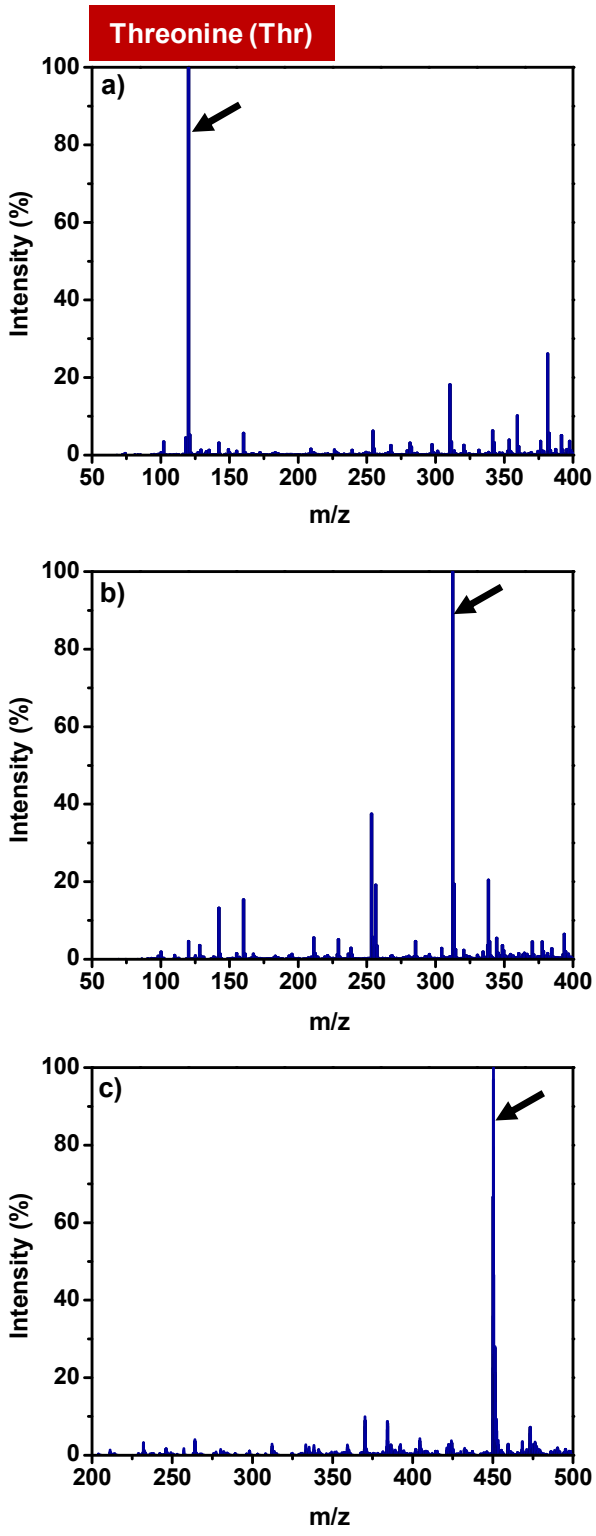

Figure 2.8 ESI-MS spectra generated from a) pure reactant solution of threonine (Thr) (m/z 120), b) on-chip synthesized peptide-based macrocycle containing Thr (m/z 312), and c) on-chip synthesized aziridine ring-opened derivative (m/z 450).

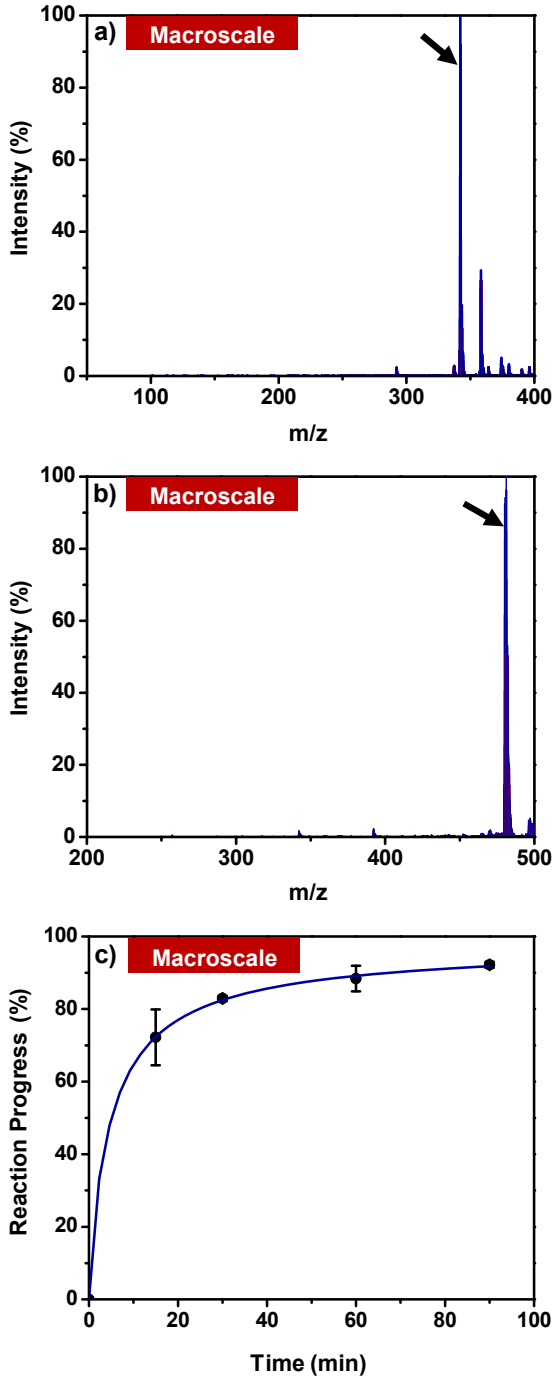

Figure 2.9 ESI-MS spectra of a) macroscale synthesized peptide-based macrocycle containing Met (m/z 342) and b) macroscale synthesized aziridine ring-opened derivative (m/z 480). c) Macroscale reaction progress as % conversion of Met over time. Each data point represents the mean ± S.D. of 4 samples.

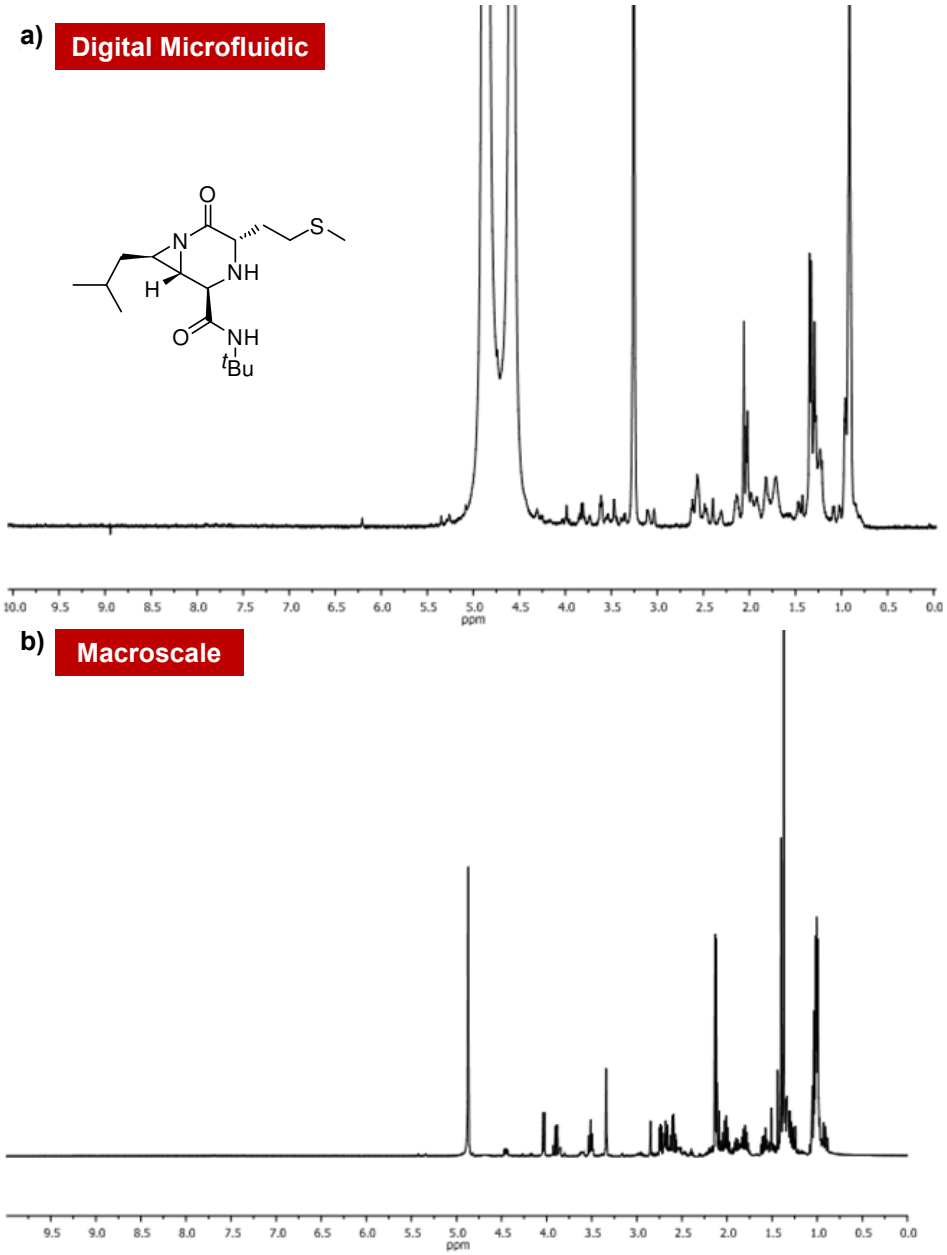

^{1}H NMR δ: 4.42 (ddd, J = 10.0, 4.3, 1.9 Hz, 1H), 4.00 (d, J = 5.9 Hz, 1H), 3.58 (dd, J = 7.7, 4.1 Hz, 1H), 3.48 (dd, J = 8.6, 6.6 Hz, 1H), 2.71 (dd, J = 5.9, 3.7 Hz, 2H), 2.10 (s, 3H), 1.98 (ddd, J = 10.4, 8.0, 4.7 Hz, 2H), 1.87 (m, 2H), 1.77 (m, 1H), 1.34 (s, 9H), 0.98 (d, J = 5.1 Hz, 3H), 0.97 (d, J = 5.0 Hz, 3H) ppm.

Figure 2.10 NMR spectra generated from a) on-chip and b) macroscale synthesized cyclic peptide-Met in MeOH-d4. Below are the chemical shifts of proton.

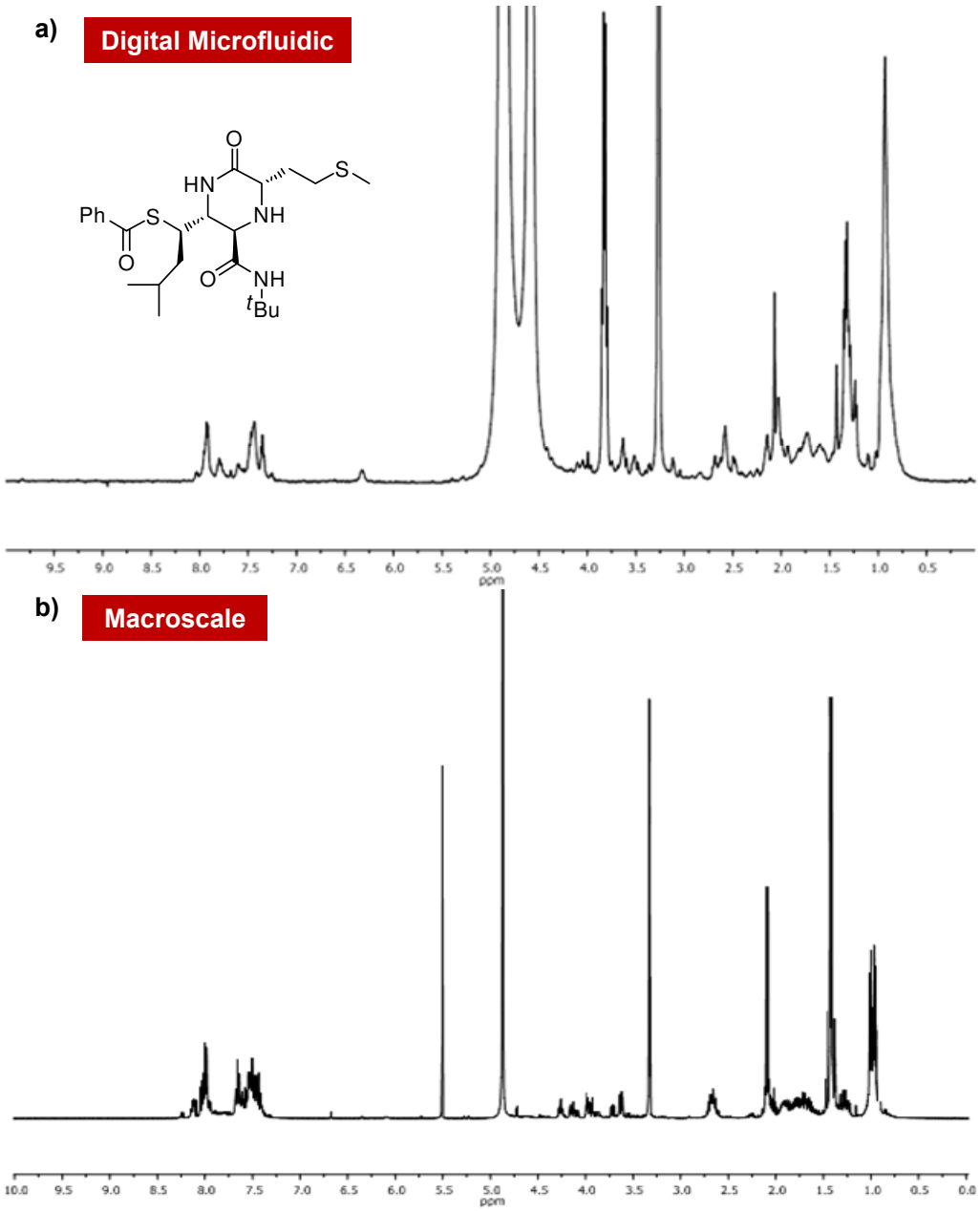

^{1}H NMR δ: 8.09 (m, 2H), 7.58 (m, 2H), 7.41 (dd, J = 8.0, 7.5 Hz, 1H), 4.70 (d, J = 6.7 Hz, 1H), 4.23 (ddd, J = 11.5, 5.8, 2.6 Hz, 1H), 4.13 (t, J = 3.4 Hz, 2 H), 4.10 (t, J = 3.5 Hz, 2 H), 3.60 (dd, J = 10.2, 3.8 Hz, 1H), 2.63 (m, 1H), 2.05 (s, 3H), 1.89 (m, 2H), 1.74 (m, 1H), 1.39 (s, 9H), 0.98 (d, J = 6.4 Hz, 3H), 0.93 (d, J = 6.3 Hz, 3H) ppm.

Figure 2.11 NMR spectra generated from a) on-chip and b) macroscale synthesized ring opened cyclic peptide-Met in MeOH-d4. Below are the chemical shifts of protons.

To further show the application of the technique, a nine-membered macrocycle was synthesized on-chip (Figure 2.12a). In this method, a Pro–Leu-derived macrocycle was prepared in three steps. Droplets of 900 nL volumes containing dipeptide, aziridine aldehyde, and isocyanide were dispensed from respective reservoirs, merged, mixed, and incubated. Figure 2.12b shows a mass spectrum from a Pro–Leu-derived macrocycle synthesized on a digital microfluidic device, which further demonstrates the reaction selectivity. Of note is an exciting possibility offered by this new on-chip conjugation strategy: thioesters are well-known precursors to native chemical ligation.[105]

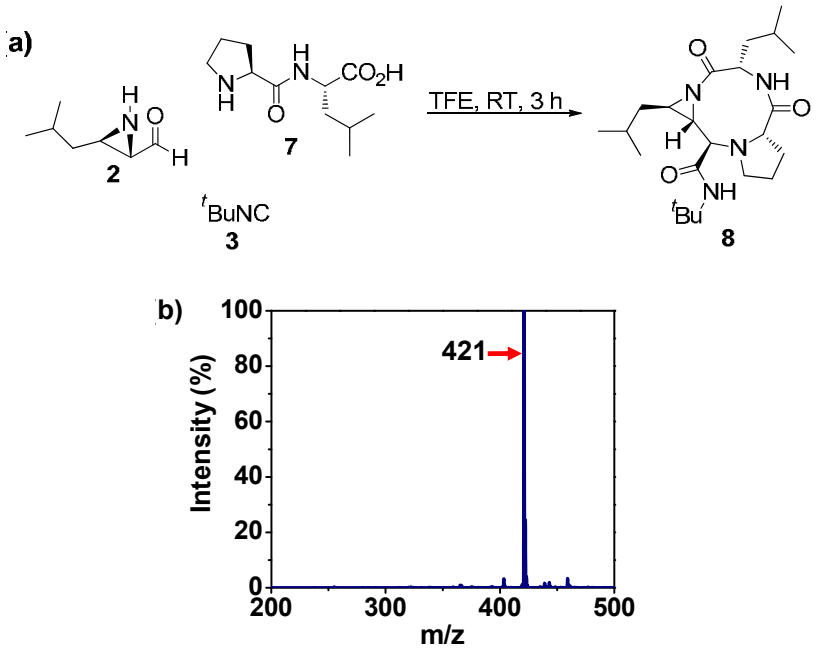

Figure 2.12 a) Synthesis of a nine-membered macrocycle. b) ESI-MS spectrum of 8.

The new digital microfluidic method is capable of synthesizing peptide-based macrocycles and aziridine ring opened derivatives that are analogous to the macroscale method, as shown by MS and NMR results. In comparison with other miniaturized fluidic technologies, digital microfluidics is particularly well-suited for applications in synthesis, as it allows precise control over multiple reagent phases. Importantly, it supports the critical step of solvent removal and re-dissolution of product for further processing (Figure 2.3, frames 1,2). This highlights the flexibility of digital microfluidics: there are no limits on the volume of solvent used to re-dissolve a particular solid (for example, in this method, four droplets of trifluoroethanol

representing a combined volume of 3.5 μL were dispensed to facilitate dissolution of each solid macrocycle). The salient features of digital microfluidics for synthesis include individual addressing of all reagents with no need for complex networks of microvalves,[45,46] a chemically inert Teflon-based device surface that diversifies the scope of compatible reagents to include organic solvents and corrosive chemicals, and easy access to reasonably large amounts of products for off-chip analysis (such as simply removing the top plate on a device). Last but not least, the technique will likely be well-suited for evaluating macrocyclic libraries if the solvent is removed by evaporation.

2.4 Conclusion

In summary, a new microfluidic technique for synchronized synthesis of peptide-based macrocycles and their analogues with side chains appended during aziridine ring-opening was described. The device was designed to handle diverse reagents and thirty reaction steps, and was capable of forming five products in parallel. The multiplexing demonstrated here is likely just the beginning; future systems might be capable of synthesis of tens or hundreds of products simultaneously, which would streamline the formation of spatially addressable crystalline peptide based macrocycles. These advantages suggest a significant potential for digital microfluidics for fast and automated synthesis of libraries of compounds for applications such as drug discovery and high-throughput screening.

Chapter 3 A Digital Microfluidic Method For Protein Extraction by Precipitation

In this chapter, we report the first microfluidic method for extracting proteins from heterogeneous fluids by precipitation. The method comprises an automated protocol for precipitation of proteins onto surfaces, rinsing the precipitates to remove impurities, and resolubilization in buffer for further analysis. The method is compatible with proteins representing a range of different physicochemical properties, as well as with complex mixtures such as fetal bovine serum and cell lysate. In all cases, the quantitative performance (measured using a fluorescent assay for % recovery) was comparable to that of conventional techniques, which are manual and require more time. we believe this work is an important first step towards developing a fully automated microfluidic method for proteomic analyses.

3.1 Introduction

In the post-genome era, proteomics has emerged as the next great scientific challenge. While methodologies vary widely, a near-universal first step for proteomic analyses of physiological samples (e.g., blood, serum, tissue extract, etc.) is removal of the non-relevant solution constituents (e.g., nucleic acids and lipids).[106-109] A common method used to accomplish this task is protein precipitation. In this technique, one or more precipitants (organic solvents, salts, or pH modulators) is mixed with the protein-containing sample, which causes proteins to precipitate and settle to the bottom of the reaction vessel.[106-108,110-113] After centrifuging, removal of supernatant, and washing in appropriate rinse solvents, the precipitate can be re-dissolved, and the now-purified solution can be used for subsequent processing and analysis.

Here, the development of an automated microfluidic method for extracting proteins from heterogeneous fluids by precipitation is described. Although there has been a myriad applications of microfluidic technologies to proteomics,[114] there have been no work describing protein extraction by precipitation in microchannels. Precipitation has been used in channels to remove proteins for analysis of other analytes,[115] but not as a technique to extract and collect proteins for further analysis. This shortfall is a function of complexity and heterogeneity – in protein extraction by precipitation, liquids (samples, precipitants, rinse solutions), solids (precipitates), and vapor phases (air for drying precipitates) all play prominent roles and must be precisely controlled. These requirements seem like a poor match for the conventional format of microfluidics, enclosed microchannels, thus digital microfluidics (DMF) was used for this work.

In DMF, discrete droplets of sample and reagents are controlled (i.e., moved, merged, mixed, and dispensed from reservoirs) by applying a series of electrical potentials to an array of electrodes coated with a hydrophobic insulator.[23,24] Although microchannels can also be used to manipulate droplets, DMF is a distinct paradigm; the principal difference is that in DMF, samples are addressed individually, while in channels, they are controlled in series.[14] DMF has recently become popular for a wide range biochemical applications including cell-based assays,[70] enzyme assays,[36,49,63] protein profiling,[37,52,53] and the polymerase chain reaction.[69] More importantly, the DMF format seems well suited for complex procedures such as protein

extraction by precipitation, as DMF can be used to precisely control liquid-, solid-, and gas-phase reagents in heterogeneous systems.[21,116-118]

In the work described here, we present a DMF-based protocol for extracting and purifying proteins from heterogeneous mixtures, including the key steps of precipitation, rinsing, and resolubilization. The effectiveness of the new method was determined using electrospray ionization mass spectrometry (ESI-MS), and the % recovery was quantified using fluorescence. The method was demonstrated to be compatible with protein standards representing a range of different physicochemical properties, as well as with complex mixtures such as fetal bovine serum and cell lysate. In all cases, the performance of the new method was comparable to that of conventional techniques, with the advantages of automation and reduced analysis time. we believe this may be an important an important first step in efforts to develop a fully automated microfluidic methods for proteomic analyses.

3.2 Experimental

3.2.1 Reagents and Materials

Acetone, acetonitrile (ACN), chloroform, methanol, boric acid, 50% formic acid, fluorinert FC-40, sodium hydroxide, Pluronic F127, trichloroacetic acid (TCA), Triton X-100, phenylmethylsulfonyl fluoride (PMSF), sodium dodecyl sulfate (SDS), fluorescamine, ammonium sulfate, bovine serum albumin (BSA), fibrinogen (Fb), and myoglobin (Mb) were purchased from Sigma Chemical (Oakville, ON). Dulbecco's phosphate buffered saline (PBS) and fetal bovine serum (FBS) were purchased from Invitrogen Canada (Burlington, Ontario). 1,2-Dibutyroyl-*sn*-glycero-3-phosphocholine (PC) was purchased from Avanti Polar Lipids Inc. (Alabaster, AL). In all experiments, solvents of HPLC-grade and deionized (DI) water with a resistivity of 18 MΩ·cm at 25°C were used.

Working solutions of all proteins were prepared in 10 mM borate buffer (pH 8.5) with 0.08% Pluronics F127 (w/v).[50] For qualitative analysis of protein extraction, a test solution containing 0.71 mM protein (Mb) and 62 mM lipid (PC) was prepared. For quantitative analysis of protein recovery, solutions of BSA (50 mg/mL), Mb (30 mg/mL), and Fb (20 mg/mL) were prepared. For experiments involving FBS and cell lysate, solutions were spiked with 0.08 % Pluronics F127. Protein precipitation methods used trichloroacetic acid (TCA) (20% in DI water), acetonitrile (ACN), and ammonium sulfate (saturated solution in DI water) as the precipitants and acetone, chloroform/ACN (70/30 v/v), and chloroform/acetone (60/40 v/v) as rinse solutions.

Clean-room reagents and supplies included Shipley S1811 photoresist and MF321 developer from Rohm and Haas (Marlborough, MA), AZ300T photoresist stripper from AZ Electronic Materials (Somerville, NJ), parylene C dimer from Specialty Coating Systems (Indianapolis, IN), Teflon-AF from DuPont (Wilmington, DE), solid chromium from Kurt J. Lesker Canada (Toronto, ON), CR-4 chromium etchant from Cyantek (Fremont, CA), hexamethyldisilazane (HMDS) from Shin-Etsu MicroSi (Phoenix, AZ), and concentrated sulfuric acid and hydrogen peroxide (30%) from Fisher Scientific Canada (Ottawa, ON). Piranha solution was prepared as a 3/1 v/v mixture of sulfuric acid/hydrogen peroxide.

3.2.2 Cell Culture and Analysis

Jurkat T-cells were maintained in a humidified atmosphere (5% CO_2, 37°C) in RPMI 1640 medium supplemented with 10% fetal bovine serum, penicillin (100 IU mL^{-1}), and streptomycin (100 μg mL^{-1}). Cells were subcultured every 3–4 days at 5×10^5 cells mL^{-1}. Lysing medium was PBS with 0.08% (wt/v) F 127, 1% Triton X-100, and 1 mM PMSF. For precipitation experiments, cells were washed once in PBS, suspended in lysing medium at 6×10^7 cells mL^{-1}, incubated on ice (30 min), and centrifuged (13,000 rpm, 5 min). The supernatant was collected and stored at −80°C until use.

3.2.3 Device Fabrication and Operation

Digital microfluidic devices were fabricated using conventional methods in the University of Toronto Emerging Communications Technology Institute (ECTI) cleanroom facility, using a transparent photomask printed at Norwood Graphics (Toronto, ON). Glass wafers (Howard Glass Co. Inc., Worcester, MA) were cleaned in piranha solution (10 min), and then coated with chromium (250 nm) by electron beam deposition. After rinsing and drying, the substrates were primed by spin-coating with HMDS (3000 rpm, 30 s) and then spin-coated again with Shipley S1811 photoresist (3000 rpm, 30 s). Substrates were pre-baked on a hotplate (100°C, 2 min), and then exposed to UV radiation (35.5 mW cm^{-2}, 365 nm, 4 s) through a photomask using a Karl Suss MA6 mask aligner (Garching, Germany). After exposure, substrates were developed in MF-321 (3 min), and then post-baked on a hot plate (100 °C, 1 min). Following photolithography, substrates were immersed in chromium etchant (30 s). The remaining photoresist was stripped in AZ-300T (10 min). After forming electrodes and cleaning in piranha solution (30 s), substrates were coated with 2.5 μm of Parylene-C and 50 nm of Teflon-AF. Parylene-C was applied using a vapor deposition instrument (Specialty Coating Systems), and Teflon-AF was spin-coated (1 % wt/wt in Fluorinert FC-40, 2000 rpm, 60 s) followed by post-baking on a hot-plate (160 ºC, 10 min). The polymer coatings were removed from contact pads by gentle scraping with a scalpel to facilitate electrical contact for droplet actuation. In addition to patterned devices, unpatterned indium tin oxide (ITO) coated glass substrates (Delta Technologies Ltd, Stillwater, MN) were coated with Teflon-AF (50 nm, as above).

The devices had a double-cross geometry as shown in Fig. 3.1a, with 1 × 1 and 1.5 × 1.5 mm actuation electrodes, 2.5 × 2.5 mm and 3.0 × 3.0 mm reservoir electrodes, and inter-electrode gaps of 40 μm. Devices were assembled with an unpatterned ITO–glass top plate and a patterned bottom plate separated by a spacer formed from one or two pieces of double-sided tape (70 or 140 μm thick). Driving potentials (70–100 VRMS) were generated by amplifying the output of a function generator (Agilent Technologies, Santa Clara, CA) operating at 18 kHz. As described elsewhere,[70] droplets were sandwiched between the two plates and actuated by applying driving potentials between the top electrode (ground) and sequential electrodes on the bottom plate via the exposed contact pads. Droplet actuation was monitored and recorded by a CCD camera mounted on a lens.

3.2.4 Digital Microfluidics-Driven Protein Extraction

Protocols were developed using digital microfluidics to implement protein extraction by precipitation and resolubilization. In each experiment, droplets containing the sample (i.e., protein standards, mixtures, FBS, or cell lysate) and a precipitant were dispensed from their respective reservoirs and merged on the extraction electrode. In some cases, a third droplet containing a secondary precipitant was also dispensed and merged. The combined droplet was allowed to incubate until the protein was observed to precipitate from solution (~5 min, room temperature), after which the supernatant was actuated away from the extraction electrode (to the waste reservoir). The precipitate was then washed by dispensing and driving three droplets of rinse solution across the extraction electrode to waste. The precipitate was dried and a droplet of resolubilization solution was dispensed and driven to the extraction electrode to dissolve the protein. In some cases the precipitate was baked on a hot plate (95°C, 5 min) prior to resolubilization to ensure complete removal of any solvent residue.

The composition of precipitant(s), rinse solutions, and resolubilization solutions were optimized for each analyte by trial-and-error, and are recorded in Table 1. For protocols applied to standards, mixtures, and serum, sample and precipitant droplet volumes were ~140 nL and rinse and resolubilization solution droplet volumes were ~315 nL. For the protocol applied to cell lysate, the corresponding volumes were ~70 and ~158 nL, respectively.

3.2.5 Conventional Protein Extraction

Protein samples were extracted on the macroscale by combining 10 μL of sample with 10 μL chilled precipitant in a microcentrifuge tube. The solution was incubated (5 min, 4 ºC) and then centrifuged (13,000 rpm, 5 min), and the supernatant was discarded. The pellet was washed three times by iteratively suspending in rinse solution (22.5 μL) and centrifuging (13,000 rpm, 5 min) and discarding the supernatant. The final pellet was dissolved in 100 μL. The precipitant, rinse solution, and resolubilization solution for each analyte were identical to those used for DMF.

3.2.6 Mass Spectrometry

Extracts of PC/Mb mixtures were evaluated qualitatively by mass spectrometry. Briefly, 315-nL samples (prepared by DMF as described above) were diluted into 50 μL of 50/50 water/ACN containing 0.1% formic acid and injected into an LTQ linear ion trap mass spectrometer (Thermo Fischer Scientific, Waltham, MA) operating in positive ion mode. Samples were delivered *via* a fused silica capillary transfer line (100 μm i.d.) mated to a New Objective Inc. (Woburn, MA) nanoelectrospray emitter (100 μm i.d. tapering to 30 μm i.d.). The samples were delivered at a flow rate of 0.5 μL min^{-1}, with an applied voltage of 1.7–1.9 kV and capillary temperature of 170ºC. Spectra were collected as an average of 50 acquisitions, and data shown here are representative of analysis of samples in triplicate.

3.2.7 Fluorescence

Extraction efficiency was evaluated quantitatively using a fluorescence-based assay. For samples prepared by DMF, 315- or 158-nL droplets (as above) of sample were diluted into 13-μL aliquots of pH 8.5 working buffer in wells in a 384-well low-volume microplate. The working buffers were identical to the resolubilizing buffers (Table 1). Upon addition of 2 μL of fluorescamine (5 mg/mL in acetone) the microplate was inserted into a fluorescence microplate reader (Pherastar, BMG Labtech, Durham, NC) equipped with a module for 390 nm excitation and 510 nm emission. The plate was shaken (1 min), allowed to sit (2 min), and then the fluorescence was measured.

As a control, for each analyte, identical samples that had not been extracted were evaluated using the same fluorescent assay. To ensure that controls were processed in identical

volumes relative to extracted samples, each control was prepared by dispensing a droplet on a device, delivering it to the extraction electrode, and allowing it to dry. A droplet of resolubilization solution was then dispensed, driven to the dried spot, incubated to allow for full dissolution, and the droplet was collected and analyzed. Four replicate measurements were made for each sample and control.

For samples extracted using conventional methods, the quantitative analysis protocol was similar to that used for samples prepared by DMF, with identical working buffers and reagents. The difference was volume – in each case, precipitate from 10 μL samples was resolubilized in 100-μL of working buffer. Each sample was mixed with 13 μL fluorescamine (5 mg/mL in acetone) in a well in a 96-well plate. As with samples prepared by DMF, controls were evaluated, and four replicate trials were conducted for each sample and control.

3.3 Results and Discussion

3.3.1 Device and Method Optimization

In an automated method for protein extraction by precipitation, at least four different solutions must be managed: sample, precipitant, rinse solution, and resolubilization solution. To facilitate this goal, as shown in Figure 3.1a, we designed and built a digital microfluidic device with a "double T" pattern of electrodes, with four reservoirs (with dedicated droplet movement paths) for the various reagents, and a fifth reservoir for waste. The dimensions of the electrodes were chosen such that (in normal circumstances) the droplet volumes were 140 nL (sample and precipitant) and 315 nL (rinse and resolubilization solutions), respectively. As shown, a key position in the design is the extraction electrode – the surface above this electrode is where the precipitation and purification of proteins takes place.

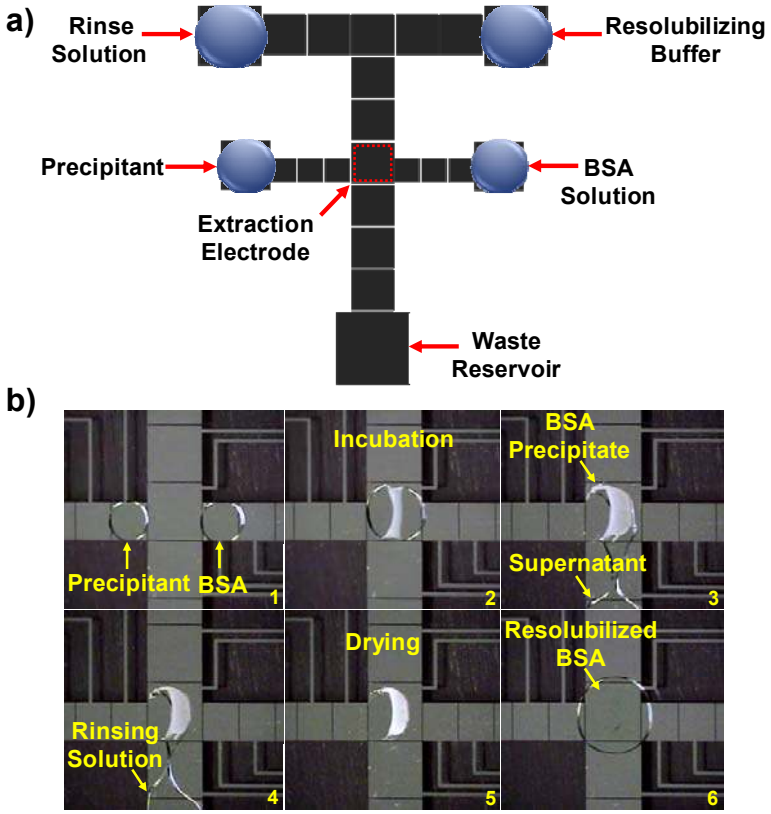

Figure 3.1 Digital microfluidic device and method for protein precipitation. a) Schematic of device depicting the four reagent reservoirs, the waste reservoir, and extraction electrode. b) Frames from a movie depicting the extraction and purification of BSA (50 mg/mL) in 20% TCA (precipitant) and washing with 70/30 v/v chloroform/acetonitrile (rinse solution). In the final frame, the precipitated protein is redissolved in a droplet of 100 mM borate buffer containing 1% SDS.

In practice, samples were sequentially precipitated onto the extraction electrode, washed in rinse solution, and then resolubilized in solvent. Figure 3.1b shows a series of frames from a movie depicting this process for a sample containing BSA. As shown, a droplet containing BSA was merged with a droplet containing 20% TCA to precipitate the protein. After precipitation, the supernatant was driven away to the waste reservoir leaving the precipitate on the extraction electrode. The precipitate was then washed in three droplets of 70/30 chloroform/ACN and allowed to dry. Finally, the purified protein was resolubilized in a droplet of 100 mM borate (pH 8.5) buffer containing 1% SDS.

As is the case for conventional methods,[112] we found that the optimal DMF-driven recipe for protein precipitation varied from sample to sample (Table 2.1). For example, ACN worked well as a precipitant for highly concentrated solutions of Mb and Fb. Low concentrations (<1 mM) were more challenging – for example, reproducible precipitation and extraction of 0.71 mM myoglobin required two different precipitants, including concentrated ammonium sulfate. For samples containing proteins and phospholipids, chloroform was found to be a useful rinsing agent to remove residues of the phospholipid from the precipitate. However, because neat chloroform is not amenable to actuation at low driving potentials (as reported previously[25]), a mixture of chloroform and ACN (70/30 v/v) (which was readily movable) was used. As has been reported,[106,107,111] TCA was the best precipitant for large proteins and complex mixtures (BSA, FBS, and cell lysate). For BSA and FBS, acetone was found to be a useful rinsing agent to remove traces of TCA from the precipitate. For cell lysate, however, neat acetone was found to dissolve some of the precipitated protein; thus, a mixture of chloroform and acetone (60/40 v/v) was used. In all experiments, borate buffer containing SDS worked well for resolubilization, although in future work, alternatives such as acid labile surfactants and urea will be used.

The protein extraction method reported here differs from conventional techniques in many respects, but one difference stands out: no centrifugation is required. In initial experiments, we observed that precipitates in droplets settle much more quickly than they do in centrifuge tubes. This is largely a function of distance – the maximum path in DMF samples is ~0.1 mm, while the comparable parameter in microcentrifuge tubes or well plates is several millimetres. Moreover, once settled, precipitates in DMF devices adhere strongly to the Teflon-AF device surfaces. This is fortuitous, as it facilitates the process of separating the liquid phase from solid

(Figure 3.1b, frames 3,4). These characteristics make the DMF-based extraction procedure faster by a factor of two relative to the macroscale equivalent (from ~30 to ~15 min).

Table 2.1 Solutions used for extracting, purifying, and resolubilizing proteins.

Sample	Primary Precipitant	Secondary Precipitant	Rinse Solution	Resolubilizing Solution
Mb	ACN	—	Chloroform/ACN (70/30 v/v)	10mM Borate with 1% SDS
Fb	"	—	"	"
Mb/PC	"	Ammonium Sulfate (saturated in DI water)	"	"
BSA	20% TCA	—	"	100mM Borate with 1% SDS
FBS	"	—	Acetone	100mM Borate with 10% SDS
Cell Lysate	"	—	Chloroform/Acetone (60/40 v/v)	"

3.3.2 Evaluation of Method Efficiency

To qualitatively evaluate the effectiveness of on-chip protein extraction, we used a model system comprising a protein analyte (Mb) and a phospholipid contaminant (PC). To approximate a demanding scenario, the concentrations were chosen to have a large excess (80:1) of contaminant. Figure 3.2 shows representative mass spectra generated from control and extracted solutions. As shown, in the spectrum of the control sample (Figure 3.2a), there are two prominent peaks at *m/z* 398 and 795 representing the $[M+1]^{+1}$ and $[2M+1]^{+1}$ ions of PC. A close look at the spectrum reveals a noisy baseline in the 600 – 1,800 *m/z* region corresponding to a low signal from Mb, which is suppressed by the high concentration of contaminant. In the spectrum of the extracted sample (Figure 3.2b), the peaks in the 600 – 1,800 *m/z* region correspond to the multiply charged ions of Mb (+27 to +10). An additional peak at *m/z* 616 represents the $[M+1]^{+1}$ ion of dissociated Heme cofactor. A very small peak at *m/z* 398 corresponds to the trace PC that remains in the solution. As shown, this method is a qualitative success, transforming a contaminated sample with very little analyte signal into a much purer solution that contains primarily analyte.

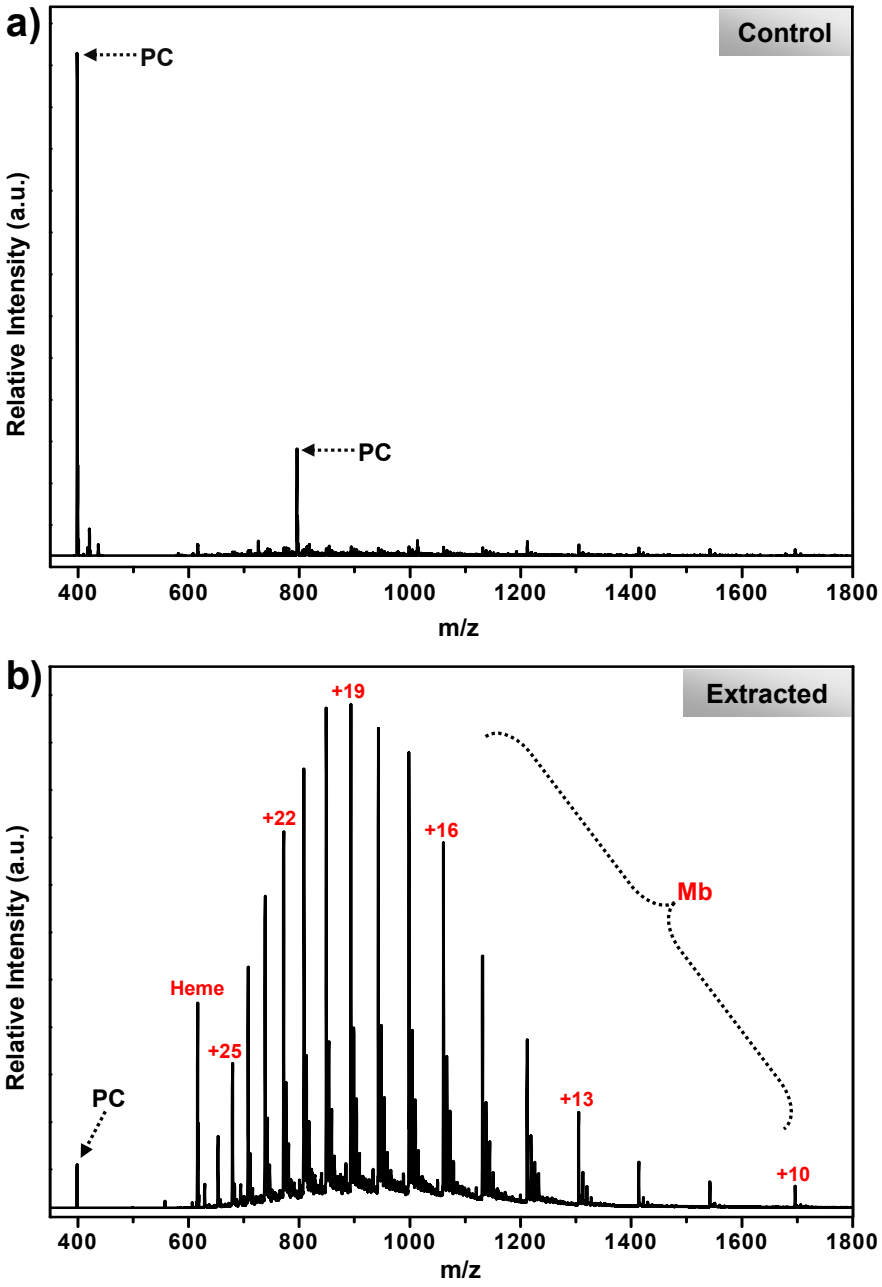

Figure 3.2 ESI-MS spectra of a) control and b) extracted samples containing model analyte, Mb (0.71 mM) and model contaminant, PC (62 mM).

To quantitatively evaluate the extraction efficiency of the new DMF techniques, we used a fluorescence-based assay similar to the widely used absorbance-based Bradford test.[119] The fluorescent method relies on fluorescamine, a fluorogenic reagent that exhibits no fluorescence until it reacts with primary amines, such as those at the N-terminus of proteins.[120,121] The reaction is immediate, and is used for non-specific labelling and quantification of proteins in

solution.[122,123] Three proteins representing a range of physicochemical characteristics, BSA (MW 66 kDa, pI 4.7), Mb (17 kDa, pI 7.3), and Fb (MW 340 kDa, pI 5.5) were evaluated at different concentrations to determine the range of linear response. Concentrations found to be in this range (50, 30, and 20 mg/mL of BSA, Mb, and Fb respectively) were chosen for quantitative analysis, and % recovery was determined by comparing the fluorescence intensity of multiple samples before and after extraction. For comparison, the same samples and concentrations were also extracted from 10 μL aliquots in microcentrifuge tubes.

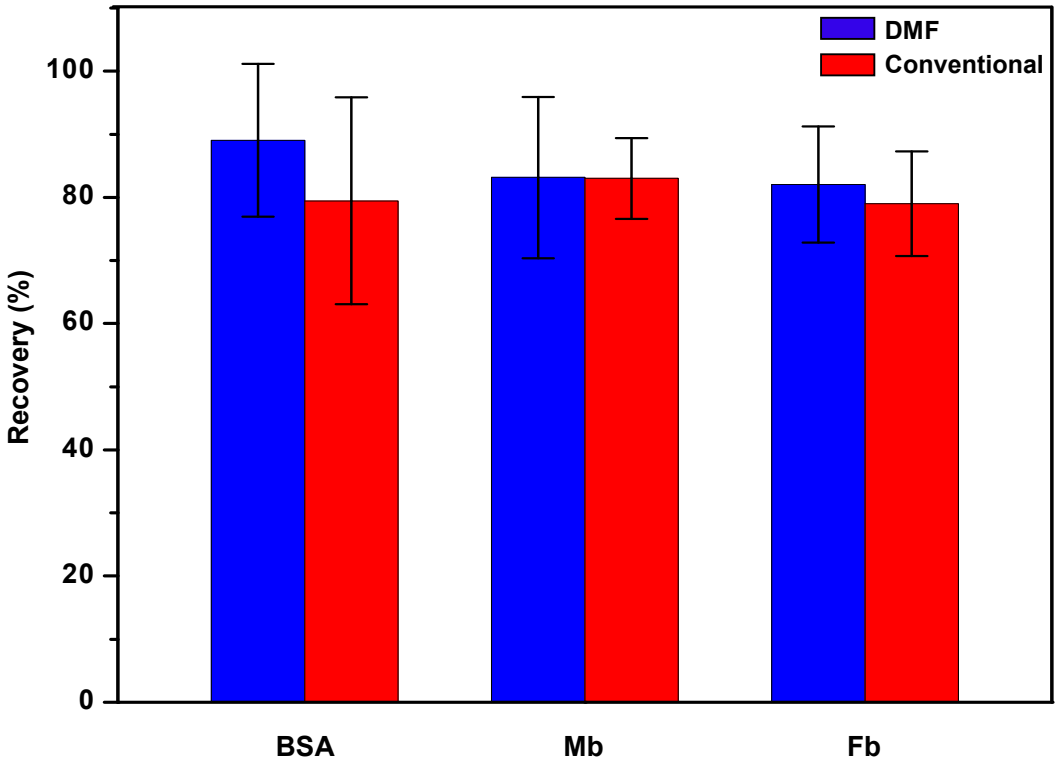

Figure 3.3 Bar graph comparing the recovery efficiency for protein standards using the DMF method (blue bars) and conventional macroscale techniques (pipette, centrifuge, etc.) (red bars). In each experiment, BSA (50 mg/mL), Mb (30 mg/mL), or Fb (20 mg/mL) samples were precipitated, washed, resolubilized, and reacted with fluorescamine, and the fluorescence intensity was compared with that of a control. The data represent the mean ± S.D. of 4 extractions for each condition.

As shown in Figure 3.3, the new digital microfluidic method proved to be very efficient – over 80% was recovered for each protein standard evaluated. In initial experiments, we hypothesized that macroscale methods might have better recovery, as the centrifugation step might facilitate collection of very small, non-settling precipitate particles. However, we did not observe this to be the case – as shown; the efficiencies determined for the new method were comparable or better than those calculated for standard techniques. Note that protein recovery in

conventional precipitation methods scales with concentration, and the use of lower concentrations (e.g., < 1mg/mL) results in reduced recovery rates (low concentrations were not evaluated here). Regardless, for the concentration ranges described here (which overlap with those commonly encountered in clinical samples) the new microfluidic method seems to be an analogous procedure to the macroscale technique, with the advantages of automation and shorter processing times.

3.3.3 Application to Complex Solutions

Protein precipitation is most useful as a sample cleanup step applied to complex mixtures – for example, precipitation is often used to purify proteins from plasma for proteome profiling.[124,125] To evaluate the potential for the new digital microfluidic method for such applications, we tested two model systems: fetal bovine serum (FBS) and cell lysate (CL). In both cases, the samples were found to be compatible with digital microfluidic manipulation and extraction. Figure 3.4 shows images of dried protein precipitates generated from droplets of FBS and CL.

FBS and CL solutions were more challenging to work with than protein standard solutions. First, dispensing droplets of cell lysate was difficult because the solution was so viscous. To solve this problem, the spacing between the top plate and the patterned bottom plate was decreased from 140 to 70 μm (resulting in a smaller droplet volume) – this strategy (reducing the spacing between plates) has been shown to enhance dispensing of viscous solutions in DMF.[32] Second, precipitates formed from FBS and CL were particularly sticky, and in rare cases, the supernatant droplet could not be driven away from the extraction electrode. In such cases, we found that if a supplemental droplet of rinse solution was dispensed and driven to the extraction electrode, the combined droplet (rinse solvent + supernatant) could be successfully driven to waste. Upon application of these strategies (reduced inter-plate spacing and supplemental rinse droplets), the extraction process for FBS and CL became reliable and reproducible.

Protein recovery efficiencies from FBS and CL were determined using the fluorescent assay described above. In each case, performance was excellent (mean ± S.D.) – 84.0% (± 7.8%) for FBS and 82.4% (± 11.5%) for CL. These values are comparable to those reported for macro-scale techniques.[107] Note that higher protein recovery can be achieved by using less rigorous

rinsing; however, multiple rinse steps are typically used to ensure high purity of the processed sample. In summary, the performance of the new DMF-driven method is comparable to conventional techniques even for complex mixtures, which bodes well for plans to integrate this procedure with other processing steps (such as enzymatic digestion[50]) for automated, miniaturized proteomic analysis.

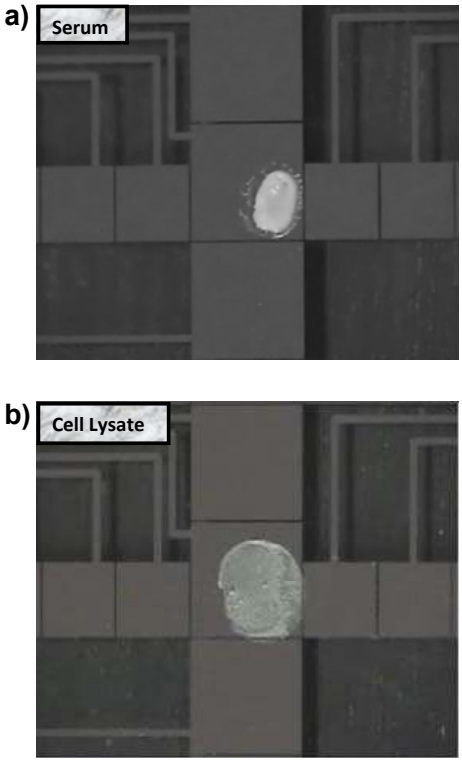

Figure 3.4 Images of protein precipitates generated from droplets of a) fetal bovine serum (140 nL) and b) cell lysate (70 nL) using the DMF method.

3.4 Conclusion

Here, the first application of microfluidics to protein extraction by precipitation is described. In this work, digital microfluidics (DMF) was used to extract and purify proteins from protein standards and heterogeneous mixtures. The new method had comparable performance relative to conventional techniques, combined with the advantages of reduced reagent and sample consumption, no centrifugation, and automated liquid handling. These results suggest great potential for the development of integrated, multistep processes incorporating sample reduction, alkylation, and digestion. we believe this work represents an important first step in developing a fully automated microfluidic method for proteomic analyses.

Chapter 4 Multilayer Hybrid Microfluidics: A Digital-to-Channel Interface for Sample Processing and Separations

Microchannels can separate analytes faster with higher resolution, higher efficiency and with lower reagent consumption than typical column techniques. Unfortunately, an impediment in the path toward fully integrated microchannel-based labs-on-a-chip is the integration of pre-separation sample processing. In contrast, the alternative format of digital microfluidics (DMF), in which discrete droplets are manipulated on an array of electrodes, is well-suited for carrying out sequential chemical reactions such as those commonly employed in proteomic sample preparation. Recently, Abdelgawad et al.[40] reported a new paradigm of "hybrid microfluidics", integrating DMF with microchannels for in-line sample processing and separations. Here, we build on initial efforts, introducing a second-generation hybrid microfluidic device architecture. In the new multilayer design, droplets are manipulated by DMF in the two-plate format, an improvement that facilitates dispensing samples from reservoirs, as well as droplet splitting and storage for subsequent analysis. To demonstrate the capabilities of the new method, we implemented an on-chip serial dilution experiment, as well as multi-step enzymatic digestion followed by separation. Given the myriad applications requiring pre-processing and chemical separations, we believe the hybrid digital-channel format has the potential to become a powerful new tool for micro total analysis systems.

4.1 Introduction

Microchannels have revolutionized separation science, allowing for rapid, efficient analyses with miniscule reagent and sample consumption.[126] To complement chemical separations, microchannel-based systems have been developed incorporating precolumn reactions, including enzymatic digestion,[127] organic synthesis,[128] and fluorescent derivatization.[129] These techniques represent the promise of the "lab-on-a-chip". Unfortunately, the scope of laboratories-on-a-chip capable of integrating precolumn reactions with separations is limited. For example, there are no microchannel-based methods reported that are useful for shotgun proteomics, in which samples are subjected to a rigorous, multistep processing regimen requiring several days to complete.[130] This deficit is largely mechanistic managing multiple reagents with precise control over position and reaction time in microchannels is complicated by the near-universal effects of hydrostatic and capillary flows.[131,132] On-chip microvalves[133] offer some relief from this problem; however, the complicated fabrication and control infrastructure required for this technology limits their widespread adoption and use.[134] Another technique that might be useful for precolumn reactions and separations is multiphase microchannel systems (i.e., droplets-in-channels).[15] Several groups[135-137] recently reported methods capable of delivering droplets from such systems directly into separation channels. This is an exciting development, but we posit that the droplets-in-channels paradigm is not ideally suited for controlling multistep chemical reactions between many different reagents (as is required for shotgun proteomics[130]), as the droplets in such systems (regardless of their contents) are controlled in series.

An alternative miniaturized fluid handling format to microchannels is digital microfluidics (DMF), a technique in which discrete fluidic droplets are manipulated by electrostatic forces on an array of electrodes coated with an insulating dielectric.[14,23,24] DMF is well-suited for carrying out sequential chemical reactions; this is particularly true for the two-plate format, in which droplets are sandwiched between a top substrate bearing a ground electrode and a bottom substrate bearing driving electrodes. In this configuration, droplets containing different reagents can be dispensed from reservoirs, moved, merged, mixed, and split,[32] which facilitates multistep proteomic sample processing in which protein samples are sequentially reduced, alkylated, and digested prior to mass spectrometric analysis.[54,55,57]

Likewise, two-plate DMF can be used to purify proteins from serum in a multistep process comprising precipitation, rinsing, and resolubilization.[17,57] Ideally, digital microfluidics could be coupled with microchannels (as noted, microchannels are well-suited for chemical separation analysis) on a single platform for a fully integrated lab-on-a-chip.

Recently, Abdelgawad et al. developed the first device architecture combining reactions and processing by digital microfluidics with separations in microchannels.[40] This method called "hybrid microfluidics" comprised of a single-plate digital microfluidic device interfaced in a "side-on" configuration with a network of microchannels. Using this design, proof-of-concept experiments including on-chip fluorescent labeling of amines in cell lysate and enzymatic digestion of proteins, followed by separation of the products were performed. However, preliminary hybrid microfluidics design[138] was limited in that the DMF portion of the device was operated in single-plate format. The single-plate format is not compatible with some key fluidic manipulation steps, including dispensing samples from reservoirs and splitting sample droplets. Evaporation is also a concern for this format, as droplets are directly exposed to the environment. Furthermore, the PDMS channel used in the initial design was not ideal, as this material suffers from well-known disadvantages[139] for lab-on-a-chip applications (e.g., surface adsorption of analytes, solvent compatibilities).

Here, we present a second-generation interface between digital microfluidics and microchannels, using a two-plate configuration for the digital platform. In this device, the side-to-side junction between DMF and microchannels (i.e., the previous design[138]) is replaced with a multi-layer junction between an actuation electrode on a top layer and a vertical access hole to a microchannel network on a layer below. In the following, we describe the implementation of this second-generation of hybrid microfluidics paradigm, and present its application to sample processing and separations.

4.2 Experimental

4.2.1 Reagents and Materials

All chemicals, unless otherwise stated, were purchased from Sigma Aldrich (Oakville, ON) and used without further purification. Alexa Fluor 488 labeled bovine serum albumin (AF-BSA) was from Invitrogen-Molecular Probes (Eugene, OR) and food coloring dyes from McCormick Canada (London, ON). Sodium borate and acetate buffers were dissolved in deionized water (diH_2O, 18 MΩ cm), filtered through Millipore nylon syringe filters (Billerica, MA, 0.2 μm pore dia.) and degassed by ultrasonication (5 min) prior to use. Materials required for device fabrication included Parafilm-M laboratory film (Pechiney Plastic Packaging, Menasha, WI) chromium pellets (Kurt J. Lesker Canada, Toronto, ON), parylene-C (Specialty Coating Systems, Indianapolis, IN), and Teflon-AF1600 (DuPont, Wilmington, DE).

4.2.2 Device Fabrication and Operation

Glass slides bearing a simple cross network of microchannels (substrate 3 in Figure 4.1) thermally bonded to slides with drilled-hole (1.5 mm dia.) inlets (substrate 2 in Figure 3.1) were obtained from Caliper Life Science (Hopkinton, MA). The devices were then modified by patterning a digital microfluidic device (an array of chromium electrodes coated with Parylene-C and Teflon-AF) on top of substrate 2. As shown in Figure 4.1, the DMF design comprised thirteen driving electrodes (2.2 mm x 2.2 mm) and three reservoir electrodes (3 mm x 3 mm or 5 mm x 5 mm) and was positioned such that one of the driving electrodes was adjacent to one of the inlets – this inlet served as the "digital-channel interface".

The digital microfluidic device architecture was formed in the University of Toronto Emerging Communications and Technology Institute (ECTI) using methods described elsewhere[17,57] with two modifications. First, prior to coating with chromium, the channel inlets were protected by inserting small plugs of Parafilm-M. After coating with chromium, the plugs were carefully removed. Second, after electrode patterning, the channels were inspected and rinsed with acetone and methanol, and the vertical inlets were sealed with dicing tape (Semiconductor Equipment Corp., Moorpark, CA). After coating with Parylene-C and Teflon-AF the tape was removed.

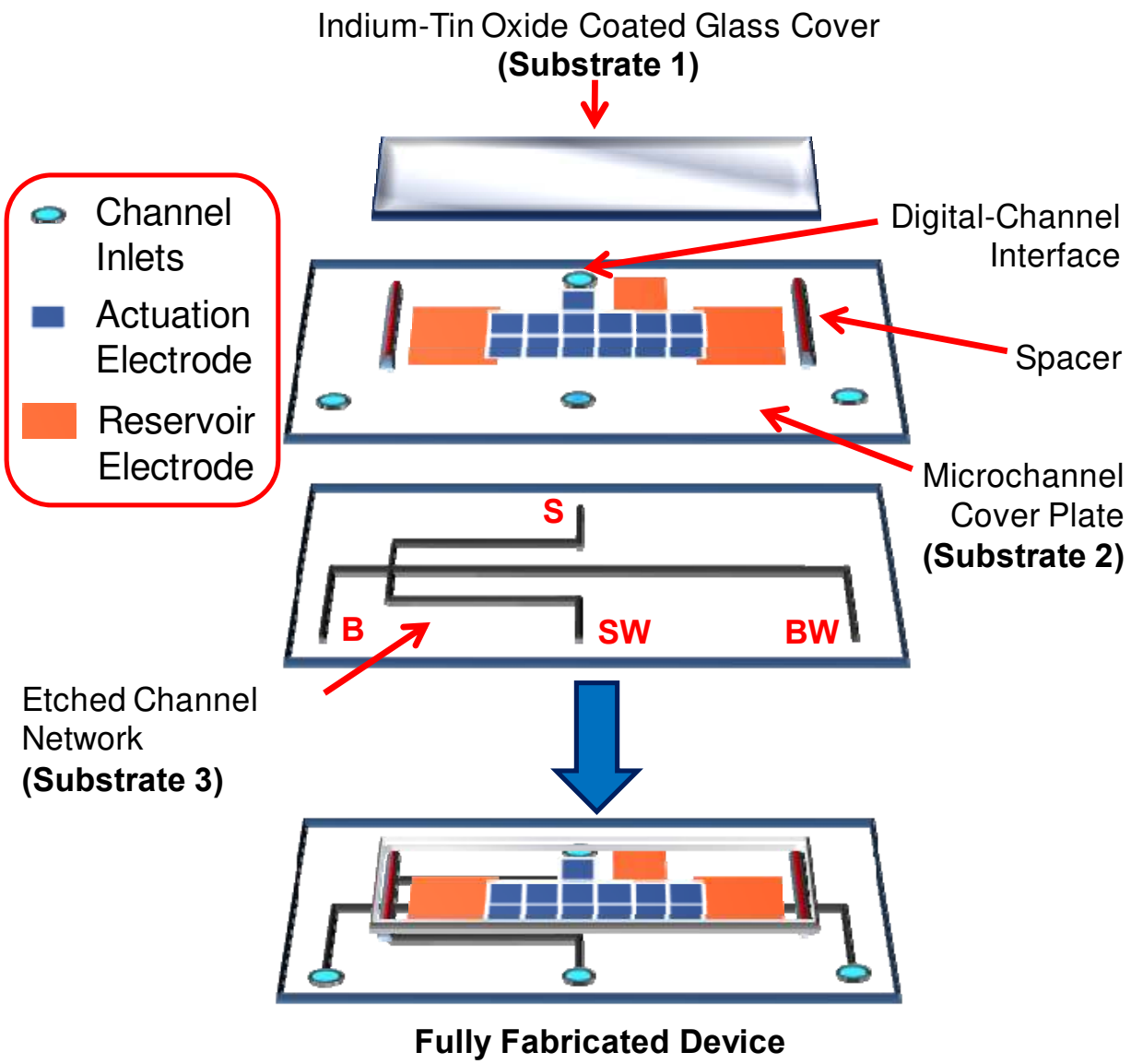

Figure 4.1 Exploded view of a multilayer hybrid microfluidic device. A two-plate digital microfluidic (DMF) structure is defined by substrates 1 and 2, and the network of microchannels is defined by substrates 2 and 3. In practice, the DMF architecture was fabricated on the top of pre-formed commercially available glass microchannel devices. Pipet tip buffer reservoirs were inserted into the B, SW and BW channel inlets.

After coating, hybrid devices were largely complete, save for the final preparation steps. Pipette tips were trimmed (into pieces capable of holding ~20 µL) and were inserted into all of the microchannel access holes except for the digital-channel interface. Platinum wires were inserted into each of these reservoirs. At the digital-channel interface, a platinum wire was affixed such that it was flat on the surface of the top substrate, terminating in a hook that penetrated the access hole. Samples and reagents were pipetted into the DMF reservoirs, and a top plate (substrate 1 in Figure 4.1) comprising an indium-tin oxide (ITO) and Teflon-AF coated

glass slide formed as described elsewhere[17,57] was positioned on top of the device. The top plate was separated from the array of electrodes by spaces formed from 4 pieces of double-sided tape (280 μm total thickness). Finally, the network of microchannels was filled with separation buffer (20 mM or 100 mM borate buffer, pH 9.0, for on-chip dilutions or enzyme digests, respectively). Device operation comprised two stages: sample processing by droplet actuation followed by chemical separation by electrophoresis. In the first stage, droplet actuation (i.e. dispensing, merging, mixing and splitting) was implemented in two-plate format. Voltages for actuation of droplets were generated by applying an AC signal (20 kHz, 100-200V_{RMS}) originating from a function generator (Agilent, Santa Clara, CA) and high-voltage amplifier (Trek, Medina, NY). After sample processing in droplets (described in detail below) was complete, samples to be analyzed were driven to the digital-channel interface inlet for sampling into the microchannels below. In the second device operation stage (analysis by separation), DC signals were applied at the sample inlet (S), sample waste outlet (SW), buffer inlet (B) and buffer waste outlet (BW) using a high voltage sequencer (LabSmith, Livermore, CA). Initially, the solution in the droplet at the interface was driven through the injection cross by applying high voltage between S and SW (S = 900 V; SW = 0 V; B = 650 V; BW = 850 V). A plug of sample was then injected onto the separation column by switching voltage to drop between B and BW (S = 500 V; SW = 500 V; B = 1000 V; BW = 0 V).

Analytes were detected 3 cm downstream from the injection cross by LIF using an inverted microscope (Olympus IX-71) mated to an argon ion laser (Melles Griot, Carlsbad, CA). The 488 nm laser line (20 mW) was focused into the channel using an objective (60 X); the fluorescent signal was collected by the same lens and filtered optically (536/40 nm band-pass and 488 nm notch filter) and spatially (500 μm pinhole), and imaged onto a photomultiplier tube (PMT, Hamamatsu, Bridgewater, NJ). PMT current was converted to a voltage using a picoammeter (Keithley Instruments, Cleveland, OH) and then collected using an A-D converter and a PC running a custom LabVIEW (National Instruments) program to generate electropherograms.

4.2.3 On-Chip Calibration Curves

To generate on-chip calibration curves, a droplet containing both rhodamine 123 and fluorescein (1 μM each in 20 mM borate buffer, pH 9.0) was dispensed and merged with a

second droplet containing only rhodamine (1 μM) and mixed by moving the droplet across several electrodes. The mixed droplet (~0.5 μM fluorescein and 1 μM rhodamine) was then split into two sub-droplets; one sub-droplet was stored on the array while the other was driven to the interface and analyzed. The stored droplet was then merged and mixed with a third droplet of rhodamine (1 μM), to create the next dilution (~0.25 μM fluorescein and 1 μM rhodamine). Again, this droplet was split, and one sub-droplet was driven to the interface for analysis, while the other sub-droplet was stored. Between each analysis, the remaining portion of the previous sample was removed by suction with a fine needle connected to a vacuum flask.

After collecting electropherograms, peak areas were quantified using PeakFit (SeaSolve Software Inc., Framingham, MA). In each case, the peak area of fluorescein was measured relative to that of the internal standard, rhodamine 123. The resulting ratio was plotted as a function of fluorescein concentration to generate calibration curves. The variance of this method was probed by assessing the percent relative standard deviation (% RSD) from 5 replicates.

4.2.4 On-Chip Protein Digestion

A model protein, AF-BSA, was used to demonstrate the compatibility of the new device architecture with multi-step sample processing. In each experiment, a droplet of AF-BSA (20 μg/mL in DI water containing 0.1 %wt. F-68) was dispensed, merged and mixed with a droplet containing either pepsin (1 mg/mL in 1 mM acetate buffer containing 0.1%wt. F-68, pH 4.5) or trypsin (1 mg/mL in 50 mM borate buffer containing 0.1%wt. F-68, pH 9.0). After droplet merging, the device was incubated (30 min) in a humidified chamber (a Petri dish containing a water-saturated wipe), after which the combined droplet was split and one sub-droplet was delivered to the interface for analysis. Experiments included analysis of AF-BSA alone, AF-BSA digested by pepsin alone, AF-BSA digested by trypsin alone, and AF-BSA digested by pepsin followed by trypsin. Each condition was repeated in triplicate.

4.3 Results and Discussion

4.3.1 Device fabrication and operation

A new architecture mating digital microfluidics (useful for sample processing) to microchannels (useful for separations) has been developed. The new hybrid devices were formed by creating a DMF device on the top surface of a commercially available glass device bearing a network of microchannels. An exploded view is shown in Figure 4.1, the digital microfluidic device is defined by substrates 1 and 2, and the network of microchannels is defined substrates 2 and 3. Critically, the new multilayer architecture facilitates manipulation of droplets in the two-plate format, representing an advance over the previous hybrid microfluidics device configuration (which relied on single-plate droplet actuation[40]).

The new device was designed such that the two fluid manipulation paradigms – electrostatic droplet manipulation in the top layer and electrokinetic flow in the bottom layer – are orthogonal and independent. For the former, droplets were dispensed from reservoirs, merged, mixed, and split by applying a series of AC potentials to sequential driving electrodes. Adsorption of proteins and reagents from droplets onto device surfaces was minimized by the addition of pluronic as a buffer additive,[50] and droplet evaporation was controlled by storing devices in a humidified chamber.[70] For the latter, sample at the digital-channel interface was loaded and separated by applying DC voltage to drive electroosmotic flow (EOF) through the channels. Channels and reservoirs were filled prior to actuation of droplets and were cleaned and refilled after performing electrophoretic separations.

As shown in Figure 4.1, the central feature of this design is the digital-channel interface formed at the intersection of a DMF electrode and one of the drilled-hole channel inlets. Thus, in this scheme, droplets are manipulated on the top of the device, and are subsequently transferred to microchannels on the bottom of the device through the interface. This process is depicted in Figure 4.2. As shown, a droplet is actuated on the array of electrodes (not visible in the perspective of Figure 4.2) such that it approaches the digital-channel interface. As the droplet reaches the inlet, it spontaneously wets the exposed glass, settling into the bottom of the hole. In this design, unit droplet volumes (~3 μL) were chosen to approximate the volume bounded by the hole (2 mm. dia., 1 mm deep), but this is not a requirement for operation.

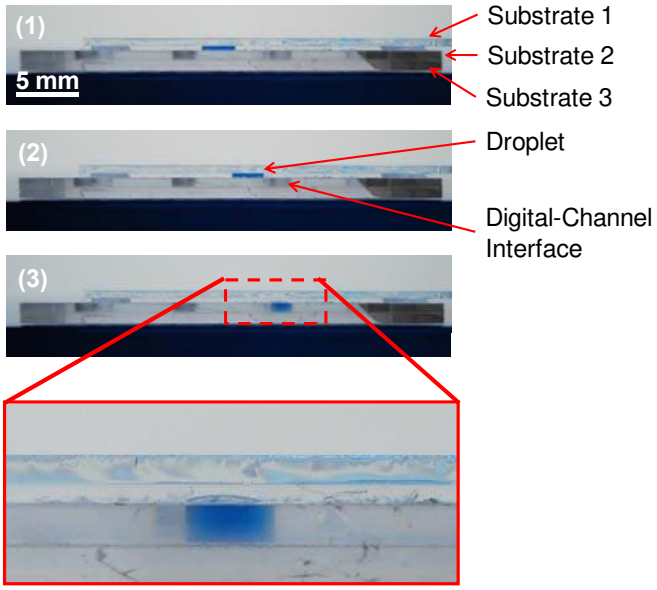

Figure 4.2 Series of images from a movie (side-view) depicting sample transfer from the digital microfluidic platform (above) to the network of microchannels (below). As the droplet (colored blue for visualization) approaches the digital-channel interface (a drilled hole in the glass), it spontaneously wets and settles into the hole. A magnified image of the droplet settled in the inlet is shown in the bottom panel.

In initial work, the design and fabrication protocol for hybrid microfluidic devices was optimized to address two challenges: droplet transition into the network of microchannels, and protection of the channel network during cleanroom processing. For the former challenge, it was found that reliable sample transfer into the interface hole required that the actuation electrode (2.2 x 2.2 mm) be aligned to partially overlap with the vertical hole (2 mm dia.). In initial experiments, it was found that if the electrode and hole do not overlap, the droplet will not contact the exposed glass. However, if the electrode and hole overlap too much, the electrode will not be sufficiently attractive to the droplet. In the final design, the interface electrode was patterned such that it overlapped the interface access hole by ~1 mm, which facilitated reliable droplet transfer. For the latter challenge, it was found that protection of the channels during electrode patterning and coating was necessary to prevent channel clogging. During metal deposition and photoresist coating, channel inlets were protected with plugs of parafilm, which is easy to mould and forms a tight seal. Paraffin was also explored as a channel protectant.[140] However, the high temperatures required for metal deposition and photoresist curing sometimes caused the paraffin to melt. During Parylene-C and Teflon-AF coating, it was found that the best method for channel protection was covering the inlets with dicing tape. This was particularly important at the digital-channel interface – the tape must be carefully positioned such that the

electrode is exposed but the hole is covered. Parafilm plugs were not used for this step because the conformal Parylene-C coating makes extraction of the plugs difficult, leading to pealing or blistering of the dielectric layer.

An additional challenge for device operation was optimization of sample/buffer volumes. In microchannel electrophoresis, large reservoir volumes are often used to limit the effects of buffer depletion and evaporation, which can lead to unpredictable EOF rates. Moreover, it is often advisable to match the fluid heights in reservoirs to avoid siphoning and unwanted pressure-driven flows.[131] Unfortunately, in the new hybrid device design, the sample volume is small (i.e., a 3 μL droplet). In response to this challenge, strategy was adopted in which large volumes (15 μL) were used for buffer, buffer waste, and sample waste reservoirs, and a small volume (3 μL droplet) for the sample. Pressure-driven flow towards the sample inlet is observed under these conditions. However, it is predictable, and the voltages for electrokinetic loading and electrokinetic separations were chosen to compensate for the pressure-driven flow. In the future, channel restrictions[141] or small-pore porous polymer plugs[142] may be used to further mitigate the effects of siphoning.

4.3.2 On-chip calibration curves

The unique hybrid architecture of the device reported here makes it straightforward to integrate sample preparation with chemical separations. As shown in Figure 4.3, droplets can be dispensed from reservoirs (frame 2), merged (frame 3), mixed (frames 3-4) and split to form sub-droplets (frames 4-5). Droplet dispensing and splitting are particularly welcome capabilities, as the initial hybrid microfluidic design[40] (relying on single-plate DMF) was incapable of these operations. After completion of processing, samples can be transferred to the network of channels below for analysis (frame 6). To illustrate this capacity, the new method was used to create a set of calibration standards on the digital platform with in-line analysis by electrophoretic separations. Serial dilutions were formed by merging a droplet containing both analyte (fluorescein) and internal standard (rhodamine 123) with a droplet of diluent (buffer containing internal standard only). Thorough mixing (by moving the merged droplet in a circular pattern for several seconds[103]) produced a droplet with a 2x dilution of analyte. This droplet was split (as in Figure 4.3, frames 4-5), and one daughter droplet was analyzed by electrophoresis and LIF, and the other daughter droplet was stored for further processing. Subsequent mixing of the

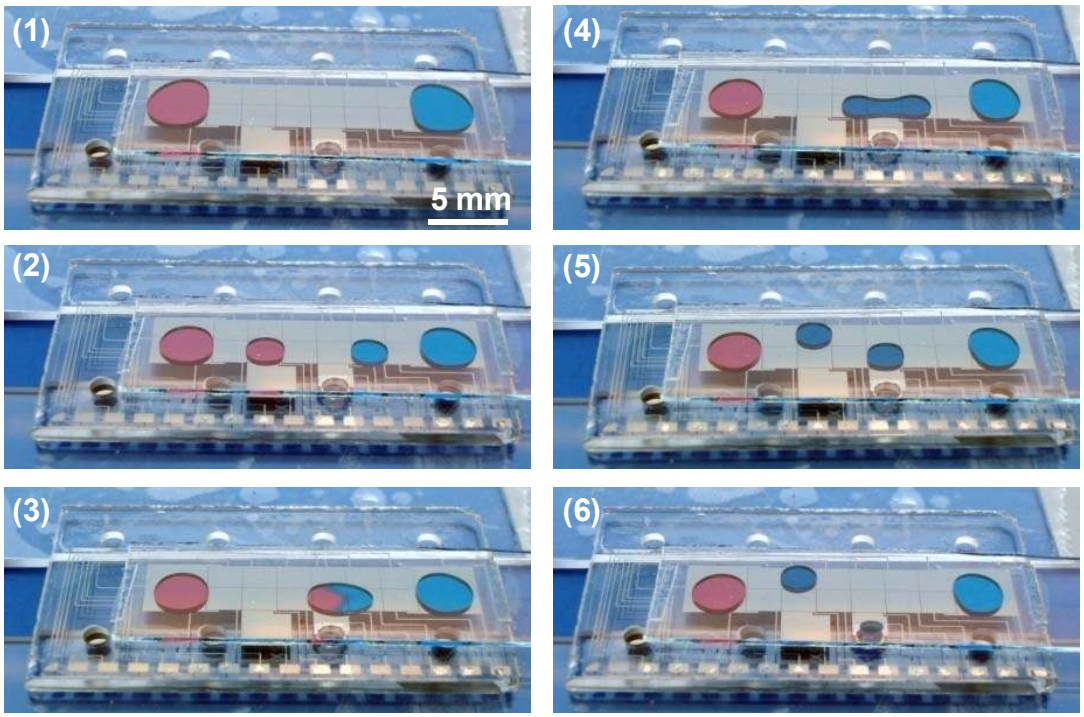

Figure 4.3 Series of images from a movie (top-view) depicting droplet manipulation on the hybrid microfluidic device. Devices were capable of all basic DMF operations: dispensing (frames 1-2), merging (frame 3), mixing (frames 3-4) and splitting (frames 4-5). Processed droplets were then delivered to the vertical interface to access the channels below (frame 6). Red and blue dyes were added for visualization.

stored droplet with another droplet of diluent resulted in a product droplet with 4x-diluted analyte concentrations. Figure 4.4 summarizes the results of replicate (n = 5) electrophoretic analyses. Figure 4.4a is a series of representative electropherograms for a dilution curve set (i.e. undiluted stock, first dilution and second dilution). Both the analyte and the internal standard are fully baseline resolved and peak area was used as the calibration metric. A calibration curve (Figure 4.4b) was generated by plotting the ratio of analyte peak area (A_A) to that of the internal standard (A_{IS}) as a function of analyte concentration. The precision in each measurement (RSD = 2.9%, 3.7%, and 7.4% for the stock, first dilution, and second dilution, respectively) and the correlation coefficient (R^2 = 0.9937) demonstrates that the method is reproducible and linear. Efficiency for the separation (29,000 plates for rhodamine 123) was also very high, and represents an improvement over what was reported for the previous design[40] (4.7×10^5 plates/m). The improvement can be attributed to the channel materials, as PDMS (used in the previous design) is known to contribute to band broadening relative to glass (used in the current design).

Devices used in this proof of concept experiment were designed with equal sized electrodes and accomplished a maximum of a 4x dilution. This limit on dilution factor derives

from both the uniform shape of the actuation electrodes and the size of the reservoir. Droplets dispensed on chip contain a volume that is proportional to the electrode size dispensed upon. Therefore if a different solution series (i.e., 10x or 100x dilution) is desired the electrode pattern can be adjusted accordingly to accomplish the correct volume metering.

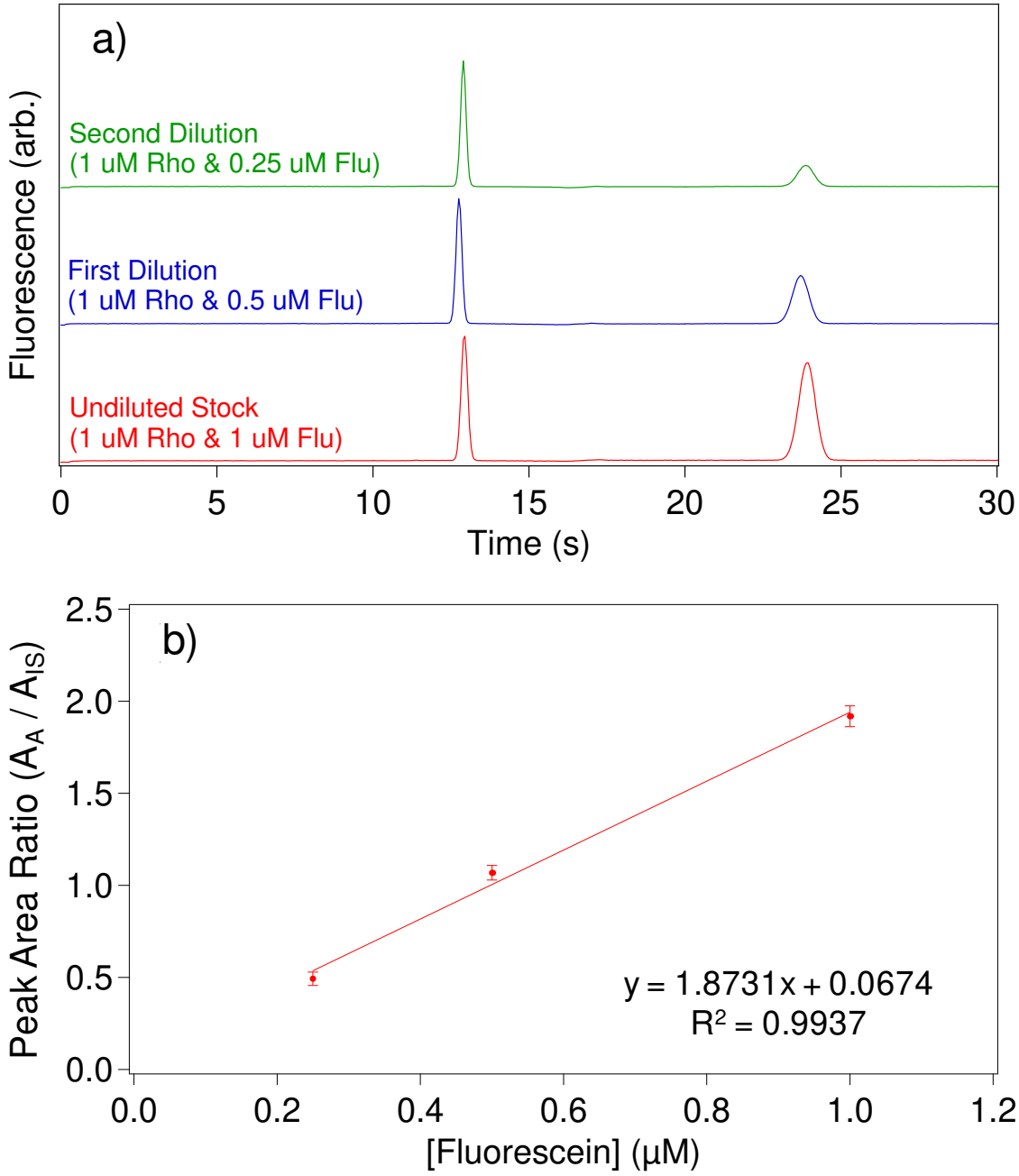

Figure 4.4 Data generated from on-chip serial dilutions and analysis. a) Representative electropherograms of analyte, fluorescein (Flu) and internal standard, rhodamine 123 (Rho) from an undiluted stock, first dilution and second dilution (offset vertically for clarity). b) Calibration curve for the ratio of peak area of analyte (A_A) to that of internal standard (A_{IS}) from five replicate analyses. Error bars are ± 1 S.D.

4.3.3 Multi-step protein processing

Analysis of complex samples often requires the combination of multi-step sample processing followed by separations. A well-known example is shotgun protoemics,[130] in which samples are exposed to a rigorous sample processing regimen and then separated by HPLC. A key step in this method is enzymatic digestion of proteins into constitutive peptides which are easier to handle and analyze. In fact, this step is so important, that samples are often digested serially with multiple enzymes that cleave at different amino acid residues.[130] Here, the new multi-layer hybrid microfluidic device was used to integrate digestion by multiple enzymes followed by separations. In this work, a model analyte (fluorescently labeled bovine serum albumin, AF-BSA) was digested by pepsin (which cleaves after Phe, Tyr and Trp) and trypsin (which cleaves after Arg and Lys). All solution processing was implemented on the DMF platform, and the resulting processed samples were delivered to the digital-channel interface for analysis by microchannel electrophoresis.

AF-BSA was analyzed in three states: undigested, digested with pepsin (30 min), and digested with pepsin (30 min) followed by digestion with trypsin (30 min each). (AF-BSA digested with trypsin-only was also analyzed, but is not shown.) As shown in Figure 4.5, each enzyme produces a unique series of peaks in the resulting electropherograms. Pepsin selectively cleaves at aromatic residues (Trp, Tyr and Phe), resulting in multiply charged peptides. The resulting electropherograms (middle trace in Figure 4.5) include several peaks that elute at a range of times relative to the AF-BSA reactant. From these data, the digestion has clearly proceeded long enough to generate a variety of subsequent peptides. Trypsin selectively cleaves at basic residues (Lsy and Arg), resulting in a reduction of multiply charged peptides from the pepsin digestion. Thus, in these electropherograms (top trace in Figure 4.5), a new series of peaks is observed, with the peptides eluting closer together. These data sufficiently proves that the new multi-layer hybrid design is capable of multi-step on-chip digestion of a model protein. In future work digestions will also be monitored by MALDI-MS to confirm protein digest progress in addition to digest sequence coverage.

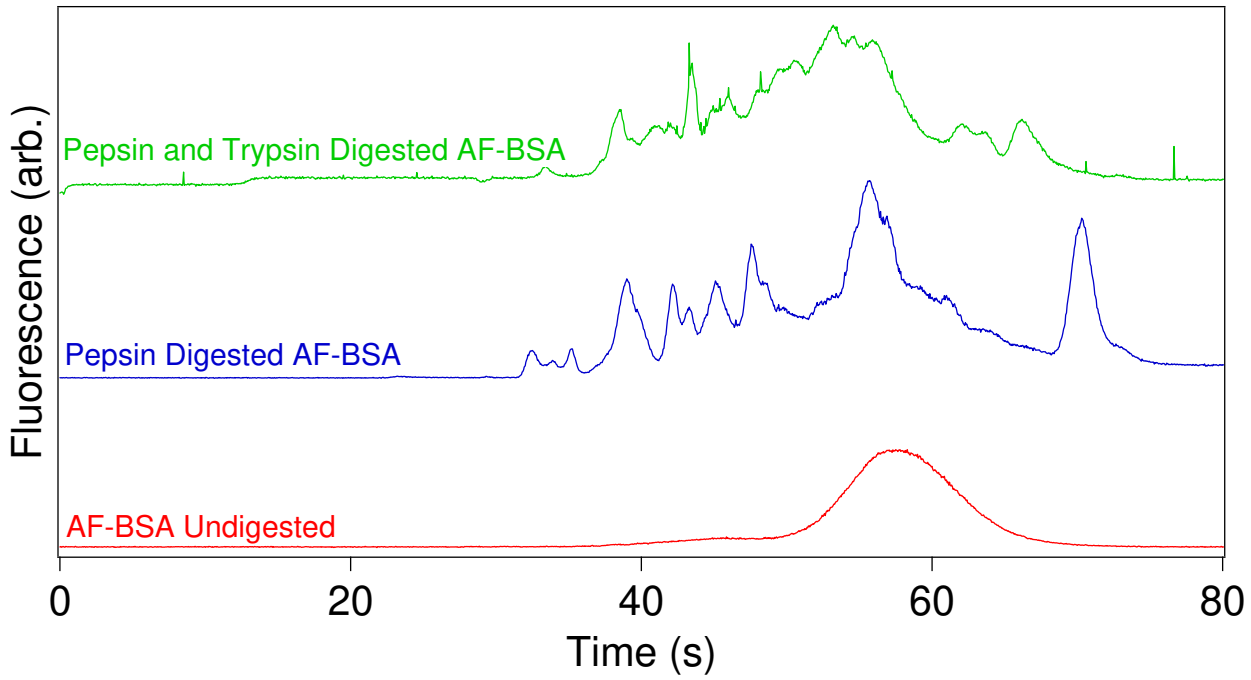

Figure 4.5 Multi-step processing of a model protein. AF-BSA was subjected to enzymatic digestion by two proteolytic enzymes; pepsin and trypsin. The three electropherograms (offset vertically for clarity) represent (1) undigested AF-BSA (20 µg/mL), (2) AF-BSA digested by pepsin (30 min) and (3) AF-BSA digested by pepsin followed by trypsin (30 min each).

The small footprint (3.5 x 2 cm) of the commercial microchannel devices used here limited the size of the DMF array to a few electrodes. In the future work, devices will be fabricated with larger DMF arrays capable of manipulating up to 10 different reagents[57] to integrate on-chip protein precipitation[17] and sample reduction, alkylation, and digestion.[54] In the long-term, it is anticipated that integration of such techniques with microchannel chromatography[143] and nanoelectrospray mass spectrometry[144] will form a powerful new tool for application to shotgun proteomics and many other applications.

4.4 Conclusions

Here, we introduced a new multi-layer hybrid microfluidic device architecture, bearing a digital microfluidic module on the top of the device and a network of microchannels below. In such devices, droplets are dispensed from reservoirs, merged, mixed, and split on the top layer, and are subsequently transferred to microchannels on the bottom of the device through a vertical interface. To validate the capabilities of the new method, an on-chip serial dilution experiments, as well as multi-step enzymatic digestion were implemented. Given the many applications require pre-processing and a chemical separation, the two-layer hybrid digital-channel format has the potential to become a powerful new tool for micro total analysis systems.

Chapter 5 Droplet-Scale Estrogen Assays in Breast Tissue, Blood, and Serum

Estrogen is a key hormone in human reproductive physiology, controlling ovulation and secondary sexual characteristics. In addition, it plays important role in the pathogenesis of breast cancer. Indeed, estrogen receptor antagonists and aromatase inhibitors (which block estrogen biosynthesis) are primary drugs used for treatment and prevention in at-risk populations. In spite of its importance, tissue concentrations of estrogens are not routinely measured because conventional techniques require large samples of biopsies for analysis. In response to this need, we have developed a digital microfluidic method and applied it to the extraction of estrogen in one-microliter samples of breast tissue homogenate (as would be collected with fine-needle aspiration), as well as in whole blood and serum. we believe this method has potential for application to conditions requiring frequent analysis of hormones in clinical samples (for example, infertility and cancer).

5.1 Introduction

In addition to its well-known role as a blood-borne hormone, estrogen is an important intracrine and paracrine messenger in many tissues including the breast.[145-147] Indeed, in situ biosynthesis of estrogen contributes up to 75% of the total estrogen produced in the breasts of premenopausal women (menstruating women of reproductive age) and almost 100% in menopausal women.[148] There is a need for measuring estrogen concentrations in breast tissue to identify women at risk for developing breast cancer or to monitor the effect of anti-estrogen breast cancer therapies such as aromatase inhibitors.[149,150] Unfortunately, local breast tissue estrogen concentrations are not routinely measured because existing methods require invasive biopsies of hundreds to thousands of milligrams of tissue.[151,152] Such procedures are not performed in part because they require local anesthesia and carry the risk of scarring or deformity. Moreover, prior to analysis, large tissue samples must be processed (including lysis, homogenization, extraction, purification, and resolubilization), which requires many hours of laboratory time.[153,154] These procedures are ill-suited for routine testing. Although most problematic for tissue samples, many of these same limitations apply to blood and serum samples [for example, in applications related to monitoring low levels of hormones[155-158] or in management of infertility].

In response to these challenges, we have developed a miniaturized, automated and integrated method for hormone analysis in one-microliter samples. The method relies on digital microfluidics (DMF), a technique in which sample and reagent droplets are moved across an open surface by applying electrical potentials to an array of electrodes.[159] This technique is particularly well suited to multistep sample processing, and, in this chapter, we describe the application of DMF to sample clean-up and extraction of estradiol (the most biologically active form of estrogen) in breast tissue from postmenopausal breast cancer patients, as well as from samples of whole blood and serum.

5.2 Experimental

5.2.1 Study Subjects

Breast tissue was obtained from apparently normal areas adjacent to breast cancer tumors during surgery in two postmenopausal breast cancer patients and kept at –80°C until analysis. Blood and serum samples were collected from a healthy female volunteer during 5 different reproductive cycles (mid luteal phase) and kept at –20°C until analysis. Human ethics approvals were obtained from Mount Sinai Hospital and the Ontario Tumor Bank Research Ethics Boards.

5.2.2 Reagents and Materials

Dichloromethane (DCM) and 2,2,4 Trimethylpentane (Isooctane) 99.8% and HPLC-grade water were purchased from Sigma. Methyl alcohol (Methanol, HPLC grade) was from Fisher Scientific. Estradiol (17-ß) was purchased from Steraloids Inc. Shipley S1811 photoresist and MF321 developer from Rohm and Haas, AZ300T photoresist stripper from AZ Electronic Materials, parylene C dimer from Specialty Coating Systems, Teflon-AF from DuPont, solid chromium from Kurt J. Lesker Canada, CR-4 chromium etchant from Cyantek, hexamethyldisilazane (HMDS) from Shin-Etsu MicroSi, concentrated sulfuric acid and hydrogen peroxide (30%) from Fisher Scientific Canada, Fluorinert FC-40 from Sigma, and SU-8 and SU-8 developer from MicroChem.

5.2.3 Device fabrication and Operation

Digital microfluidic devices were fabricated in the University of Toronto Emerging Communications Technology Institute (ECTI) clean room facility, using transparency photomasks printed at City Graphics. Glass wafers (Howard Glass Co. Inc.) were cleaned in piranha solution (a 3/1 v/v mixture of sulfuric acid/hydrogen peroxide) for 10 min, and coated with chromium (150 nm) by electron beam deposition (BOC Edwards). After rinsing (acetone, methanol, DI water) and baking on a hot plate (115°C, 5 min), substrates were primed by spin-coating HMDS (3000 rpm, 30 s) and then spin-coating Shipley S1811 photoresist (3000 rpm, 30 s). Substrates were baked on a hot plate (100 °C, 2 min) and exposed (35.5 mW/cm^2, 4 s) through a transparency photomask using a Karl Suss MA6 mask aligner. Then substrates were developed (MF321 developer, 3 min) and postbaked on a hot plate (100 °C, 1 min). After

photolithography, exposed chromium was etched (CR-4, 2 min) and the remaining photoresist was stripped by sonicating in AZ300T (5 min).

After forming electrodes and cleaning in piranha solution (30 s), a photoresist wall was formed, using methods similar to those reported by Moon et al. [37] Briefly, substrates were spin-coated with SU-8-25 (500 rpm, 5 s, then 1000 rpm, 30 s), baked on a hotplate (65°C, 5 min, then 95°C, 15 min), and then exposed to UV light (35.5 W/cm^2, 7 s). After baking (65°C, 1 min, then 95°C, 4 min), and developing in SU-8 developer, substrates were coated with 2 μm of parylene-C and 100 nm of Teflon-AF. Parylene-C was applied using a vapor deposition instrument (Specialty Coating Systems) and Teflon-AF was spin-coated (1% by weight in Fluorinert FC-40, 1000 rpm, 1 min) followed by baking on a hot plate (160°C, 10 min). The polymer coatings were removed from contact pads by gentle scraping with a scalpel to facilitate electrical contact for droplet actuation. In addition to patterned devices, unpatterned indium-tin oxide (ITO) coated glass substrates (Delta Technologies Ltd) were coated with Teflon-AF using the conditions described above, to serve as the top plate on assembled devices.

The device design included three input reservoir electrodes (3.5 x 3.5 mm) for the raw sample, lysing solvent, and polar extraction solvent, respectively, and a fourth reservoir electrode for collection of the processed sample. Actuation electrodes (1.5 mm x 1.5 mm with a 40 μm inter-electrode gap) formed a path linking the input reservoirs, which passed through a fifth reservoir (delineated by a photoresist wall) containing non-polar extraction solvent. Devices were assembled with an unpatterned ITO–glass top plate and a patterned bottom plate separated by a spacer formed from one or two pieces of double-sided tape (90 or 180 μm thick). Thus, depending on the spacer thickness, reservoir volumes were ~1.1 or 2.2 μl, and unit droplets (covering a single actuation electrode) were ~200 or 400 nl. A single spacer was used to process standard solutions of estradiol, while a double spacer was used for blood, serum, and tissue. Droplets were sandwiched between the two plates and actuated by applying AC potentials (18 kHz, 100 V) between the top electrode (ground) and sequential electrodes on the bottom plate via the exposed contact pads. Droplet motion was monitored by a CCD camera mated to an imaging lens positioned over the top of the device.

5.2.4 Digital Microfluidic Estrogen Extraction

The DMF-driven estrogen extraction technique was comprised of four steps. First, an aliquot of whole blood, serum, breast tissue homogenate, or estradiol standard solution was positioned in the sample reservoir of a device. Standard solutions were used immediately, and blood, serum, or tissue homogenate samples were allowed to dry on the surface. The top plate was then affixed and the solvents (DCM/acetone 80:20 v/v as lysing solvent, methanol as polar extracting solvent, and isooctane as non-polar extracting solvent) were loaded. Second, a series of reservoir volumes (9 x 1.1 µl or 5 x 2.2 µl) of DCM/acetone was dispensed and driven by DMF drop-wise to the sample, each of which was allowed to incubate at room temperature until dry (~1 min per reservoir volume). Third, a reservoir volume of methanol (1.1 or 2.2 µl) was dispensed and driven by DMF to the dried lysate to dissolve the steroids. A unit droplet of the dissolved sample (200 or 400 nl) was dispensed and delivered by DMF to the isooctane reservoir and circulated within the pool for ~20 s prior to driving the droplet out of the isooctane and towards the collection reservoir. This process was repeated until the sample reservoir was empty of the methanol. Fourth, step three was repeated with successive reservoir volumes of methanol (for a total of 9 x 1.1 µl or 5 x 2.2 µl) to ensure the extraction of all of the free estradiol. Finally, all extractate droplets were pooled in the output reservoir and allowed to dry. After collecting and drying the extract, the devices were stored at –20°C. Immediately prior to analysis, each extract was resolubilized in an aliquot (30 µl) of methanol/DCM (2:1 v/v).

5.2.5 Liquid Chromatography and Tandem Mass Spectrometry (LC-MS/MS)

LC-MS/MS with selected reaction monitoring (SRM) was used to evaluate estradiol in extractates from standard solutions, breast tissue homogenate, and blood. SRM is a highly selective method used to quantify a known analyte by tandem mass spectrometry. In SRM, two sequential mass selections are carried out, the first to isolate the analyte parent ion, and the second to isolate a fragment ion after reaction with a collision gas. The intensity of the fragment ion is recorded. Standard solutions (1 µl, 2 mg/ml in methanol) and blood (dried from 1 µl) were extracted by DMF (method one, as above) with no prior processing, while breast tissue (400 mg) was manually homogenized in DCM (1 ml), from which 1 µl samples were dried and processed similarly. In all cases, after extraction, samples were resuspended in 100 µl of methanol:water

(80:20 v/v), 10 µl of which was injected onto an HPLC (HP-Agilent 1100 series LC) interfaced by electrospray to a QTRAP LC-MS/MS (Applied Biosystems). The samples were analyzed in negative mode with SRM, evaluating an ion transition of *m/z* 271/145 to identify and determine the abundance of estradiol.[160] Operating parameters included 300 µl/min flow rate, 4200 V spray potential, 60 V collision energy and 400°C nebulizing temperature. A microbore (2.1 mm i.d. x 50 mm) Thermo Gold C18 (2.2 µm) column with isocratic elution via a mobile phase of methanol:water (80:20 v/v) was used for LC separation.

5.3 Results and Discussion

Estrogen and other steroid hormones are fundamental for growth and reproduction, and disturbances in their physiological levels can be associated with a multitude of clinical disorders, including hormone-sensitive cancers (for example, breast, endometrial and prostate cancers), infertility, and pregnancy complications such as intrauterine growth restriction.[161-165] Moreover, hormonal therapeutics have been used for decades as anti-cancer medications, contraceptives, hormone replacement, and fertility drugs.[166-171] Thus, there are a wide range of clinical conditions that require frequent monitoring of these hormones in tissue or blood for accurate diagnosis and treatment. Here, we report the extraction of the sex steroid estrogen in 1 μl volume samples using digital microfluidics (DMF). Figure 5.1a depicts the DMF device designed to adapt conventional techniques for estrogen extraction to the DMF format. As shown, an array of electrodes connects a series of reservoirs containing the sample and reagents. The process of estrogen extraction from a sample of human blood is depicted in Figure 5.1b. As shown, in typical assays, samples were lysed, the estradiol was extracted into a polar solvent (methanol), unwanted constituents were extracted into a non-polar solvent (isooctane), and the extractate was delivered to a collection reservoir. The device illustrated in Figure 5.1 could be used with breast tissue homogenate, whole blood, serum, and standard solutions.

The sample size required by DMF is 1000-4000 times smaller than that required for conventional methods of extraction and quantification of steroids including extraction followed by immunoassays or mass spectrometry.[151,152,172-175] As shown in Figure 5.2, the method could be applied to routine screening of breast estrogen concentrations in microaspirates as a potential marker of cancer risk, or blood estrogen in finger pricks to monitor hormone levels in infertility patients. In addition to the advantages that come with smaller samples, automation of the digital microfluidic method allows considerably less time- and labor-intensive assays relative to conventional processing techniques. Specifically, the conventional 5 to 6 hour hormone extraction techniques (including various liquid-liquid extraction and solid phase extraction based protocols) that require extensive pipetting, centrifugation and drying but could be replaced with the 10 to 20-min digital microfluidic process described here.

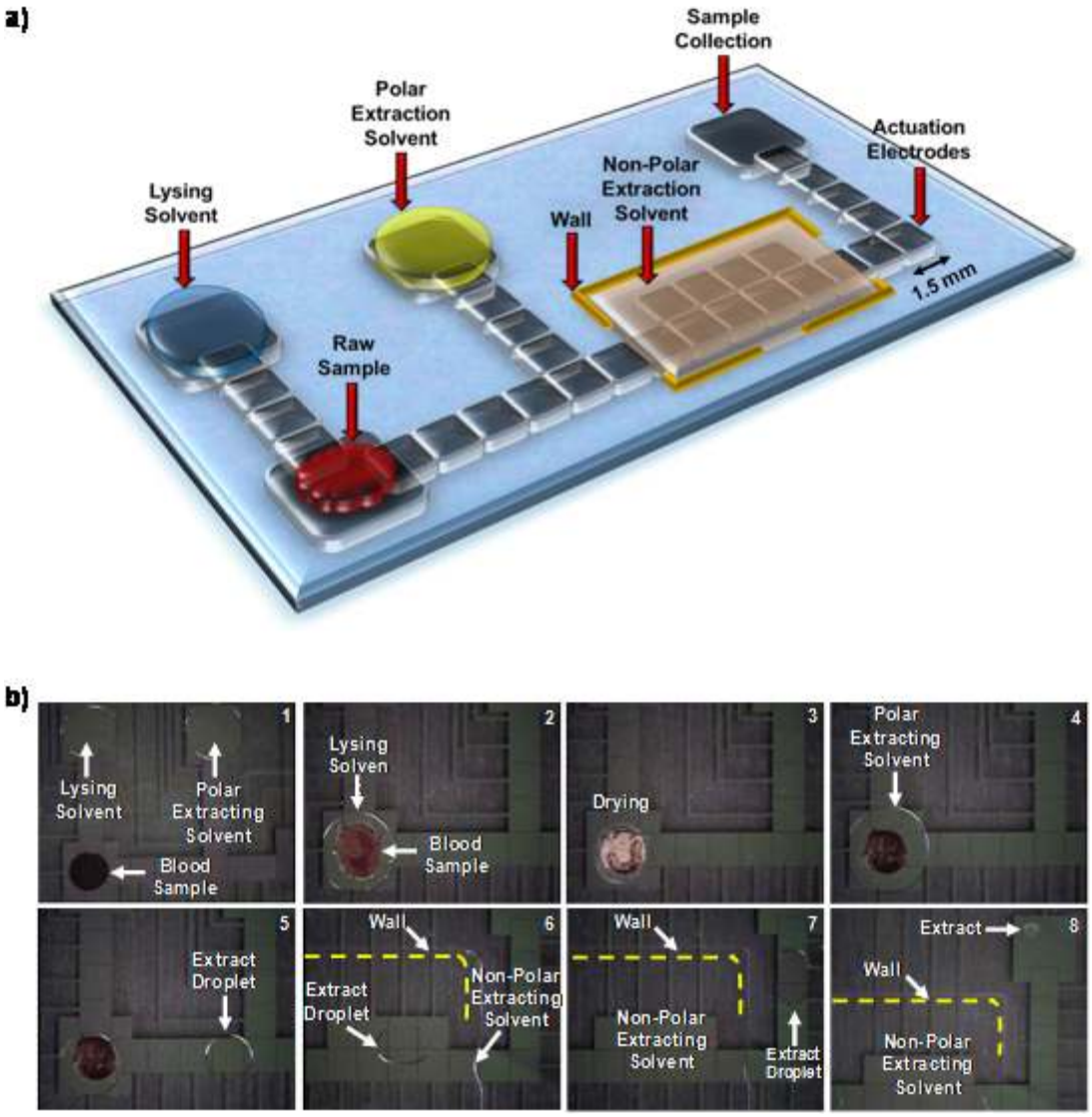

Figure 5.1 Digital Microfluidic (DMF) Device Design and Operation. a) Schematic of the DMF device, which includes sample and solvent reservoirs and the liquid-liquid extraction zone (bounded by a photoresist "wall"). b) A series of frames from a movie (1-8) illustrating the key steps in the DMF-based extraction of estrogen from a droplet of human blood (1 µl). As shown, samples are lysed, the estradiol is extracted into a polar solvent (methanol), unwanted constituents are extracted into a non-polar solvent (isooctane), and the extractate is delivered to a collection reservoir. Among the remarkable features of this technique is the ease with which the methanolic phase is controlled within the isooctane phase (frame 6) and then separated from it after liquid-liquid extraction (frame 7).

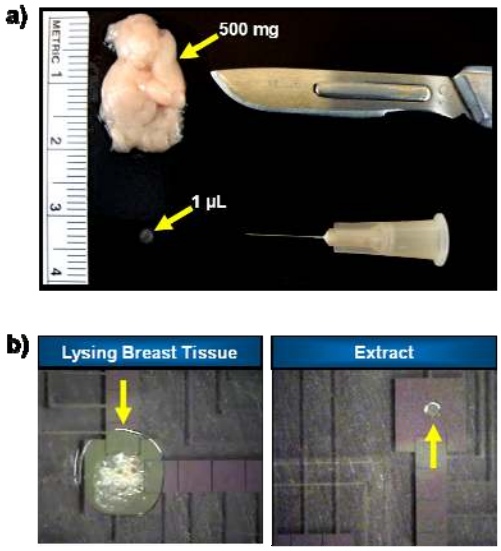

Figure 5.2 Reduction in Sample Volume. a) Picture of 500 mg of breast tissue collected by incisional biopsy (representing the sample size required for conventional analysis methods) compared to a 1 µl microaspirate collected using a 30 ga. needle (representing the sample size used with the new method). b) Pictures of breast tissue microaspirate (1 µl) being lysed on the DMF device and of the dried estrogen extracted from it.

To test whether estradiol can be quantified in samples extracted by the digital microfluidic method, liquid chromatography and tandem mass spectrometry (LC-MS/MS) with selected reaction monitoring (SRM) was used to evaluate estradiol extracted by DMF from standard solutions (Figure 5.3a), from breast tissue homogenate from a postmenopausal breast cancer patient (Figure 5.3b) and from whole blood from a female volunteer (Figure 5.3c). As shown, estradiol was detected with high signal-to-noise ratio (S/N) at retention time ~3.2 min for all cases. Further work will include developing ELISA and LC-MS/MS based methods for quantifying estradiol.

The method described here is powered by digital microfluidics,[23,159,176] a technology similar to but distinct from microchannel-based fluidics. Although microchannels are well suited for many applications (for example, electrophoresis, in vitro culture and analysis of cells), microchannel-based fluidics would likely be a poor match for the application described here. Indeed, in few reports[177-179] of microchannel-powered methods for liquid-liquid extraction (representing only one of the series of steps required for estrogen processing from clinical samples), the techniques have been inherently limited by the challenge of separating and collecting one liquid phase from the other after they have come into contact. In contrast, this step is straightforward in the method we have reported here (Fig. 5.1b, frame 7). The precise control

over different reagents,[180] phases[17] (see chapter 3) and volumes[21] afforded by digital microfluidics makes it a good match for this application.

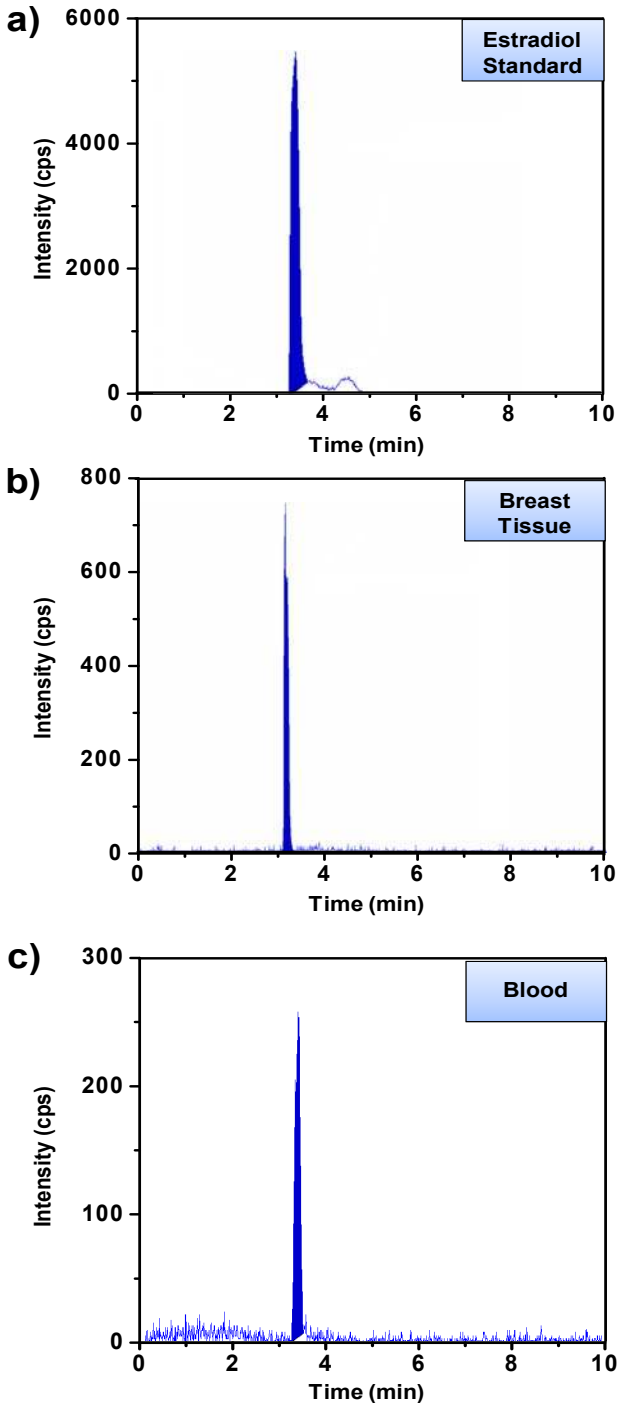

Figure 5.3 LC-MS/MS Analysis of DMF-Extracted Samples. Chromatograms generated by LC-MS/MS with selective reaction monitoring (SRM) from 1 µl samples of a) estradiol standard solution (2 mg/ml), b) breast tissue homogenate from a postmenopausal patient with breast cancer, and c) whole blood. The estradiol-specific ion pair evaluated for SRM was m/z 271/145.

5.4 Conclusion

In this chapter, we described a lab-on-a-chip method powered by digital microfluidics for sample clean-up and extraction of estradiol in microdrops of samples (breast tissue homogenate, whole blood, serum and standard solutions). We anticipate that integrated sample cleanup methods, such as the one described here, may prove useful for a wide range of clinically relevant applications in many different sample types.

Chapter 6 A Digital Microfluidic Method For Amino Acid Quantification in Dried Blood Spots

Screening the population for treatable congenital diseases is a major public health endeavor in countries around the world. In Ontario, Canada, for example, the Newborn Screening Ontario (NSO) facility at the Children's Hospital of Eastern Ontario evaluates approximately 140,000 babies each year for at least 28 diseases, including several inborn errors of amino acid metabolism. Each screening test requires collection of a blood sample which is spotted onto a piece of filter paper and dried. This dried blood spot (DBS) is then sent to NSO for analysis by tandem mass spectrometry (MS/MS). MS/MS is particularly powerful for this application, as it facilitates the detection of many analytes simultaneously in a single run. Unfortunately, this technique is slowed by an extensive sample preparation regimen (including excision/punching, extraction, evaporation, derivatization, and resolubilization), and in addition, high-throughput screening requires robotic sample handling. As a first-step towards solving these challenges, we have developed an integrated microfluidic system for processing samples for quantification of amino acids in blood. The new method is fast, robust, precise, and is capable of quantifying analytes associated with common congenital disorders such as homocystinuria, phenylketonuria, and tyrosinemia. We propose that the new method can potentially contribute to a new generation of sample preparation techniques for inborn errors of amino acid metabolism and other diseases. If widely applied, this could have a major impact on the bottom line for newborn screening programs around the world.

6.1 Introduction

Inborn errors of amino acid (AA) metabolism are a class of inherited diseases characterized by the inability to metabolize AAs; examples include homocystinuria (build-up of excess methionine and homocysteine), phenylketonuria (build-up of excess phenylalanine), and tyrosinemia (build-up of excess tyrosine and its metabolites).[181-184] If left untreated, these diseases can have serious consequences including mental and physical retardation, seizures, and death.[181,183,185,186] Because a symptom-free period is often present early in life, babies are routinely screened in the first days after birth. For example, a blood sample from every baby born in the province of Ontario, Canada is analyzed at the Newborn Screening Ontario (NSO) facility at the Children's Hospital of Eastern Ontario.[187] This represents a significant public health undertaking, requiring the evaluation of approximately 2,800 blood samples each week. Many jurisdictions around the world have instituted similar programs.[188-190]

In each newborn blood analysis,[187,191-193] a sample is obtained by pricking the subject's heel (or by venipuncture) and spotting the blood on a piece of filter paper; this is referred to as a "dried blood spot" (DBS). The DBS is couriered to the central facility, where 3.2 mm diameter circular discs are punched, and the analytes are extracted, mixed with isotope-labelled internal standards, derivatized, and then reconstituted for analysis by tandem mass spectrometry (MS/MS). As shown in Figure 6.1a, the derivatization step transforms each AA to its corresponding butyl ester (derivatized AA) that allows for a characteristic fragmentation pattern (neutral loss of 102) via collision induced dissociation (CID). This allows for quantification of most AAs in a single scan. Figure 6.1b-c contains representative primary (MS1) and secondary (MS2) mass spectra for the amino acid, phenylalanine, with peaks at m/z 222 and 120. In addition to amino acids, the same derivatization step butylates acylcarnitines (AC), which serve as markers of inborn errors of fatty acid and organic acid metabolism.[184,192]

As reviewed in a recent cover story in *Chemical and Engineering News*,[194] the success of DBS and MS/MS for newborn screening has led to a surge in popularity for these techniques for a wide spectrum of applications in clinical labs and the pharmaceutical industry. DBS methods allow for the collection of tiny amounts of sample and are convenient for long-term storage and cataloguing. MS/MS methods allow for the measurement of many different analytes in a single shot. But despite these advantages, a number of important challenges remain. For example,

maintenance of instruments (sample preparation robots and mass spectrometers) and plumbing (capillary tubes and associated connections) requires expertise and time.[192,195] In addition, the costs (~$20 per sample[196]) are magnified by the scale of operation (e.g., nearly 140,000 samples/year for NSO). Finally, collection procedures (i.e., spotting blood samples on filter paper) can suffer from challenges (e.g., uneven distribution or overlapping blood spots and supersaturated filter paper) that can skew results.[187,191,197] Thus, programs relying on DBS and MS/MS are continuously seeking innovative laboratory approaches and technologies that can improve sample preparation throughput and quality of analysis.

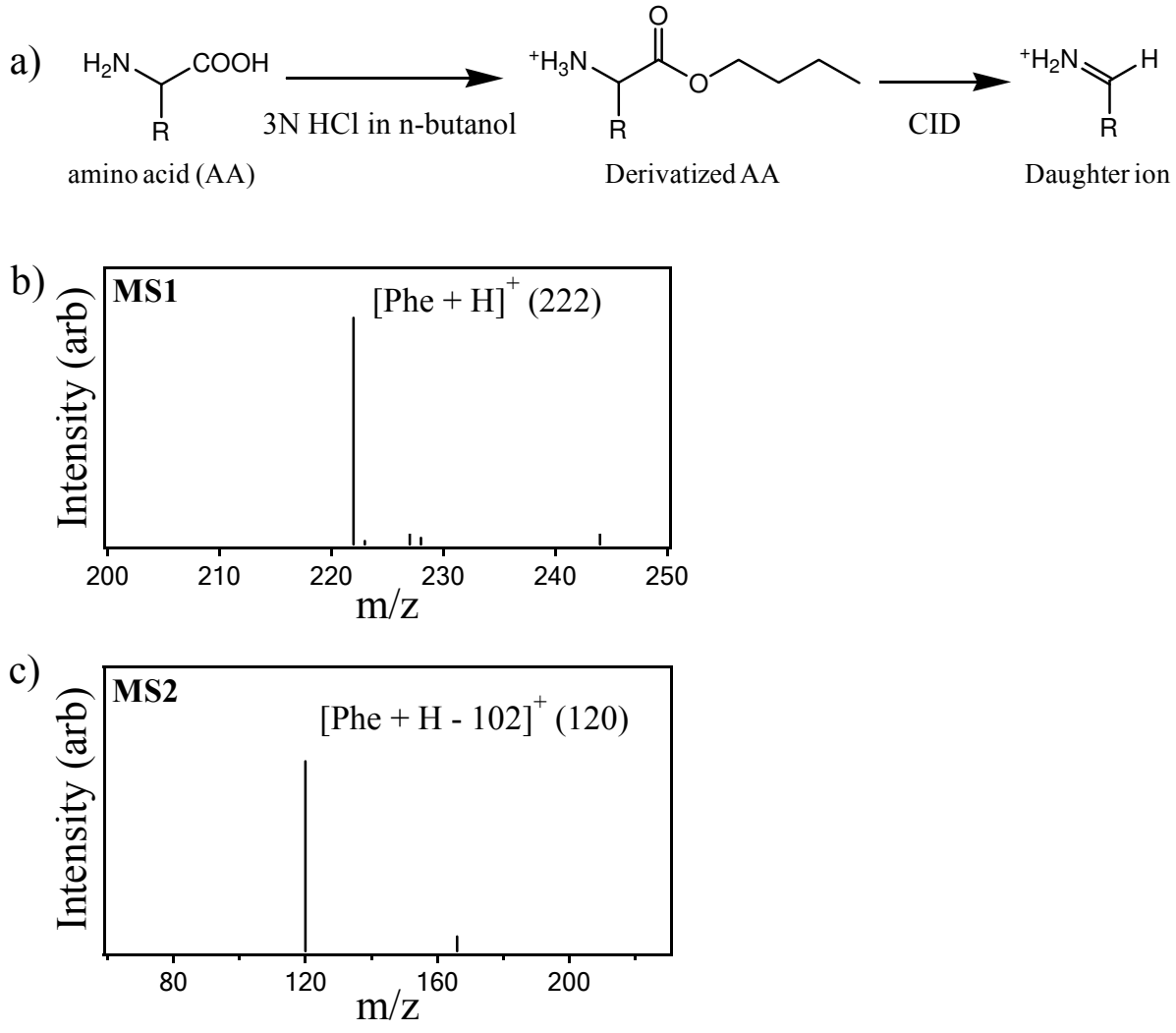

Figure 6.1 Processing blood samples for quantification of amino acids (AAs) by tandem mass spectrometry. (a) Reaction scheme involving derivatization of the extracted AA, followed by derivatization with n-butanol, followed by the formation of a daughter ion by collision induced dissociation (CID) in the mass spectrometer. (b) Mass spectrum generated from primary analysis (MS1) of derivatized phenyalanine (Phe). (c) Mass spectrum generated from the secondary analysis (MS2) of derivatized Phe showing the loss of 102 amu as a result of CID.

In this Chapter, we report a new automated method for quantifying analytes related to genetic diseases in newborn blood samples powered by digital microfluidics (DMF). DMF is a relatively new technique in which droplets are manipulated on an array of electrodes by application of electromechanical forces[14] and is useful for precise control of complex samples and reagents for biochemical analyses.[198] Moreover, as described previously,[18] DMF is particularly useful for extracting analytes from dried blood, as the solids stick to the device surface, allowing the extracted analytes to be ferried away for analysis in moving droplets. We report here a series of new DMF-driven methods for analyzing amino acids in newborn blood samples. This is the first report of microfluidic methods that are capable of direct analysis of analytes in DBS samples. The new methods are automated and have significant advantages relative to the conventional techniques in terms of sample preparation and reagent use. Moreover, the new technology is liberated from reliance on robots and capillary-plumbing. We propose that the methods may someday be a useful tool for newborn screening or other applications.

6.2 Experimental

6.2.1 Study Subjects

Blood samples were collected from a healthy adult male volunteer after a 10 h fasting period, and were kept at –20°C until analysis. Punches from residual dried blood spots from three infants screened by Newborn Screening Ontario (NSO, Ottawa, ON) were stored at -80°C until analysis.

6.2.2 Reagents and Materials

L-Methionine (Met), L-Phenylalanine (Phe), L-Tyrosine (Tyr), acetonitrile (ACN), acetone, methanol (MeOH), boric acid and fluorescamine were purchased from Sigma Chemical (Oakville, ON). Deuterated Methionine (Met-d_3), Phenylalanine (Phe-d_5), and Tyrosine (Tyr-d_4) were obtained from Cambridge Isotope Laboratories (Andover, MA). Concentrated hydrochloric acid (HCl) was purchased from Fisher Scientific (Ottawa, ON) and *n*-butanol from ACP Chemicals (Montreal, QC). In all experiments, organic solvents were HPLC grade and deionized (DI) water had a resistivity of 18 MΩ·cm at 25 °C.

Working solutions of all amino acids (AAs) (25, 50, 100 and 500 μM ea.) were prepared in DI water. For derivatization of extracted AAs, a 3 N HCl-butanol solution was prepared from a mixture of 12 N HCl/neat butanol (1:3 v/v). For analysis of AAs in blood samples, the extracting solvent (MeOH) contained 50 μM of the appropriate deuterated AA (d_3-Met, d_5-Phe or d_4-Tyr). For quantitative analysis of AA recovery from blood and for experiments mimicking diseased/healthy infant blood, samples were spiked with 200 μM of the appropriate AA (Met, Phe or Tyr). A series of 3.2 mm dia. punches of dried blood samples containing different concentrations of phenylalanine (see Table 6.1) were prepared by NSO staff as described previously.[193]

6.2.3 Non-Digital Microfluidic Sample Processing and Analysis

Amino acids were extracted and quantified from dried blood spot punches by NSO staff as described previously.[193]

6.2.4 Reagents and Materials for Fabrication

Concentrated sulfuric acid and hydrogen peroxide (30%) were from Fisher Scientific (Ottawa, ON), Parylene C dimer was from Specialty Coating Systems (Indianapolis, IN) and Teflon-AF was from DuPont (Wilmington, DE). Shipley S1811 photoresist and MF321 developer were from Rohm and Haas (Marlborough, MA), AZ300T photoresist stripper was from AZ Electronic Materials (Somerville, NJ), solid chromium was from Kurt J. Lesker Canada (Toronto, ON), CR-4 chromium etchant was from Cyantek (Fremont, CA), hexamethyldisilazane (HMDS) was from Shin-Etsu MicroSi (Phoenix, AZ), and Fluorinert was FC-40 from Sigma (Oakville, ON). Piranha solution was prepared as a 3/1 v/v mixture of sulfuric acid/hydrogen peroxide. Dicing tape (medium tack) was purchased from Semiconductor Equipment Corp. (Moorpark, CA).

Table 6.1 Measured phenylalanine (Phe) concentration in 3.2 mm dia. punches from filter paper bearing dried blood using digital microfluidic method 2 (left) and standard techniques at NSO (right). The average difference between the measurements generated by the two methods is 6.4%.

Sample	Measured Phe Concentration (μM) Using DMF Method 2	Measured Phe Concentration (μM) Using NSO Technique
1	70	70
2	550	548
3	93	88
4	93	92
5	368	302
6	534	539
7	735	871

6.2.5 DMF Device Fabrication and Operation

Digital microfluidic devices were fabricated in the University of Toronto Emerging Communications Technology Institute (ECTI) cleanroom facility, using a transparency photomask printed at Norwood Graphics (Toronto, ON). Glass devices bearing patterned chromium electrodes were formed by photolithography and etching as described previously [57], and were coated with 2.5 μm of Parylene-C and 50 nm of Teflon-AF. Parylene-C was applied using a vapor deposition instrument (Specialty Coating Systems), and Teflon-AF was spin-

coated (1% wt/wt in Fluorinert FC-40, 2000 rpm, 60 s) followed by post-baking on a hot-plate (160 ºC, 10 min). The polymer coatings were removed from contact pads by gentle scraping with a scalpel to facilitate electrical contact for droplet actuation. In addition to patterned devices, unpatterned indium tin oxide (ITO) coated glass substrates (Delta Technologies Ltd, Stillwater, MN) were coated with Teflon-AF (50 nm, as above).

The device design used in methods 1 and 2 featured an array of eighty-eight actuation electrodes (2.2 × 2.2 mm ea.) connected to ten reservoir electrodes (5 × 5 mm ea.), with inter-electrode gaps of 40 μm. For method 1, devices were assembled with an unpatterned ITO–glass top plate and a patterned bottom plate separated by a spacer formed from four pieces of double-sided tape (total spacer thickness 360 μm). For method 2, the two plates were separated by six pieces of double-sided tape (total spacer thickness 540 μm). To actuate droplets, driving potentials (70–100 V_{RMS}) were generated by amplifying the output of a function generator (Agilent Technologies, Santa Clara, CA) operating at 18 kHz. As described elsewhere,[19,57] droplets were sandwiched between the two plates and actuated by applying driving potentials between the top electrode (ground) and sequential electrodes on the bottom plate via the exposed contact pads. Droplet actuation was monitored and recorded by a CCD camera mounted on a lens.

6.2.6 Hybrid Device Fabrication and Operation

Hybrid DMF-microchannel devices used for method 3, were fabricated in four steps. First, a DMF bottom substrate (layer 2 in Figure 6.2) was fabricated as described above (but with no Teflon-AF coating). The design, shown in Figure 4 in the main text, was similar to that of the DMF-only devices, but with fewer electrodes – 2 rows of 9 actuation electrodes (2.2 x 2.2 mm) and 3 reservoir electrodes (5 x 5 mm).Moreover, the substrates were first modified by drilling an access hole (~2mm diameter) through the substrate using a micro drill-press (manufacturer, location) before the photolithographic processes. After patterning the electrodes, the opposite side was first coated with 7μm of Parylene-C for bonding with a second substrate (layer 3 in Figure 6.2). Second, a glass substrate bearing a microchannel nanoelectrospray tip (layer 3 in Figure 6.2) formed in Parylene was fabricated using methods similar to those described previously,[144] but with a few modifications. 37 grams of Parylene-C were deposited on piranha cleaned, silanized glass slide (25 x 55 mm) via vapour deposition. After Cr deposition, a

microchannel (25 µm wide x 5 mm long) was photolithographically patterned on the substrate by UV radiation (365nm, 35mW/cm^2, 50s) using a Karl-Suss MA6 mask aligner (Garching, Germany). Third, the channel side of layer 3 was mated to the non-electrode side of layer 2, placed under pressre in a precision vise (~20 MPa), and thermally bonded in a vacuum oven (200˚C, 24 h). After cooling, the top of layer 2 was first coated with 2 µm of parylene followed by spin-coating 50 nm of Teflon-AF with a small piece of dicing tape covering the accessing hole. The tape was removed before post-baking on a hot plate (160˚C, 10min). Fourth, the top plate (layer 1 in Figure 6.2) was assembled with spacers formed from four pieces of double-sided tape as described above for droplet actuation.

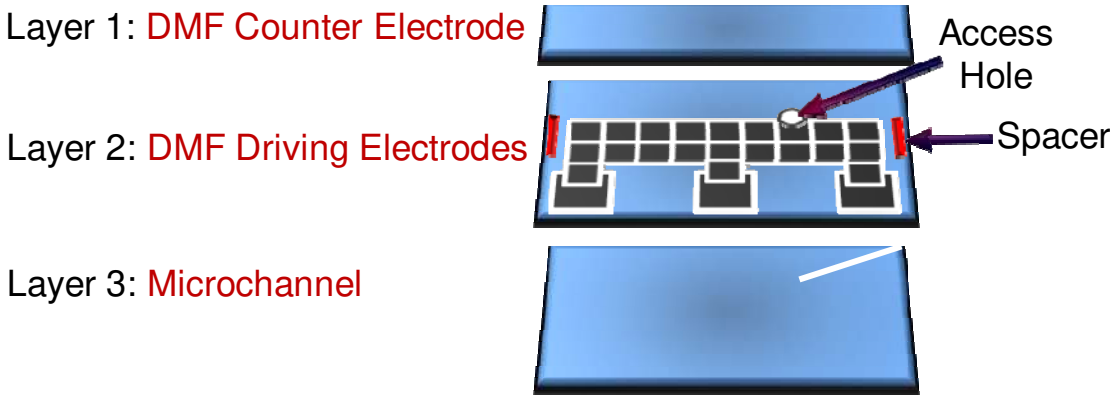

Figure 6.2. Exploded view schematic of the hybrid DMF-microchannel device used for method 3 for in-line analysis by mass spectrometry.

6.2.7 Digital Microfluidic-Driven Sample Processing

For samples analyzed by digital microfluidic methods 1 and 3, 5-µL droplets of blood were spotted onto the bottom plate of a device and dried. The top plate was then affixed and two solvents were loaded into the appropriate reservoirs, including MeOH containing 50 µM of deuterated AA (extraction solvent), and 3 N HCl-butanol (derivatization solvent). A reservoir volume (10 µL) of extraction solvent was dispensed and driven by DMF to the dried sample and allowed to incubate (5 min). The extraction solvent was then actuated away from the sample and dried (~15 min, room temperature) at a second site, after which a reservoir volume (10 µL) of derivatization solvent was dispensed to the dried extract and incubated for 15 min at 75ºC. Following the reaction, the top plate was removed and the solvent was allowed to evaporate (~15 min, room temperature). For samples analyzed by method 2, the process was identical to the

above, but with two differences: (1) punches (3.2 mm dia.) from filter paper bearing dried blood were positioned on the bottom plate of a device in place of liquid blood, and (2) a larger volume (15 μL) of extraction solvent was used.

6.2.8 Digital Microfluidic-Driven Sample Analysis

Samples processed by digital microfluidic methods 1 and 2 were analyzed offline by nanoelectrospray tandem mass spectrometry (nESI-MS/MS). Such samples (stored dry on device or in centrifuge tube until analysis) were reconstituted in 70 μl of acetonitrile/water (4:1 v/v); samples originating from blood were, in addition, passed through PVDF membrane centrifuge-filters with 0.1 μm pore diameter (Millipore, ON). Samples were injected into an LTQ Mass Spectrometer (Thermo Scientific) via a fused silica capillary transfer line (100 μm i.d.) mated to a New Objective Inc. (Woburn, MA) nanoelectrospray emitter (100 μm i.d. tapering to 50 μm i.d.) at a flow rate of 0.8 μL min^{-1}, with an applied voltage of 1.7-1.9 kV and capillary temperature of 200°C. Tandem MS/MS analysis was carried out by introducing 30% collision energy to the parent ions and then the fragments over the *m/z* range of 100-300 were scanned. AA daughter ions detected in the second mass selection, which exhibit a loss of butylformate ($HCOOC_4H_9$, 102 *m/z*), were observed and used for quantification. Spectra were collected as an average of 50 acquisitions, and replicate spectra were obtained for DMF-derivatized samples of both control and blood. For samples processed by method 3 (Fig. 6.3c), devices bearing an integrated nESI emitter were mounted on a 3-axis micromanipulator (Edmund Optics, NJ) positioned near the inlet of the LTQ MS. After sample processing, a spray was generated by applying 2.5-3.0 kV to a platinum wire inserted in the access hole, with parameters identical to the above.

For samples processed by digital microfluidic method 1, calibration plots were generated by plotting the MS/MS intensity ratio of daughter ions from the extracted AAs relative to the those of the internal standards (i.e., Met *m/z* 104:107, Phe *m/z* 120:125, and Tyr *m/z* 136:140) as a function of AA concentration in standard solutions (25-500 μM in DI water). Data points included in the calibration plots represent an average of at least 4 replicate measurements, and the data in each plot were fit with a linear regression. Blood samples were then evaluated (with on-chip derivatization and extraction, and measurement by MS/MS relative to internal standards,

as above), and the values were compared to the calibration plots to determine the AA concentrations.

For samples processed by digital microfluidic method 2, quantitation was similar to that for method 1, except that standards were formed from adult male blood spiked with Phe to different concentrations (25-900 μM) which was pipetted onto sheets of filter paper (Whatman, NJ) allowed to dry, and punched (3.2 mm dia.). Newborn blood samples (as DBS filter paper punches) from NSO were then analyzed as above and compared with the calibration plot to determine the Phe concentrations.

6.2.9 Digital Microfluidic-Driven Sample Recovery Determination

The % recovery of AAs in Method 1 was evaluated quantitatively using (i) a fluorescence-based assay and (ii) MS/MS. For (i), control samples (Met, Phe or Tyr; 50 μM of each) were processed by DMF (as above), excluding the derivatization step. The dried extracts were diluted into 95 μL aliquots of borate buffer (20 mM, pH 8.5) in wells in a 96-well microplate. Upon addition of 5 μL of fluorescamine (5 mg/mL in acetone) the microplate was inserted into a fluorescence microplate reader (Pherastar, BMG Labtech, Durham, NC) equipped with a module for 390 nm excitation and 510 nm emission. The plate was shaken (5 s) and the fluorescence was measured. As a control, identical samples that had not been extracted were evaluated using the same fluorescence assay. To ensure that controls were processed in identical manner relative to extracted samples, each control sample was spotted on a device, dried and then reconstituted in buffer for analyses. Four replicate measurements were made for each sample and control. For (ii), blood samples of known AA concentrations were spiked with 200 μM of AA standards and extracted (as above). Knowing the total concentration of AAs in blood spots (e.g. native methionine concentration plus spiked methionine), % recovery was obtained by comparing the concentration values (obtained from calibration curves) vs. the known values.

6.3 Results and Discussion

Digital microfluidic methods were developed to automate the quantification of methionine as a marker for homocystinuria, phenylalanine as a marker for phenylketonuria, and tyrosine as a marker for tyrosinemia in newborn blood samples. (Note that for Type 1 Tyrosinemia, succinylacetone[184] is typically measured as a primary screen.) To accommodate different sampling and analysis needs, three related methods were developed. As shown in Figure 6.3, in method 1, a sample of liquid blood is spotted directly onto a device and allowed to dry. In method 2, a punched sample of filter paper bearing dried blood is deposited onto a device for analysis. In methods 1 and 2, analysis is carried out off-line, while in method 3, an integrated nanoelectrospray emitter facilitates in-line analysis with mass spectrometry.

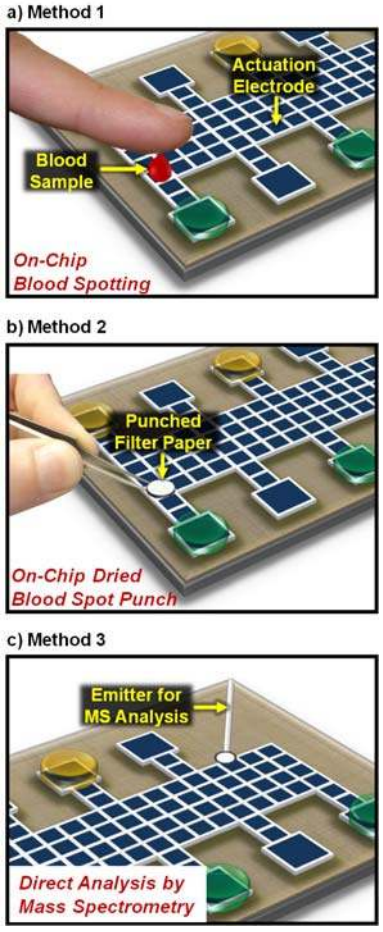

Figure 6.3 Three digital microfluidic methods designed to quantify amino acids in newborn samples of blood. In method 1 (a), a 5 µL droplet of blood is spotted directly onto the device surface and allowed to dry. In method 2 (b), a 3.2-mm diameter punch from filter paper bearing dried blood is positioned on the device surface. In method 3 (c), a microchannel nanoelectrospray emitter is coupled to the device to facilitate inline analysis by tandem mass spectrometry (MS/MS).

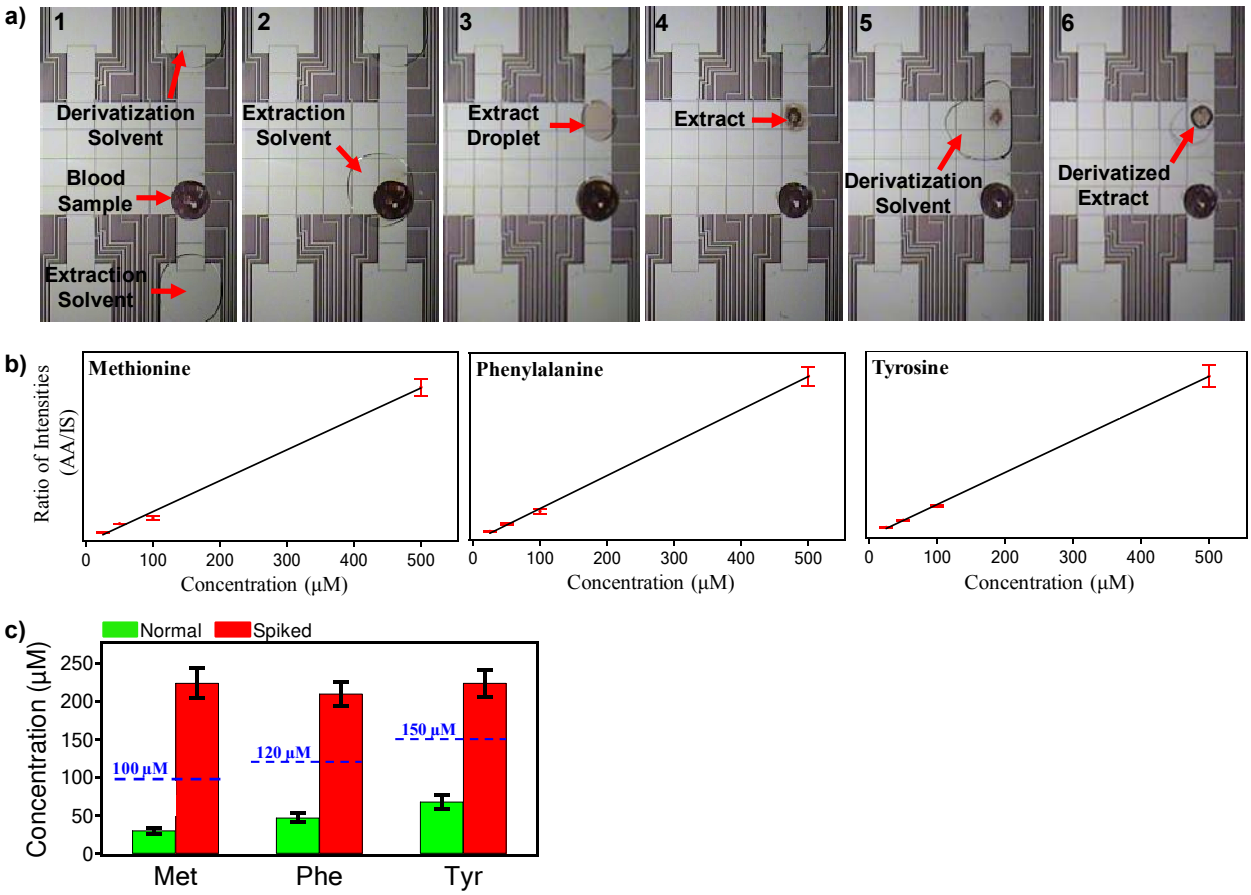

Figure 6.4 Analysis of amino acids in blood by digital microfliudic method 1. a) Sequence of frames from a movie depicting several stages in sample processing by DMF including: (1) a dried blood sample prior to processing; (2) mixing and incubating an extractant droplet with the sample; (3) a droplet containing sample extract after translation away from the dried sample; (4) a dried extract; (5) mixing and incubating a derivatization reagent droplet with the dried extract; and (6) the dried, derivatized product. b) Calibration curves generated by DMF method 1 for quantification of methionine (Met), phenylalanine (Phe), and tyrosine (Tyr). Data were generated by plotting the intensity ratios of the daughter ions of each amino acid (AA) relative to their deuterated internal standard (IS) (i.e., d3-Met, d5-Phe, d4-Tyr, respectively) as a function of AA concentration. Each data point represents at least four replicate measurements, and error bars represent ±1 S.D. Regression lines were linear with $R^2 > 0.996$ for each analyte. c) Comparison of Met, Phe, and Tyr concentrations in normal (green) and spiked (red) blood samples as biomarkers for homocystinuria, phenylketonuria, and tyrosinemia, respectively. The dashed lines indicate the upper levels for normal concentrations in newborn blood samples. Each data point represents at least four replicate measurements, and error bars represent ±1 S.D.

While the most common method for newborn screening relies on DBS samples on filter paper, we propose that for some cases, it may be useful to analyze blood samples that are dried directly onto the surface of a device, as in method 1 (Figure 6.3a). An experiment using method 1 is depicted in Figure 6.4a. As shown, a blood sample is spotted onto the device, dried, extracted into methanol containing isotope-labelled standards, and the solvent is allowed to evaporate. The extract and standards are then derivatized, and the products are isolated by allowing the solvent to evaporate. The entire process requires 50 min to complete. Samples processed by method 1 were collected and analyzed off-line by nanoelectrospray ionization tandem mass spectrometry (nESI-MS/MS) to quantify AAs. Calibration curves with R^2 greater than 0.996 (Figure 6.4b) were generated for Met, Phe, and Tyr by analyzing standards processed by DMF at known concentrations from the abundance ratio of each AA to its deuterated standard peak in the secondary (MS2) spectra. As listed in Table 6.2, when method 1 was used to evaluate blood collected from an adult male volunteer, the values obtained were in the expected physiological range and the precision in the method was high with coefficients of variation (CVs) ranging from 5 to 11%.

Table 6.2. Concentrations of amino acids in blood of an adulte male volunteer measured by digital microfluidic method 1 (left column) and normal concentration ranges (right column).

Amino Acid	Measured Blood Concentration (μM) ± 1 S.D.	Normal Blood Concentration (μM)
Methionine	25 ± 2	16-33[199,200]
Phenylalanine	38 ± 2	41-68[199,201]
Tyrosine	46 ± 5	45-74[199,202]

To evaluate the potential of DMF method 1 as a platform for discriminating between disease and healthy states in blood, spiked blood samples (mimicking diseased states) and non-spiked blood samples (mimicking healthy state) were analyzed by mass spectrometry. Figure 6.4c shows a comparison of measured concentration of AAs in normal and spiked blood samples. The dashed line indicates typical threshold values indicative of homocysteinuria (100 μM Met)[187,203] phenylketonuria (120 μM Phe)[204,205] and tyrosinemia (150 μM Tyr)[184,203]. As shown, the method is useful for distinguishing between these concentrations.

Extraction efficiency is an important parameter for any new analytical method. To evaluate the extraction efficiency of DMF method 1, two orthogonal tests were used: fluorescence and MS/MS. In the former test, fluorescamine, a fluorogenic reagent that exhibits no fluorescence until it reacts with primary amines[121] was used to label standard samples before and after extraction to determine concentrations. In the latter test, blood samples were spiked with AA and recovery was determined by comparing the AA concentration (endogenous plus spiked AA) vs. known concentration. As listed in Table 6.3, the two orthogonal methods (fluorescence and MS/MS) agree and reveal the new DMF technique to be very efficient. Recovery was ≥80% for each sample evaluated. As above, the precision of these measurements was high, with CVs ranging from 1 to 10%.

Table 6.3. % Recovery of digital microfluidic method 1 measured by fluorescence (left) and MS/MS (right)

Amino Acid	% Recovery by Fluorescence ± 1 S.D.	% Recovery by MS/MS ± 1 S.D.
Methionine	98 ± 10	100 ± 1
Phenylalanine	86 ± 9	85 ± 5
Tyrosine	82 ± 10	84 ± 7

As noted above, dried blood spots (DBS) are surging in popularity for a wide range of applications in clinical chemistry and the pharmaceutical industry.[194] We developed digital microfluidic method 2 (Figure 6.3b) to analyze punched discs from DBS. A portion of an experiment is depicted in Figure 6.5a. As shown, a droplet of extraction solvent was dispensed and driven to a 3.2 mm diameter filter paper punch, and the extract was then moved away for further processing (i.e., derivatization and solvent exchange, similar to Figure 6.4a). Like method 1, this process requires ~50 min to complete. Although analytes extracted from DBS samples (using conventional means) have been analyzed by microfluidic methods,[206] as far as we are aware, DMF method 2 is the first microfluidic method that has been reported that can accept a DBS punch directly as a sample input.

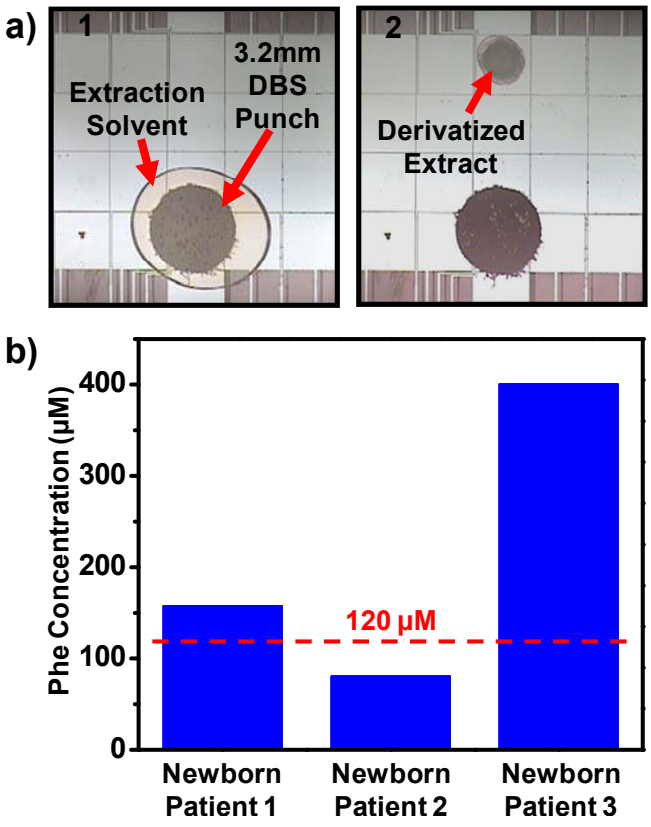

Figure 6.5 Analysis of amino acids in blood by digital microfliudic method 2. a) Frames from a movie depicting sample processing of 3.2 mm diameter punch of a dried blood spot (DBS) on filter paper by digital microfluidics (DMF). b) Graph of Phe concentrations measured by the digital microfluidic method in DBS punches from three NSO patients. As shown, patients 1 and 3 were correctly diagnosed as having phenylketonuria, and patient 2 was correctly identified as being unaffected. The dashed lines indicates the upper level for normal concentrations of Phe in newborn blood samples.

To evaluate digital microfluidic method 2 relative to gold standard practices, a series of punches from blood samples containing various concentrations of Phe were processed by DMF method 2 and analyzed in Toronto, and identical punches were evaluated using the routine newborn screening technique in Ottawa. As listed in Table 6.1, a paired *t*-test revealed no significant difference between the two data sets at a 95% confidence level. To validate the new technique for application to clinical samples, DBS punches from three newborn patients of NSO were evaluated by the DMF method. As shown in Figure 6.5b, the new technique correctly identified patients 1 and 3 as suffering from phenylketonuria, and patient 2 as being unaffected.

While the data described above were generated with microfluidic sample processing and off-line analysis, there may be some cases in which a fully integrated (processing + analysis) method is useful. To accommodate this need, method 3 (Figure 6.3c) was developed in which a digital microfluidic platform was coupled directly to a nanoelectrospray emitter for in-line analysis by mass spectrometry. As shown in Figure 6.2, the central feature of this method (building on recent work with hybrid microfluidics[39]) is an intersection of a DMF electrode and a microchannel through a vertical hole. In this device, droplets are manipulated on the top surface, and are subsequently transferred to microchannels on the bottom of the device through the hole. A portion of an experiment using method 3 is depicted in Figure 6.6a. A blood sample was first spotted on the device as in method 1 (note that analogous methods could be developed using DBS samples similar to method 2) and the AAs were extracted and derivatized as described above. The dried, derivatized sample was then resuspended and the droplet was actuated to the access hole such that it filled the channel below by capillary action. A nanoelectrospray is generated at a corner of the device[144,207] (Figure 6.6b) by applying a high voltage to the counter electrode. Representative mass spectra generated from samples processed and analyzed on-chip are shown in Figure 6.6c. The entire process requires ~1 h from sampling to analysis, and requires only the hybrid DMF device and a mass spectrometer (i.e., no nanoflow pumps, capillary connections, robots, or samplers).

Newborn screening programs have been implemented around the world to detect aminoacidopathies at an early stage.[188,190,208] Tandem mass spectrometry, which facilitates the simultaneous quantification of multiple analytes, is particularly useful for such programs, but the technique is hampered by disadvantages associated with sample preparation. Here, we report a new automated microfluidic method powered by DMF for quantifying amino acids in blood

samples, and present proof-of-concept results demonstrating that it may be useful for screening samples for homocystinuria, phenylketonuria, and certain types of tyrosinemia. The new method has several advantages relative to the conventional techniques, which are discussed below.

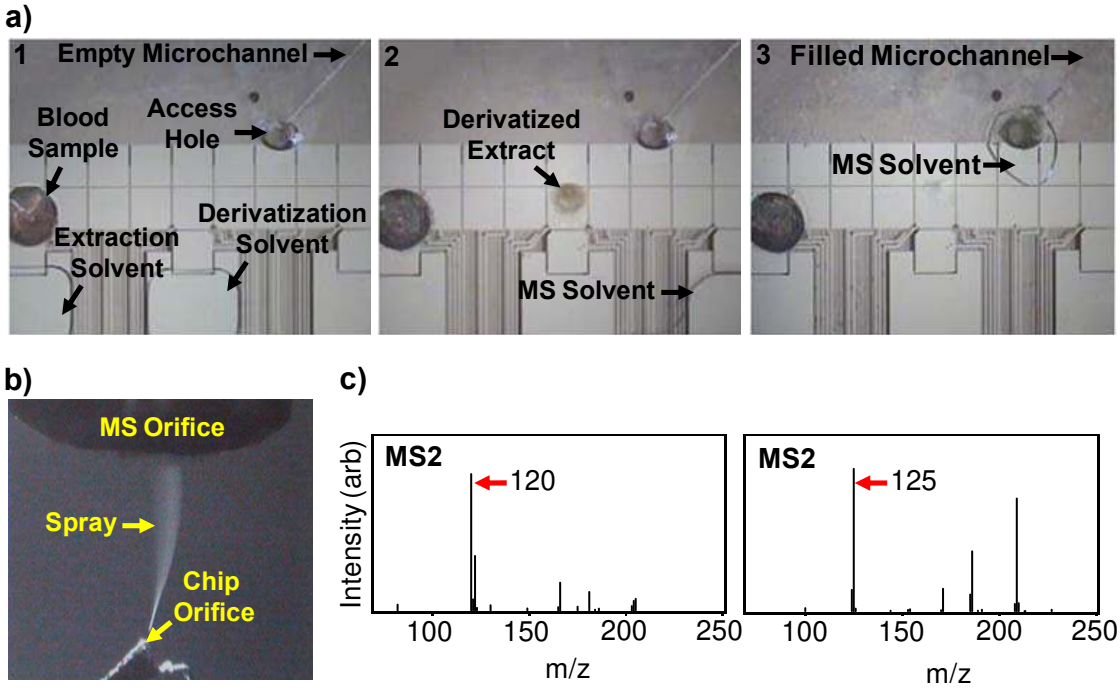

Figure 6.6 Analysis of amino acids in blood by digital microfliudic method 3. a) Frames from a movie (left-to-right) demonstrating derivatization and extraction of AA from dried blood, resolubilization in solvent, and analyte solution in spray microchannel. b) Image of sample spraying from an integrated emitter. c) MS2 spectra of Phe (left) and d_5-Phe (right) generated from blood samples.

An obvious advantage of the microfluidic methods relative to conventional techniques is automation -- a single technician using instruments powered by digital microfluidics could likely do the work of several technicians using conventional methods. Furthermore, the digital microfluidic techniques facilitate reduction in reagent use [20 µL vs. 170-450 µL[184,209,210]], and a reduction in analysis time [~1 h vs. >3.5 h[192,195]]. Note that the 3.5 h required by the conventional method is for analysis of 96 samples, while the 1 h required by the new method is for the analysis of 3 samples. We propose that future generations of the digital microfluidic technique should be capable of accommodating 96 samples in parallel.

Another advantage of the new technique is the potential for integration directly with mass spectrometry (Figure 6.6). Nanoflow electrospray ionization (nESI) is used in nearly all newborn screening laboratories, and is a finicky technique requiring operator expertise and vigilance to

achieve reproducible results. This is a serious limitation, and is part of the reason why all newborn blood samples in Ontario are mailed to a single facility.[187] Indeed, a recent editorial on this subject decried the inherent limitations of systems relying on "conventional electrospray plumbing including capillary tubes etc".[192] The device shown in Figure 6.6a is the first ever reported to integrate digital microfluidics with in-line mass spectrometry. In this design, the nESI plumbing is built-in to the device by standard batch-processing. Sample analysis is realized simply by positioning a device in front of the mass spectrometer and applying an electrical potential.

Over the past two decades MS/MS has revolutionized newborn screening, replacing the tests used historically for diagnosing amino acid disorders (i.e., Guthrie's bacterial inhibition[211] and fluorometric[212] and enzymatic[213] tests). This is mainly because MS/MS facilitates the analysis of multiple analytes simultaneously in a single run in comparison to the traditional single-analyte assays, which improves efficiency and reduces costs.[183,192] In this work, we present the first method to combine microfluidic sample handling and preparation with MS/MS for analysis of amino acids. Note that there are other metabolic and non-metabolic disorders (e.g., cystic fibrosis, congenital hypothyroidism, biotinidase deficiency, galactosemia) that are commonly screened in newborns that are not routinely detected by MS/MS. Instead, these diseases are evaluated by enzyme-, DNA-, or immunoassay-based tests[183,214] and a variety of new technologies[214,215] (including digital microfluidics[216]) are being developed to implement them. We speculate that future microfluidic systems might be capable of implementing all of the necessary tests, including those that rely on mass spectrometry and those that do not.

The current work demonstrates proof-of-concept for quantification of three amino acids (methionine, phenylalanine, and tyrosine) that are often measured for early diagnosis of diseases in newborn screening, and in on-going work, the goal is to extend the technique to be compatible with the full suite of diseases tested by MS/MS by NSO.[187] If successful, we propose that these methods might be useful for a wide range of applications. For example, we propose that blood samples could be spotted directly onto inexpensive devices[217,218] (or removable device coverings[51]), after which they would be returned to a laboratory for analysis, with results obtained more efficiently than they are today. Alternatively, punches from DBS samples could be used (i.e., method 2), and either sampling technique might be combined with in-line analysis (i.e., method 3). Given the nature of the problem (quantifying multiple analytes from tiny blood

samples) and context (soaring medical and drug discovery costs), these new methods, which combine rapid, efficient microfluidic sample preparation with tandem mass spectrometry, are an attractive advance for the field of analytical science.

6.4 Conclusion

In this chapter, we report new a method for sample processing and analysis of markers of amino acids in dried blood samples using an integrated microfluidic device. The new methods are automated, and facilitate significant reductions in reagent consumption. In addition, the new methods have built-in plumbing for direct interfacing with mass spectrometry. We propose that these advances have the potential to contribute to a new paradigm of fast, inexpensive screening.

Concluding Remarks and Future Potentials

In the work described in this dissertation, digital microfluidics (DMF) was used for applications in chemistry, biology and medicine. Here, I summarize my contributions in each of these areas and propose suggestions for directions for future work.

Chemistry

A DMF-driven method for parallel-scale synthesis was developed and is described in chapter 2. The device was designed to handle diverse reagents and multiple reaction steps and was capable of forming five products in parallel with no need for complex networks of tubing and microvalves. The multiplexing demonstrated here is likely just the beginning; I propose that in the future, the device architecture should be expanded to facilitate split-and-pool combinatorial synthesis of tens or even hundreds of products simultaneously. Additionally, I propose that the device would be improved through interfacing to microchannels (as in chapter 4) for interfacing to a mass spectrometer (MS) for in-line analyses (as in chapter 6). Finally, it's worth mentioning that in its conventional format, DMF is not appropriate for all synthetic applications (e.g., reactions performed at high temperature and pressure). Thus, I propose that there is tremendous room for innovation in device format and operation.

Biology

I presented the first DMF-driven method for extracting proteins from heterogeneous mixtures via precipitation in chapter 3. The new method has comparable performance relative to conventional techniques, combined with the advantages of reduced reagent and sample consumption, and no centrifugation. The results suggest great potential for digital microfluidics for automated proteomic biomarker discovery, but the results in chapter 3 represent only the first step of many. To reach that goal, several new methods must be developed, including: (1) an integrated DMF device incorporating sample reduction, alkylation, and digestion; (2) a microfluidic platform comprising a sample preparation DMF platform coupled to a network of microchannels for separations. A prototype of the latter method is described in chapter 4 -- a multilayer hybrid microfluidic configuration in which a digital microfluidic module is interfaced to a network of microchannels. This platform was capable of performing multi-step enzymatic digestion followed by electrophoretic separations. Additional future experiments will include equipping microchannels with monoliths to carry out two-dimensional chromatography (i.e.,

Strong cation-exchange followed by reverse phase separations), which is a key requirement prior to tandem MS/MS analyses in the proteomic technology.

Medicine

The first DMF-driven method for sample clean-up and extraction of estradiol in 1μL of clinical samples (i.e., whole blood, serum and breast-tissue homogenates) is presented in chapter 5. The new method is fast and features >1000x reduction in sample use relative to conventional techniques. But estradiol is just the beginning. Future experiments will include validating the compatibility of the new method with the extraction of other hormones (e.g., progesterone and testosterone) that are involved in hormone-sensitive diseases such as infertility. In chapter 6, a new method for rapid processing and analysis of inborn amino acid diseases using an integrated microfluidic device was presented. The new method has built-in plumbing for direct interfacing with mass spectrometry, which has the potential to contribute to a new generation of fast, inexpensive screening for congenital diseases. The current work demonstrates proof-of-concept for quantification of three amino acids (methionine, phenylalanine, and tyrosine) that are often measured for early diagnosis of diseases in newborn screening, and for future work, I anticipate the extension of the technique to be compatible with the full suite of diseases tested by newborn screening programs. For example, future DMF platforms will incorporate more reagents for extracting and derivatizing other sets of biomarkers such as organic acids and acylcarnitines to screen for many diseases at once.

Appendix 1 Digital Microfluidics For Automated Proteomic Processing

Digital Microfluidics (DMF) is a technique characterized by the manipulation of discrete droplets (~nL - mL) on an array of electrodes by the application of electrical fields. It is well-suited for carrying out rapid, sequential, miniaturized automated biochemical assays. Here, I report a DMF platform capable of automating several processing steps (extraction, reduction, alkylation, digestion) used in proteomic analyses.

A1.1 Protocol

A1.1.1 Device Fabrication

1. Clean glass substrates in piranha solution (3:1 conc. sulfuric acid: 30% hydrogen peroxide). Leave the substrates in piranha solution for 10 min with frequent agitation.
2. After rinsing in deionized (DI) water and drying the substrates with N_2 gas, place the substrates inside the electron beam deposition chamber for chromium deposition (thickness of 250 nm).
3. To dehydrate the chromium-coated substrate, rinse in isopropanol and then bake on a hot plate for 5 min at 115°C.
4. Dry the substrates and prime with hexamethyldisilazane (HMDS) by spin-coating (30 s, 3000 rpm). Spin-coat again (using identical parameters) with Shipley S1811 photoresist.
5. Pre-bake the substrate on a hot-plate (100°C, 2 min), then pattern the photoresist by exposure to ultraviolet (UV) irradiation for 5 s through a photomask.
6. Develop the UV-exposed substrates in Shipley MF 321 developer for 3 min and wash in DI water. Post-bake on a hot-plate at 100°C for 1 min.
7. Etch the exposed chromium by immersing in chromium etchant for 30 s. Rinse and immerse in AZ300T stripper for 10 min to remove the remaining photoresist. Rinse in DI water and dry with N2 gas.
8. Deposit 2-5 μm Parylene-C (an insulating polymer) by chemical vapour deposition onto a substrate bearing patterned chromium. Deposit 50 nm of Teflon-AF (to make the surface hydrophobic) by spin-coating a solution (1% wt/wt in Fluorinert FC-40) at 2000 rpm for 60 s. Post-bake on a hot-plate (160 °C, 10 min).
9. To form the top plate, coat an un-patterned indium tin oxide (ITO) glass substrates 50 nm Teflon-AF, as above.

A1.1.2 Device Setup and Automation

1. In digital microfluidic devices operated in "two-plate" configuration,[13] droplets are positioned between a bottom substrate (with patterned electrodes) and a top substrate (with one contiguous, transparent electrode, typically formed from ITO).
2. To set the device up, remove polymer coatings from the contact pads of a bottom substrate by gentle scraping with a scalpel. Couple the exposed pads of the bottom substrate with 40-pin connectors (Fig. 1a).
3. Power-on a computer running LabView (National Instruments, Austin, TX), a home-built control box (featuring an array of high-voltage relays that are controlled by signals from a National Instruments DaqPad), a function generator, and an amplifier. The computer/control box facilitates user control over application of 100 VRMS/18 kHz signals to the device via the 40-pin connectors.
4. Assemble the device by positioning two pieces of double-sided tape (140 μm total thickness) on the edges of the bottom substrate and complete with unpatterned ITO slides (top plate).
5. To initialize the control system, run the LabView calibration program (written in-house) to calibrate the feedback control.
6. Load the sample and reagents into the appropriate reservoirs and enclose them under the top substrate (Teflon-coated side facing down). Attach the ground connector to the top substrate.
7. Load the actuation code in LabView (written in-house) and execute the program to initiate droplet actuation.

A1.1.3 Sample and Reagent Preparation

1. Prepare working buffer (WB): 100 mM TrisHCl (pH 7.8) and 0.08% Pluronic F127 w/v.
2. Dissolve protein(s) to be analyzed in WB and pipette sample into reservoir 1 (R-1) on the device, as shown in Fig. 1b.
3. Prepare precipitant, 20% Trichloroacetic acid (TCA) in DI water, and pipette into R-2.
4. Prepare wash buffer, 70/30 Chloroform/acetonitrile (ACN) and pipette into R-4.

5. Prepare resolubilizing buffer, 100 mM Ammonium Bicarbonate (pH 8.0) and 0.08% Pluronic F127 w/v, and pipette into R-5.
6. Dissolve reductant, *tris*(2-carboxyethyl) phosphine (TCEP), at 10 mM in WB and pipette into R-6.
7. Dissolve alkylating agent, iodoacetamide (IAM), at 12 mM in WB and pipette into R-7.
8. Dissolve trypsin in WB at a concentration equal to1/5 of the concentration of the total protein sample and pipette into R-8.

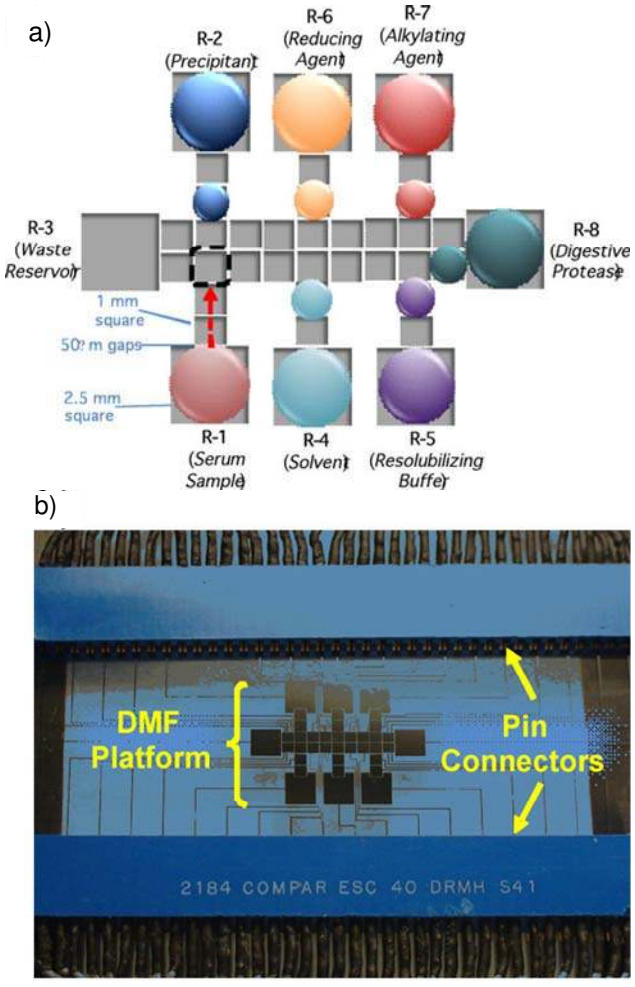

Figure A1.1 a) A picture a DMF device mated to 40-pin connectors for automated droplet actuation. b) A schematic of a device depicting the positioning of sample and reagents required for a proteomic workup.

A1.1.4 Digital Microfluidics Sample Processing

1. The following procedure is implemented automatically by means of LabView code written in-house. The volume of droplets dispensed from reservoirs is defined by the dimensions of the electrodes (in this case, dispensed droplets are ~600nL).
2. Dispense a droplet of protein-containing sample from R-1 and a droplet of precipitant from R-2 (Fig. 2, frame 1). Merge the two droplets and allow the combined droplet to incubate for 5 min, resulting in the precipitation of proteins onto the surface (Fig. 2, frames 2-3). Actuate the supernatant away from the precipitated protein to the waste reservoir, R-3 (Fig. 2, frame 4).
3. Dispense three droplets of wash buffer from R-4 and drive them across the precipitated protein to the waste reservoir, R-3 (Fig. 2, frame 5).
4. Allow the precipitate to dry, and dispense a droplet of resolubilizing buffer from R-5 to the protein. Allow the buffer to incubate for 20 min until the precipitate has dissolved (Fig. 2, frame 6).

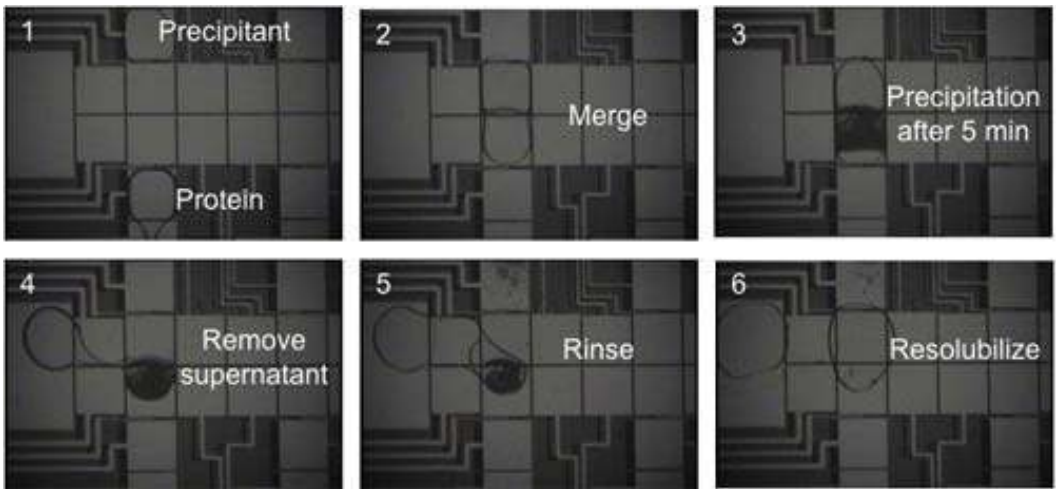

Figure A1.2 Frames from a movie depicting the automated extraction and purification of BSA in 20% TCA (precipitant) and 70/30% chloroform/acetonitrile (rinse solution). In frame 6, the precipitated protein is redissolved in a droplet of 100 mM ammonium bicarbonate.

5. Dispense a droplet of reductant from R-6 and merge it with the sample droplet. Mix the combined droplet by actuating it across 6 electrodes in a circular pattern. Allow the droplet to incubate for 1 h at room temperature in a humidified chamber (Fig. 3, frames 1-2).
6. Dispense a droplet of alkylating agent from R-7 and merge it with the sample droplet, followed by mixing (as in 4.5). Allow the droplet to incubate for 15 min at room temperature in a humidified chamber, protected from light (Fig. 3, frames 2-3).
7. Dispense a droplet of trypsin from R-8, and merge it with the sample droplet, followed by mixing (as in 4.5). Allow the droplet to incubate for 3 h at 37°C in a humidified chamber on a hot plate (Fig. 3, frames 3-4).

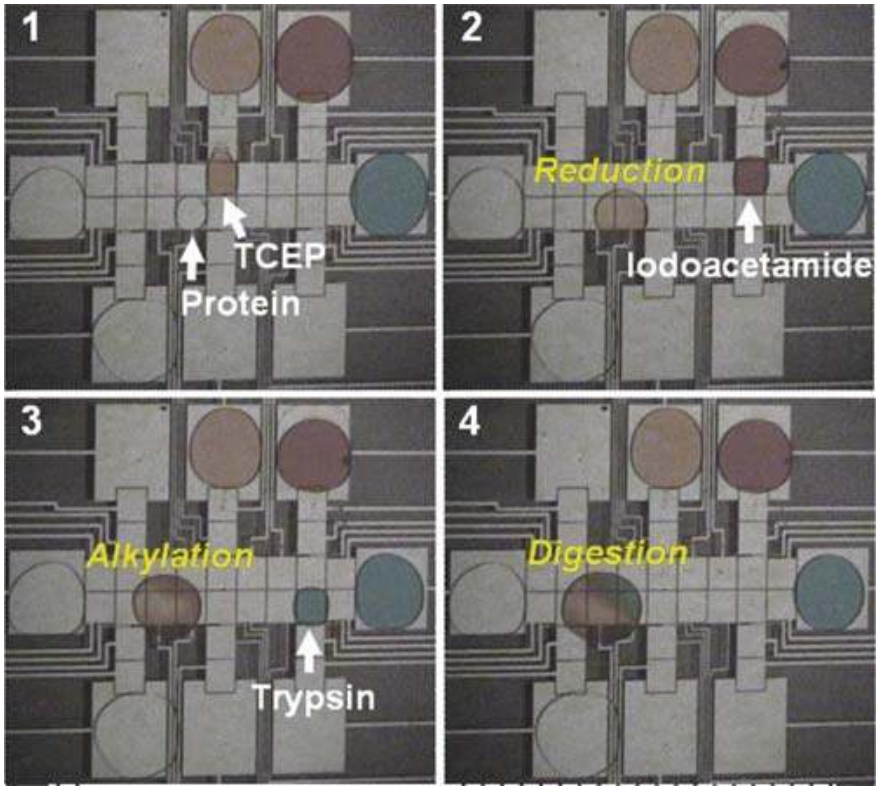

Figure A1.3 Frames from a movie illustrating sequential reduction, alkylation, and digestion of a droplet of resolubilized protein. In this figure, the reagents are colored with dyes for clarity; in practice, the reagents are not colored.

A1.1.5 Post-Processing Sample Preparation

1. Remove top substrate and quench digestion reaction by adding 0.6 mL of 2.5% trifluoroacetic acid in water.
2. Purify quenched reaction product using C18 ZipTips (Millipore, Billerica, MA) according to manufacturer's instructions.
3. Dilute purified sample in DI water to a final volume of 100 mL.

A1.1.6 Mass Spectrometry

1. Evaluate the processed sample on a nano-HPLC mated to a tandem mass spectrometer. The HPLC system used here is from Eksigent Technologies and is equipped with a trap column (3 mm dia. C18 beads, 150 μm ID x 2.5 cm) and a reversed-phase separation column (3 μm dia. C18 beads, 75 μm ID x 15 cm). The mass spectrometer used here is an LTQ from Thermo-Fisher Scientific.
2. Load a 2 μL sample onto the trap column at 5μL/min in a mobile phase comprising 5% acetonitrile in water. Separate the sample on the reversed phase column at 0.5μL/min using a linear gradient from 20% acetonitrile to 80% acetonitrile over 25 min. Continue running at 80% acetonitrile for another 10 min.
3. Analyze the bands eluting off the column by tandem mass spectrometry. In the work reported here, the eluent is sampled into the mass spectrometer via a nanoelectrospray emitter (20 μm ID tapered to 10 μm ID) from NewObjective.
4. Identify the proteins in the sample using a database search program such as SEQUEST. In this work, I used the version of SEQUEST incorporated in Bioworks v3.01 (Thermo-Fisher Scientific), and identified proteins that had probability scores of less than 1.0E-03 (equivalent to 99.9% confidence interval), and sequence coverages of at least 30% (Fig. 4).

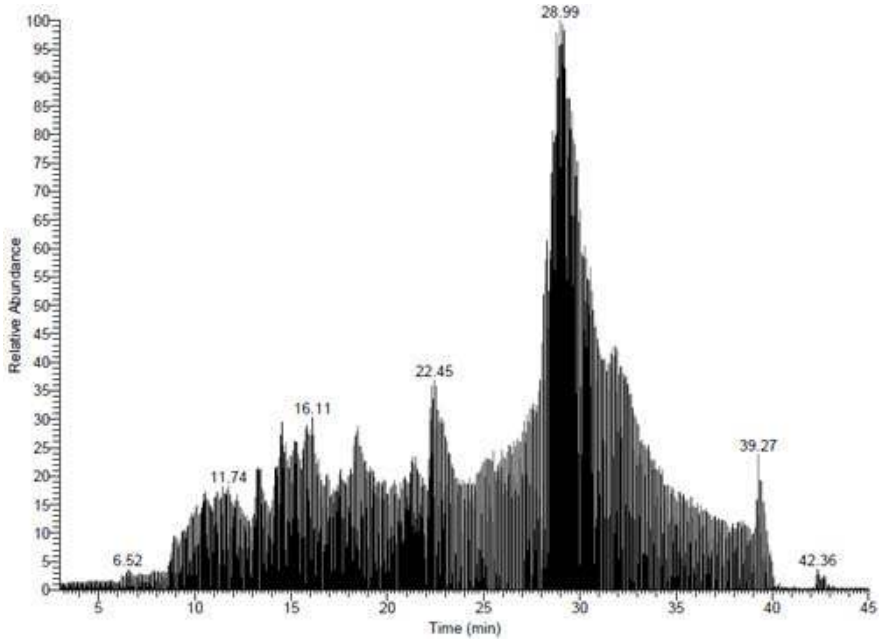

Figure A1.4 MS chromatogram of a sample of bovine serum albumin processed by digital microfluidics. 25 distinct peptides were identified (99.9% confidence interval) corresponding a sequence coverage of 44%.

A1.2 Discussion and Conclusion

The lack of standardized sample handling and processing in proteomics is a major limitation for the field. In addition, conventional macroscale sample handling involves multiple containers and solution transfers, which can lead to sample loss and contamination. A potential solution to these problems is to form integrated systems for sample processing relying on digital microfluidics (DMF).[13] In previous work, DMF was shown to be useful for efficient removal of unwanted contaminants in heterogeneous protein-containing solutions.[17] Likewise, DMF was shown to be compatible with integration of multistep solution-phase processing (reduction, alkylation and digestion) on an integrated device.[54] Here, we have demonstrated a fully integrated system with automated droplet control for protein extraction by precipitation followed by solution-phase processing. We speculate that if methods such as these are widely adopted, the human error inherent in proteomic sample processing can be largely eliminated, resulting in analyses with better reproducibility. In short, we propose that DMF has the potential for being useful for a broad cross-section of applications, as the conditions can be precisely duplicated in any laboratory in the world.

Appendix 2 A Two-for-One Dielectric and Hydrophobic Layer for Digital Microfluidics

A2.1 Why is this useful?

Digital microfluidics (DMF) is a technique in which droplets of reagents in micro- to nano-liter volumes are manipulated by applying a series of electrical potentials to an array of electrodes.[14] In DMF devices, the actuation electrodes are coated with an insulating layer. Upon application of electrical potentials, charges accumulate on either side of the insulator, a phenomenon that can be exploited to make droplets move, merge, mix, split, and dispense from reservoirs. The insulating layer is covered by an additional hydrophobic coating, which reduces droplet sticking to the surface.[24] The instruments and materials required for forming these layers are expensive (tens-to-hundreds of thousands of dollars) and the deposition methods are time-consuming (many hours). Recently, Hao et al.[51] demonstrated a new strategy for reusing DMF devices by fitting them with insulating polymer coverings (e.g., food wrap) that are spin-coated with Teflon. Here, we share an even simpler method that is cheap (tens of dollars) and fast (minutes) featuring a two-for-one insulating and hydrophobic layer formed from laboratory wrap (Parafilm®, Alcan Packaging, Neenah, WI). No Teflon is required for fabricating these devices, and we speculate that this will be useful for laboratories interested in rapid prototyping.

A2.2 What do I need?

- Bottom substrate patterned with working electrodes (typically chromium or gold on glass); electrodes can be formed using conventional cleanroom techniques[32,219] or by rapid prototyping techniques such as microcontact printing,[220] laser toner printing,[217] or marker masking[218]
- Indium-tin-oxide coated glass (can be purchased from Delta Technologies Ltd, Stillwater, MN) to serve as top substrate
- Parafilm® and wax paper backing
- Scissors
- Scalpel
- Hot plate

A2.3 What do I do?

1. With scissors, cut a piece of Parafilm® and stretch the film horizontally and vertically to its limits (Figure A2.1a), and place over the bottom plate of the DMF device (with patterned electrodes) (Figure A2.1b)

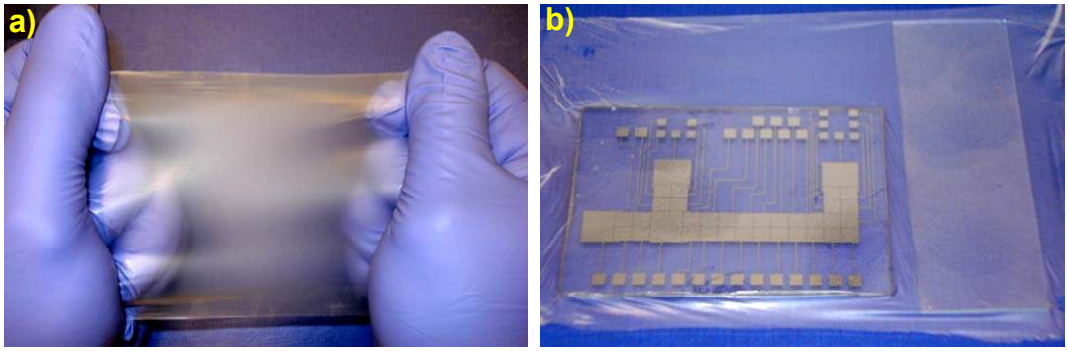

Figure A2.1 Pictures illustrating a) stretching a piece of Parafilm® and b) placing over the bottom and top plate of the DMF device.

2. With a wax paper apply pressure with your finger on the film to release any air trapped between the electrode(s) and film (Figure A2.2a). Then, score film with a scalpel and peel off excess Parafilm® (Figure A2.2b,c).

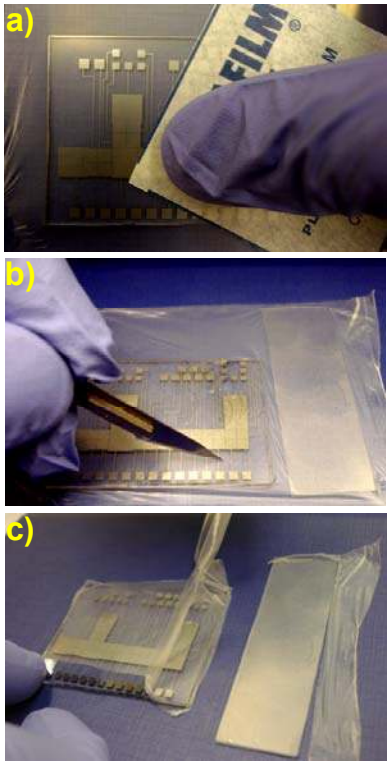

Figure A2.2. Pictures illustrating a) applying pressure on the film with finger, b) scoring the film with a scalpel and c) peeling off excess Parafilm® .

3. Repeat steps 1 and 2 to apply parafilm layer to the top substrate (indium-tin oxide coated glass)
4. Place substrates on hotplate for 30 seconds at 80-85°C.
5. Allow substrates to cool down to room temperature (Figure A2.3a), and then assemble the device with a top plate[23,32] to dispense, merge and split droplets as shown in Figure A2.3 (b-e).

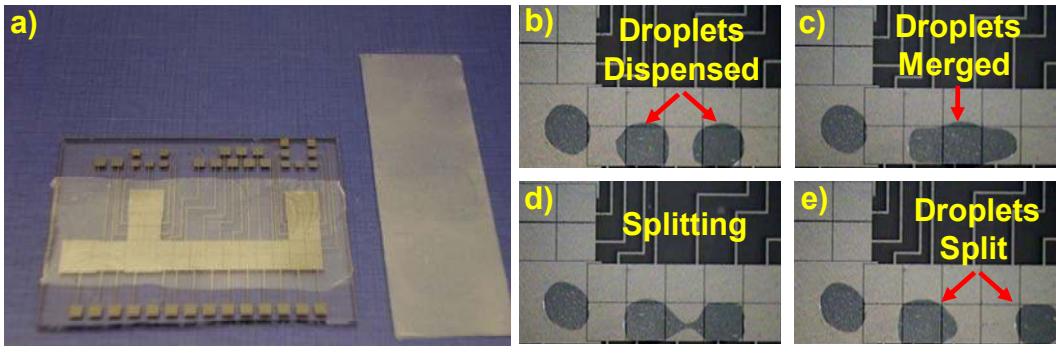

Figure A2.3 Pictures illustrating a) a DMF device fitted with Parafilm® and assembled to b) dispense, c)merge and d,e) split droplets.

A2.4 What else should I know?

- A ~4.5 x 4.5 cm piece of Parafilm® stretched to its limits will give a thickness of 6 – 9 µm.
- A voltage of 300 – 500V is appropriate for actuation for above thickness.
- Use of wax paper when applying pressure is important as it avoids contamination of Parafilm® surface.
- Device can be recycled by simply peeling off old Parafilm® and replacing it with a new film.

References

1. I. R. Baxendale, S. V. Ley, A. C. Mansfield and C. D. Smith, *Angew. Chem. Int. Edit.* , 2009, **48**, 4017-4021.
2. S. Marre and K. F. Jensen, *Chem. Soc. Rev.*, 2010, **39**, 1183-1202.
3. B. F. Cottam, S. Krishnadasan, A. J. de Mello, J. C. de Mello and M. S. P. Shaffer, *Lab Chip*, 2007, **7**, 167-169.
4. Y. J. Wang, W. Y. Lin, K. Liu, R. J. Lin, M. Selke, H. C. Kolb, N. G. Zhang, X. Z. Zhao, M. E. Phelps, C. K. F. Shen, K. F. Faull and H. R. Tseng, *Lab Chip*, 2009, **9**, 2281-2285.
5. Y. Hennequin, N. Pannacci, C. P. De Torres, G. Tetradis-Meris, S. Chapuliot, E. Bouchaud and P. Tabeling, *Langmuir*, 2009, **25**, 7857-7861.
6. D. Chen, W. Du, Y. Liu, W. Liu, A. Kuznetsov, F. E. Mendez, L. H. Philipson and R. F. Ismagilov, *Proc. Natl. Acad. Sci.*, 2008, **105**, 16843-16848.
7. A. B. Theberge, F. Courtois, Y. Schaerli, M. Fischlechner, C. Abell, F. Hollfelder and W. T. S. Huck, *Angew. Chem. Int. Edit.* , 2010, **49**, 5846-5868.
8. S. Köster, F. E. Angilè, H. Duan, J. J. Agresti, A. Wintner, C. Schmitz, A. C. Rowat, C. A. Merten, D. Pisignano, A. D. Griffiths and D. A. Weitz, *Lab Chip*, 2008, **8**, 1110-1115.
9. R. W. Doebler, B. Erwin, A. Hickerson, B. Irvine, D. Woyski, A. Nadim and J. D. Sterling, *JALA*, 2009, **14**, 119-125.
10. C. W. Yung, J. Fiering, A. J. Mueller and D. E. Ingber, *Lab Chip*, 2009, **9**, 1171-1177.
11. D. Wlodkowic and J. M. Cooper, *Curr. Opin. Chem. Biol.*, 2010, **14**, 556-567.
12. R. Fan, O. Vermesh, A. Srivastava, B. K. H. Yen, L. Qin, H. Ahmad, G. A. Kwong, C. C. Liu, J. Gould, L. Hood and J. R. Heath, *Nat. Biotechnol.*, 2008, **26**, 1373-1378.
13. M. Abdelgawad and A. R. Wheeler, *Adv. Mater.*, 2009, **21**, 920-925.
14. A. R. Wheeler, *Science*, 2008, **322**, 539-540.
15. S. Y. Teh, R. Lin, L. H. Hung and A. P. Lee, *Lab Chip*, 2008, **8**, 198-220.
16. P. Tabeling, *Lab Chip*, 2009, **9**, 2428-2436.
17. M. J. Jebrail and A. R. Wheeler, *Anal. Chem.*, 2009, **81**, 330-335.
18. N. A. Mousa, M. J. Jebrail, H. Yang, M. Abdegawad, P. Metalnikov, J. Chen, A. R. Wheeler and R. F. Casper, *Sci. Transl. Med.*, 2009, **1**, 1ra2.
19. M. J. Jebrail, A. H. C. Ng, V. Rai, R. Hili, A. K. Yudin and A. R. Wheeler, *Angew. Chem. Int. Ed.*, 2010, **49**, 8625-8629.
20. J. A. Hall, E. Felnagle, M. Fries, S. Spearing, L. Monaco and A. Steele, *Planet. Space Sci.*, 2006, **54**, 1600-1611.
21. M. Abdelgawad, S. L. S. Freire, H. Yang and A. R. Wheeler, *Lab Chip*, 2008, **8**, 672-677.
22. S. Zeng, B. Li, X. Su, J. Qin and B. Lin, *Lab Chip*, 2009, **9**, 1340-1343.
23. M. G. Pollack, R. B. Fair and A. D. Shenderov, *Appl. Phys. Lett.*, 2000, **77**, 1725-1726.
24. J. Lee, H. Moon, J. Fowler, T. Schoellhammer and C. J. Kim, *Sens. Actuators A Phys.*, 2002, **95**, 259-268.
25. D. Chatterjee, B. Hetayothin, A. R. Wheeler, D. J. King and R. L. Garrell, *Lab Chip*, 2006, **6**, 199-206.
26. T. B. Jones, *Langmuir*, 2002, **18**, 4437-4443.
27. K. H. Kang, *Langmuir*, 2002, **18**, 10318-10322.
28. E. Baird, P. Young and K. Mohseni, *Microfluid. Nanofluid.*, 2007, **3**, 635-644.
29. D. Chatterjee, H. Shepherd and R. L. Garrell, *Lab Chip*, 2009, **9**, 1219-1229.
30. D. J. Griffiths, *Introduction to Electrodynamics*, Prentice-Hall, New Jersey, 1999.

31. M. Abdelgawad, P. Park and A. R. Wheeler, *J. Appl. Phys.*, 2009, **105**, 094506-094512.
32. S. K. Cho, H. J. Moon and C. J. Kim, *J. Microelectromech. S.*, 2003, **12**, 70-80.
33. C. G. Cooney, C. Y. Chen, M. R. Emerling, A. Nadim and J. D. Sterling, *Microfluid. Nanofluid.*, 2006, **2**, 435-446.
34. L. Malic, D. Brassard, T. Veres and M. Tabrizian, *Lab Chip*, 2009, **10**, 418-431.
35. I. Barbulovic-Nad, S. H. Au and A. R. Wheeler, *Lab Chip*, 2010, **10**, 1536 - 1542.
36. V. Srinivasan, V. K. Pamula and R. B. Fair, *Lab Chip*, 2004, **4**, 310-315.
37. H. Moon, A. R. Wheeler, R. L. Garrell, J. A. Loo and C. J. Kim, *Lab Chip*, 2006, **6**, 1213-1219.
38. S. K. Fan, H. Yang and W. Hsu, *Lab Chip*, 2011, **11**, 343-347.
39. M. W. L. Watson, M. J. Jebrail and A. R. Wheeler, *Anal. Chem.*, 2010, **82**, 6680-6686.
40. M. Abdelgawad, M. W. L. Watson and A. R. Wheeler, *Lab Chip*, 2009, **9**, 1046-1051.
41. J. Gorbatsova, M. Jaanus and M. Kaljurand, *Anal. Chem.*, 2009, **81**, 8590-8595.
42. M. J. Jebrail, H. Yang, J. M. Mudrik, N. M. Lafrenière, C. McRoberts, O. Y. Al-Dirbashi, L. Fisher, P. Chakraborty and A. R. Wheeer, 2011, **Submitted**.
43. J. R. Millman, K. H. Bhatt, B. G. Prevo and O. D. Velev, *Nat. Mater.*, 2005, **4**, 98-102.
44. P. Dubois, G. Marchand, Y. Fouillet, J. Berthier, T. Douki, F. Hassine, S. Gmouh and M. Vaultier, *Anal. Chem.*, 2006, **78**, 4909-4917.
45. J. Y. Wang, G. D. Sui, V. P. Mocharla, R. J. Lin, M. E. Phelps, H. C. Kolb and H. R. Tseng, *Angew. Chem. Int. Ed.*, 2006, **45**, 5276-5281.
46. Y. Kikutani, T. Horiuchi, K. Uchiyama, H. Hisamoto, M. Tokeshi and T. Kitamori, *Lab Chip*, 2002, **2**, 188-192.
47. E. R. Murphy, J. R. Martinelli, N. Zaborenko, S. L. Buchwald and K. F. Jensen, *Angew. Chem. Int. Edit.* , 2007, **46**, 1734-1737.
48. M. Baumann, I. R. Baxendale, S. V. Ley, N. Nikbin, C. D. Smith and J. P. Tierney, *Org. Biomol. Chem.*, 2008, **6**, 1577-1586.
49. V. Srinivasan, V. K. Pamula and R. B. Fair, *Anal. Chim. Acta*, 2004, **507**, 145-150.
50. V. N. Luk, G. C. H. Mo and A. R. Wheeler, *Langmuir*, 2008, **24**, 6382-6389.
51. H. Yang, V. N. Luk, M. Abeigawad, I. Barbulovic-Nad and A. R. Wheeer, *Anal. Chem.*, 2009, **81**, 1061-1067.
52. A. R. Wheeler, H. Moon, C. J. Kim, J. A. Loo and R. L. Garrell, *Anal. Chem.*, 2004, **76**, 4833-4838.
53. A. R. Wheeler, H. Moon, C. A. Bird, R. R. O. Loo, C. J. Kim, J. A. Loo and R. L. Garrell, *Anal. Chem.*, 2005, **77**, 534-540.
54. V. N. Luk and A. R. Wheeler, *Anal. Chem.*, 2009, **81**, 4524-4530.
55. D. Chatterjee, A. J. Ytterberg, S. U. Son, J. A. Loo and R. L. Garrell, *Anal. Chem.*, 2010, **82**, 2095-2101.
56. W. C. Nelson, I. Peng, G. A. Lee, J. A. Loo, R. L. Garrell and C. J. Kim, *Anal. Chem.*, 2010, **82**, 9932-9937.
57. M. J. Jebrail, V. N. Luk, S. C. C. Shih, R. Fobel, A. H. C. Ng, H. Yang, S. L. S. Freire and A. R. Wheeler, *J. Vis. Exp.* , 2009, **33**, DOI: 10.3791/1603.
58. R. S. Sista, A. E. Eckhardt, V. Srinivasan, M. G. Pollack, S. Palanki and V. K. Pamula, *Lab Chip*, 2008, **8**, 2188-2196.
59. R. Sista, Z. S. Hua, P. Thwar, A. Sudarsan, V. Srinivasan, A. Eckhardt, M. Pollack and V. Pamula, *Lab Chip*, 2008, **8**, 2091-2104.

60. E. M. Miller, A. H. C. Ng, U. Uddayasankar and A. R. Wheeler, *Anal. Bioanal.Chem.*, 2011, **399**, 337–345.
61. T. Taniguchi, T. Torii and T. Higuchi, *Lab Chip*, 2002, **2**, 19-23.
62. K. P. Nichols and J. G. E. Gardeniers, *Anal. Chem.*, 2007, **79**, 8699-8704.
63. E. M. Miller and A. R. Wheeler, *Anal. Chem.*, 2008, **80**, 1614-1619.
64. J. G. Martin, M. Gupta, Y. M. Xu, S. Akella, J. Liu, J. S. Dordick and R. J. Linhardt, *J. Am. Chem. Soc.*, 2009, **131**, 11041-11048.
65. D. Jary, A. Chollat-Namy, Y. Fouillet, J. Boutet, C. Chabrol, G. Castellan, D. Gasparutto and C. Peponnet, *Proceedings of 2006 NSTI Nanotechnology Conference and Trade Show*, 2006, **2**, 554-557.
66. Y. J. Liu, D. J. Yao, H. C. Lin, W. Y. Chang and H. Y. Chang, *J. Micromech. Microeng.*, 2008, **18**.
67. L. Malic, T. Veres and M. Tabrizian, *Biosens. Bioelectron.*, 2009, **24**, 2218-2224.
68. Z. Hua, J. L. Rouse, A. E. Eckhardt, V. Srinivasan, V. K. Pamula, W. A. Schell, J. L. Benton, T. G. Mitchell and M. G. Pollack, *Anal. Chem.*, 2010, **82**, 2310-2316.
69. Y. H. Chang, G. B. Lee, F. C. Huang, Y. Y. Chen and J. L. Lin, *Biomed. Microdevices*, 2006, **8**, 215-225.
70. I. Barbulovic-Nad, H. Yang, P. S. Park and A. R. Wheeler, *Lab Chip*, 2008, **8**, 519-526.
71. J. Zhou, L. Lu, K. Byrapogu, D. M. Wootton, P. I. Lelkes and R. Fair, *Virt. Phys. Prototyp.*, 2007, **2**, 217-223.
72. S. K. Fan, P. W. Huang, T. T. Wang and Y. H. Peng, *Lab Chip*, 2008, **8**, 1325-1331.
73. G. J. Shah, A. T. Ohta, E. P. Y. Chiou, M. C. Wu and C. J. Kim, *Lab Chip*, 2009, **9**, 1732-1739.
74. Y. Zhao and S. K. Cho, *Lab Chip*, 2007, **7**, 273-280.
75. I. Moon and J. Kim, *Sensors and Actuators, A: Physical*, 2006, **130-131**, 537-544.
76. Y. Zhao, S. K. Chung, U. C. Yi and S. K. Cho, *J. Micromech. Microeng.*, 2008, **18**.
77. J. L. Poulos, W. C. Nelson, T. J. Jeon, C. J. Kim and J. J. Schmidt, *Appl. Phys. Lett.*, 2009, **95**.
78. S. Luckett, R. S. Garcia, J. J. Barker, A. V. Konarev, P. R. Shewry, A. R. Clarke and R. L. Brady, *J. Mol. Biol.*, 1999, **290**, 525-533.
79. R. Eisenbrandt, M. Kalkum, E. M. Lai, R. Lurz, C. I. Kado and E. Lanka, *J. Biol. Chem.*, 1999, **274**, 22548-22555.
80. P. Li, P. P. Roller and J. C. Xu, *Curr. Org. Chem.*, 2002, **6**, 411-440.
81. J. S. Davies, *J. Pept. Sci.*, 2003, **9**, 471-501.
82. J. M. Antos, M. W. L. Popp, R. Ernst, G. L. Chew, E. Spooner and H. L. Ploegh, *J. Biol. Chem.*, 2009, **284**, 16028-16036.
83. J. N. Lambert, J. P. Mitchell and K. D. Roberts, *J. Chem. Soc. Perkin Trans.*, 2001, 471-484.
84. D. J. Craik, *Science*, 2006, **311**, 1563-1564.
85. R. Hili, V. Rai and A. K. Yudin, *J. Am. Chem. Soc.*, 2010, **132**, 2889-2891.
86. S. Ceylan, C. Friese, C. Lammel, K. Mazac and A. Kirschning, *Angew. Chem. Int. Ed.*, 2008, **47**, 8950-8953.
87. P. W. Miller, N. J. Long, A. J. de Mello, R. Vilar, J. Passchier and A. Gee, *Chem. Commun.*, 2006, 546-548.
88. A. Palmieri, S. V. Ley, K. Hammond, A. Polyzos and I. R. Baxendale, *Tetrahedron Lett.*, 2009, **50**, 3287-3289.

89. T. Wu, Y. Mei, J. T. Cabral, C. Xu and K. L. Beers, *J. Am. Chem. Soc.*, 2004, **126**, 9880-9881.
90. W. Li, H. H. Pharn, Z. Nie, B. MacDonald, A. Guenther and E. Kumacheva, *J. Am. Chem. Soc.*, 2008, **130**, 9935-9941.
91. O. Flogel, J. D. C. Codee, D. Seebach and P. H. Seeberger, *Angew. Chem. Int. Ed.*, 2006, **45**, 7000-7003.
92. I. R. Baxendale, S. V. Ley, C. D. Smith and G. K. Tranmer, *Chem. Commun.*, 2006, 4835-4837.
93. Y. Y. Huang, P. Castrataro, C. C. Lee and S. R. Quake, *Lab Chip*, 2007, **7**, 24-26.
94. S. A. Khan, A. Gunther, M. A. Schmidt and K. F. Jensen, *Langmuir*, 2004, **20**, 8604-8611.
95. B. K. H. Yen, A. Gunther, M. A. Schmidt, K. F. Jensen and M. G. Bawendi, *Angew. Chem. Int. Ed.*, 2005, **44**, 5447-5451.
96. J. N. Lee, C. Park and G. M. Whitesides, *Anal. Chem.*, 2003, **75**, 6544-6554.
97. G. M. Whitesides, *Nature*, 2006, **442**, 368-373.
98. W. B. Du, L. Li, K. P. Nichols and R. F. Ismagilov, *Lab Chip*, 2009, **9**, 2286-2292.
99. L. Li, W. Du and R. Ismagilov, *J. Am. Chem. Soc.*, 2009, **132**, 106-111.
100. G. J. Shah, A. T. Ohta, E. P. Chiou, M. C. Wu and C. J. Kim, *Lab Chip*, 2009, **9**, 1732 - 1739.
101. A. Failli, H. Immer and M. Gotz, *Can. J. Chem.*, 1979, **57**, 3257-3261.
102. R. Hili and A. K. Yudin, *J. Am. Chem. Soc.*, 2006, **128**, 14772-14773.
103. P. Paik, V. K. Pamula and R. B. Fair, *Lab Chip*, 2003, **3**, 253-259.
104. P. Paik, V. K. Pamula, M. G. Pollack and R. B. Fair, *Lab Chip*, 2003, **3**, 28-33.
105. P. E. Dawson, T. W. Muir, I. Clark-Lewis and S. B. Kent, *Science*, 1994, **266**, 776-779.
106. L. Jiang, L. He and M. Fountoulakis, *J. Chromatogr. A*, 2004, **1023**, 317-320.
107. M. Zellner, W. Winkler, H. Hayden, M. Diestinger, M. Eliasen, B. Gesslbauer, I. Miller, M. Chang, A. Kungl, E. Roth and R. Oehler, *Electrophoresis*, 2005, **26**, 2481-2489.
108. J. W. Park, S. G. Lee, J. Y. Song, J. S. Joo, M. J. Chung, S. C. Kim, H. S. Youn, H. L. Kang, S. C. Baik, W. K. Lee, M. J. Cho and K. H. Rhee, *Electrophoresis*, 2008, **29**, 2891-2903.
109. C. Sandhu, M. Connor, T. Kislinger, J. Slingerland and A. Emili, *J. Proteome Res.*, 2005, **4**, 674-689.
110. S. Englard and S. Seifter, *Method Enzymol.*, 1990, **182**, 285-300.
111. M. P. Nandakumar, J. Shen, B. Raman and M. R. Marten, *J. Proteome Res.*, 2003, **2**, 89-93.
112. R. J. Simpson, *Purifying Proteins for Proteomics: A Laboratory Manual*, Cold Spring Harbor Laboratory Press, 2004.
113. M. Hirano, R. Rakwal, J. Shibato, G. K. Agrawal, N. S. Jwa, H. Iwahashi and Y. Masuo, *Mol. Cells*, 2006, **22**, 119-125.
114. S. L. S. Freire and A. R. Wheeler, *Lab Chip*, 2006, **6**, 1415-1423.
115. H. Y. Tan, W. K. Loke, Y. T. Tan and N. T. Nguyen, *Lab Chip*, 2008, **8**, 885-891.
116. Y. Fouillet, D. Jary, C. Chabrol, P. Claustre and C. Peponnet, *Microfluid. Nanofluid.*, 2008, **4**, 159-165.
117. Y. J. Zhao and S. K. Cho, *Lab Chip*, 2007, **7**, 273-280.
118. D. Brassard, L. Malic, F. Normandin, M. Tabrizian and T. Veres, *Lab Chip*, 2008, **8**, 1342-1349.
119. M. M. Bradford, *Anal. Biochem.*, 1976, **72**, 248-254.

120. P. Bohlen, S. Stein, W. Dairman and Udenfrie.S, *Arch. Biochem. Biophys.*, 1973, **155**, 213-220.
121. S. Udenfrie, S. Stein, P. Bohlen and W. Dairman, *Science*, 1972, **178**, 871-872.
122. J. E. Noble, A. E. Knight, A. J. Reason, A. Di Matola and M. J. A. Bailey, *Mol. Biotechnol.*, 2007, **37**, 99-111.
123. H. O. Bergo and C. Christiansen, *Anal. Biochem.*, 2001, **288**, 225-227.
124. P. He, H. Z. He, J. Dai, Y. Wang, Q. H. Sheng, L. P. Zhou, Z. S. Zhang, Y. L. Sun, F. Liu, K. Wang, J. S. Zhang, H. X. Wang, Z. M. Song, H. R. Zhang, R. Zeng and X. H. Zhao, *Proteomics*, 2005, **5**, 3442-3453.
125. J. N. Adkins, S. M. Varnum, K. J. Auberry, R. J. Moore, N. H. Angell, R. D. Smith, D. L. Springer and J. G. Pounds, *Mol. Cell. Proteomics*, 2002, **1**, 947-955.
126. P. Y. Chiou, Z. Chang and M. C. Wu, *J. Microelectromech. S.*, 2008, **17**, 133-138.
127. N. Gottschlich, C. T. Culbertson, T. E. McKnight, S. C. Jacobson and J. M. Ramsey, *J. Chromatogr., B*, 2000, **745**, 243-249.
128. M. Brivio, R. H. Fokkens, W. Verboom, D. N. Reinhoudt, N. R. Tas, M. Goedbloed and A. Van den Berg, *Anal. Chem.*, 2002, **74**, 3972-3976.
129. S. C. Jacobson, R. Hergenröder and A. W. Moore Jr, *Anal. Chem.*, 1994, **66**, 4127-4132.
130. M. P. Washburn, D. Wolters and J. R. Yates, *Nat. Biotechnol.*, 2001, **19**, 242-247.
131. H. J. Crabtree, E. C. S. Cheong, D. A. Tilroe and C. J. Backhouse, *Anal. Chem.*, 2001, **73**, 4079-4086.
132. D. Sinton and D. Li, *Colloids Surf., A*, 2003, **222**, 273-283.
133. M. A. Unger, H. P. Chou, T. Thorsen, A. Scherer and S. R. Quake, *Science*, 2000, **288**, 113-116.
134. G. T. Roman and R. T. Kennedy, *J. Chromatogr. A*, 2007, **1168**, 170-188.
135. J. S. Edgar, C. P. Pabbati, R. M. Lorenz, M. He, G. S. Fiorini and D. T. Chiu, *Anal. Chem.*, 2006, **78**, 6948-6954.
136. G. T. Roman, M. Wang, K. N. Shultz, C. Jennings and R. T. Kennedy, *Anal. Chem.*, 2008, **80**, 8231-8238.
137. X. Z. Niu, B. Zhang, R. T. Marszalek, O. Ces, J. B. Edel, D. R. Klug and A. J. Demello, *Chem. Commun.*, 2009, 6159-6161.
138. M. Abdelgawad, M. W. L. Watson and A. R. Wheeler, *Lab Chip*, 2009, 1046–1051.
139. J. P. Rolland, R. M. Van Dam, D. A. Schorzman, S. R. Quake and J. M. DeSimone, *J. Am. Chem. Soc.*, 2004, **126**, 2322-2323.
140. R. T. Kelly, T. Pan and A. T. Woolley, *Anal. Chem.*, 2005, **77**, 3536-3541.
141. J. Siegrist, R. Gorkin, L. Clime, E. Roy, R. Peytavi, H. Kido, M. Bergeron, T. Veres and M. Madou, *Microfluid. Nanofluid.*, 2010, **9**, 55-63.
142. Y. Fintschenko, D. Arnold, E. Peters, F. Svec and J. Frechet, *Proceedings of SPIE - The International Society for Optical Engineering*, 1999, **3877**, 202-209.
143. M. W. L. Watson, J. M. Mudrik and A. R. Wheeler, *Anal. Chem.*, 2009, **81**, 3851-3857.
144. S. L. S. Freire, H. Yang and A. R. Wheeler, *Electrophoresis*, 2008, **29**, 1836-1843.
145. H. Sasano, T. Suzuki and N. Harada, *Endocr. Pathol.*, 1998, **9**, 9-20.
146. E. R. Simpson, M. Misso, K. N. Hewitt, R. A. Hill, W. C. Boon, M. E. Jones, A. Kovacic, J. Zhou and C. D. Clyne, *Endocr. Rev.*, 2005, **26**, 322-330.
147. S. E. Bulun, L. S. Noble, K. Takayama, M. D. Michael, V. Agarwal, C. Fisher, Y. Zhao, M. M. Hinshelwood, Y. Ito and E. R. Simpson, *J. Steroid. Biochem. Mol. Biol.*, 1997, **61**, 133-139.

148. F. Labrie, *Mol Cell Endocrinol*, 1991, **78**, C113-C118.
149. C. A. Lamar, J. F. Dorgan, C. Longcope, F. Z. Stanczyk, R. T. Falk and H. E. Stephenson, Jr., *Cancer Epidemiol Biomarkers Prev*, 2003, **12**, 380-383.
150. M. S. Beattie, J. P. Costantino, S. R. Cummings, D. L. Wickerham, V. G. Vogel, M. Dowsett, E. J. Folkerd, W. C. Willett, N. Wolmark and S. E. Hankinson, *J. Natl. Cancer Inst.*, 2006, **98**, 110-115.
151. J. Szymczak, A. Milewicz, J. H. H. Thijssen, M. A. Blankenstein and J. Daroszewski, *Steroids*, 1998, **63**, 319-321.
152. M. A. Blankenstein, J. van de Ven, I. Maitimu-Smeele, G. H. Donker, P. C. de Jong, J. Daroszewski, J. Szymczak, A. Milewicz and J. H. Thijssen, *J Steroid Biochem Mol Biol*, 1999, **69**, 293-297.
153. C. Belanger, F.-S. Hould, S. Lebel, S. Biron, G. Brochu and A. Tchernof, *Steroids*, 2006, **71**, 674-682.
154. F. Labrie, A. Belanger, P. Belanger, R. Berube, C. Martel, L. Cusan, J. Gomez, B. Candas, I. Castiel and V. Chaussade, *J Steroid Biochem Mol Biol*, 2006, **99**, 182-188.
155. F. Z. Stanczyk, J. S. Lee and R. J. Santen, *Cancer Epidemiol Biomarkers Prev*, 2007, **16**, 1713-1719.
156. L. Albrecht and D. Styne, *Ped. Endocrin. Rev.*, 2007, **5**, 599-607.
157. S. N. Rahhal, J. S. Fuqua and P. A. Lee, *Steroids*, 2008, **73**, 1322-1327.
158. C. Ankarberg-Lindgren and E. Norjavaara, *Eur J Endocrinol*, 2008, **158**, 117-124.
159. A. R. Wheeler, *Science*, 2008, **322**, 539-540.
160. A. Gentili, D. Perret, S. Marchese, R. Mastropasqua, R. Curini and A. Di Corcia, *Chromatographia*, 2002, **56**, 25-32.
161. D. A. Ehrmann, *N Engl J Med*, 2005, **352**.
162. S. Smith, S. M. Pfeifer and J. A. Collins, *JAMA*, 2003, **290**, 1767-1770.
163. B. E. Henderson, R. Ross and L. Bernstein, *Cancer Res*, 1988, **48**, 246-253.
164. R. Kaaks, S. Rinaldi, T. J. Key, F. Berrinno, P. H. M. Peeters, C. Biessy, L. Dossus, A. Lukanova, S. Bingham, K. T. Khaw, N. E. Allen, H. B. Bueno-De-Mesquita, C. H. Van Gils, D. Grobbee, H. Boeing, P. H. Lahmann, G. Nagel, J. Chang-Claude, F. Clavel-Chapelon, A. Fournier, A. Thie?baut, C. A. Gonza?lez, J. R. Quiro?s, M. J. Tormo, E. Ardanaz, P. Amiano, V. Krogh, D. Palli, S. Panico, R. Tumino, P. Vineis, A. Trichopoulou, V. Kalapothaki, D. Trichopoulos, P. Ferrari, T. Norat, R. Saracci and E. Riboli, *Endocr Relat Cancer*, 2005, **12**, 1071-1082.
165. K. Allvin, C. Ankarberg-Lindgren, H. Fors and J. Dahlgren, *J. Clin. Endocrinol. Metab.*, 2008, **93**, 1464-1469.
166. F. A. Pitt and J. Brazier, *Lancet*, 1990, **335**, 978-978.
167. A. Szarewski and J. Guillebaud, *BMJ*, 1991, **302**, 1224-1226.
168. C. Djerassi, *Am. J. Obstet. Gynecol.*, 2006, **194**, 290-298.
169. R. Hertz and J. C. Bailar 3rd, *JAMA*, 1966, **198**, 1000-1006.
170. G. R. Cunningham, *Nat. Clin. Pract. Urol.*, 2006, **3**, 260-267.
171. J. Geisler, B. Haynes, G. Anker, H. Helle, D. Ekse, M. Dowsett and P. E. Lonning, *J Steroid Biochem Mol Biol*, 2005, **96**, 415-422.
172. R. T. Falk, E. Gentzschein, F. Z. Stanczyk, L. A. Brinton, M. Garcia-Closas, O. B. Ioffe and M. E. Sherman, *Cancer Epidemiol Biomarkers Prev*, 2008, **17**, 1891-1895.
173. R. J. Santen, L. Demers, S. Ohorodnik, J. Settlage, P. Langecker, D. Blanchett, P. E. Goss and S. Wang, *Steroids*, 2007, **72**, 666-671.

174. T. Yasui, M. Yamada, H. Kinoshita, H. Uemura, N. Yoneda, M. Irahara, T. Aono, S. Sunahara, Y. Mito, F. Kurimoto and K. Hata, *J. Clin. Lab. Anal.*, 1999, **13**, 266-272.
175. K. Kureckova, B. Maralikova and K. Ventura, *J Chromatogr B Analyt Technol Biomed Life Sci*, 2002, **770**, 83-89.
176. J. Lee, H. Moon, J. Fowler, T. Schoellhammer and C. J. Kim, *SENS ACTUATORS A PHYS*, 2002, **95**, 259-268.
177. Y. Okubo, T. Maki, N. Aoki, T. Hong Khoo, Y. Ohmukai and K. Mae, *Chem Eng Sci*, 2008, **63**, 4070-4077.
178. J. G. Kralj, H. R. Sahoo and K. F. Jensen, *Lab Chip*, 2007, **7**, 256-263.
179. P. Znidarsic-Plazl and I. Plazl, *Lab chip*, 2007, **7**, 883-889.
180. D. Chatterjee, B. Hetayothin, A. R. Wheeler, D. J. King and R. L. Garrell, *Lab chip*, 2006, **6**, 199-206.
181. D. H. Chace, T. A. Kalas and E. W. Naylor, *Clin. Chem.*, 2003, **49**, 1797-1817.
182. D. H. Chace and T. A. Kalas, *Clin. Biochem.*, 2005, **38**, 296-309.
183. I. Sahai and D. Marsden, *Crit. Rev. Clin. Lab. Sci.*, 2009, **46**, 55-82.
184. C. Turgeon, M. J. Magera, P. Allard, S. Tortorelli, D. Gavrilov, D. Oglesbee, K. Raymond, P. Rinaldo and D. Matern, *Clin. Chem.*, 2008, **54**, 657-664.
185. D. H. Chace, D. S. Millington, N. Terada, S. G. Kahler, C. R. Roe and L. F. Hofman, *Clin. Chem.*, 1993, **39**, 66-71.
186. M. S. Rashed, *J. Chromatogr. B*, 2001, **758**, 27-48.
187. *Educational resource on blood spot collection developed by the Ontario Newborn Screening Program, October 2009, http://www.newbornscreening.on.ca/data/1/rec_docs/195_Unsatisfactory_Sample_Educational_Resource.pdf (accessed 7 January 2010).*
188. B. L. Therrell and J. Adams, *J. Inherit. Metab. Dis.*, 2007, **30**, 447-465.
189. O. A. Bodamer, G. F. Hoffmann and M. Lindner, *J. Inherit. Metab. Dis.*, 2007, **30**, 439-444.
190. C. D. Padilla and B. L. Therrell, *J. Inherit. Metab. Dis.*, 2007, **30**, 490-506.
191. *Newborn screening guidline from British Columbia Perinatal Health Program, November 2009, http://www.bcwomens.ca/NR/rdonlyres/CD0E67F3-9D7F-48F1-BC4F-9124E748D227/42837/NBSGuideline1.pdf (accessed 7 January 2010).*
192. D. H. Chace, *J. Mass Spectrom.*, 2009, **44**, 163-170.
193. O. Y. Al-Dirbashi, L. Fisher, C. McRoberts, K. Siriwardena, M. Geraghty and P. Chakraborty, *Clin. Biochem.*, 2010, **43**, 691-693.
194. C. Arnaud, *Chem. Eng. News*, 2011, **89**, 13-17.
195. D. J. Dietzen, P. Rinaldo, R. J. Whitley, W. J. Rhead, W. H. Hannon, U. C. Garg, S. F. Lo and M. J. Bennett, *Clin. Chem.*, 2009, **55**, 1615-1626.
196. L. E. Cipriano, C. A. Rupar and G. S. Zaric, *Value Health*, 2007, **10**, 83-97.
197. *Specimen collection procedure from Michigan Newborn Screening Program, July 2009, http://www.michigan.gov/documents/Bloodco2_60773_7.pdf (accessed 10 January 2010).*
198. M. J. Jebrail and A. R. Wheeler, *Curr. Opin. Chem. Biol.*, 2010, **14**, 574-581.
199. *Measurements of plasma amino acids from Baltimore Washington Medical Center, May 2009, http://www.mybwmc.org/library/1/003361 (accessed 12 January 2010).*
200. L. D. Stegink, L. J. Filer, M. C. Brummel, G. L. Baker, W. L. Krause, E. F. Bell and E. E. Ziegler, *Am. J. Clin. Nutr.*, 1991, **53**, 670-675.
201. M. D. Armstrong and U. Stave, *Metab. Clin. Exp.*, 1973, **22**, 561-569.

202. J. C. Divino, J. Bergstrom, P. Stehle and P. Furst, *Clin. Nutr.*, 1997, **16**, 299-305.
203. D. Matern, S. Tortorelli, D. Oglesbee, D. Gavrilov and P. Rinaldo, *J. Inherit. Metab. Dis.*, 2007, **30**, 585-592.
204. M. Zaffanello, C. Maffeis and G. Zamboni, *J. Perinat. Med.*, 2005, **33**, 246-251.
205. H. L. Levy and S. Albers, *Annu. Rev. Genomics Hum. Genet.*, 2000, **1**, 139-177.
206. P. D. Rainville, *Bioanalysis*, 2011, **3**, 1-3.
207. J. S. Mellors, V. Gorbounov, R. S. Ramsey and J. M. Ramsey, *Anal. Chem.*, 2008, **80**, 6881-6887.
208. J. G. Loeber, *J. Inherit. Metab. Dis.*, 2007, **30**, 430-438.
209. D. H. Chace, S. L. Hillman, D. S. Millington, S. G. Kahler, C. R. Roe and E. W. Naylor, *Clin. Chem.*, 1995, **41**, 62-68.
210. T. H. Zytkovicz, E. F. Fitzgerald, D. Marsden, C. A. Larson, V. E. Shih, D. M. Johnson, A. W. Strauss, A. M. Comeau, R. B. Eaton and G. F. Grady, *Clin. Chem.*, 2001, **47**, 1945-1955.
211. R. Guthrie and A. Susi, *Pediatrics*, 1963, **32**, 338-&.
212. N. S. Gerasimova, I. V. Steklova and T. Tuuminen, *Clin. Chem.*, 1989, **35**, 2112-2115.
213. S. Tachibana, M. Suzuki and Y. Asano, *Anal. Biochem.*, 2006, **359**, 72-78.
214. N. S. Green and K. A. Pass, *Nat. Rev. Genet.*, 2005, **6**, 147-151.
215. S. F. Dobrowolski, R. A. Banas, E. W. Naylor, T. Powdrill and D. Thakkar, *Acta Paediatr.*, 1999, **88**, 61-64.
216. D. S. Millington, R. Sista, A. Eckhardt, J. Rouse, D. Bali, R. Goldberg, M. Cotten, R. Buckley and V. Pamula, *Semin. Perinatol.*, 2010, **34**, 163-169.
217. M. Abdelgawad and A. R. Wheeler, *Adv. Mater.*, 2007, **19**, 133-137.
218. M. Abdelgawad and A. R. Wheeler, *Microfluid. Nanofluid.*, 2008, **4**, 349-355.
219. M. G. Pollack, A. D. Shenderov and R. B. Fair, *Lab Chip*, 2002, **2**, 96-101.
220. M. W. L. Watson, M. Abdelgawad, G. Ye, N. Yonson, J. Trottier and A. R. Wheeler, *Anal. Chem.*, 2006, **78**, 7877-7885.